

Chulalongkorn University

## Chula Digital Collections

---

Chulalongkorn University Theses and Dissertations (Chula ETD)

---

2018

### Chemical composition and in vitro anticancer activity of okra (albelmoschus esculentus) seed extract to develop into polymeric micelles

Watcharaphong Chaemsawang  
*Faculty of Pharmaceutical Sciences*

Follow this and additional works at: <https://digital.car.chula.ac.th/chulaetd>



Part of the [Pharmacy and Pharmaceutical Sciences Commons](#)

---

#### Recommended Citation

Chaemsawang, Watcharaphong, "Chemical composition and in vitro anticancer activity of okra (albelmoschus esculentus) seed extract to develop into polymeric micelles" (2018). *Chulalongkorn University Theses and Dissertations (Chula ETD)*. 2561.  
<https://digital.car.chula.ac.th/chulaetd/2561>

This Thesis is brought to you for free and open access by Chula Digital Collections. It has been accepted for inclusion in Chulalongkorn University Theses and Dissertations (Chula ETD) by an authorized administrator of Chula Digital Collections. For more information, please contact [ChulaDC@car.chula.ac.th](mailto:ChulaDC@car.chula.ac.th).

CHEMICAL COMPOSITION AND *IN VITRO* ANTICANCER ACTIVITY OF OKRA  
(*ALBELMOSCHUS ESCULENTUS*) SEED EXTRACT TO DEVELOP INTO POLYMERIC  
MICELLES



Mr. Watcharaphong Chaemsawang

A Dissertation Submitted in Partial Fulfillment of the Requirements  
for the Degree of Doctor of Philosophy in Pharmaceutics  
Department of Pharmaceutics and Industrial Pharmacy  
Faculty of Pharmaceutical Sciences  
Chulalongkorn University  
Academic Year 2018  
Copyright of Chulalongkorn University

องค์ประกอบทางเคมีและฤทธิ์ต้านมะเร็งแบบนอกกายของสารสกัดเมล็ดกระเจี๊ยบเขียว เพื่อพัฒนาให้  
อยู่ในรูปพอลิเมอร์ไมเซลล์



นายวัชรพงษ์ แจ่มสว่าง

วิทยานิพนธ์นี้เป็นส่วนหนึ่งของการศึกษาตามหลักสูตรปริญญาเภสัชศาสตรดุษฎีบัณฑิต  
สาขาวิชาเภสัชกรรม ภาควิชาวิทยาการเภสัชกรรมและเภสัชอุตสาหกรรม  
คณะเภสัชศาสตร์ จุฬาลงกรณ์มหาวิทยาลัย  
ปีการศึกษา 2561  
ลิขสิทธิ์ของจุฬาลงกรณ์มหาวิทยาลัย

Thesis Title	CHEMICAL COMPOSITION AND <i>IN VITRO</i> ANTICANCER ACTIVITY OF OKRA ( <i>ALBELMOSCHUS ESCULENTUS</i> ) SEED EXTRACT TO DEVELOP INTO POLYMERIC MICELLES
By	Mr. Watcharaphong Chaemsawang
Field of Study	Pharmaceutics
Thesis Advisor	PHANPHEN WATTANAARSAKIT, Ph.D.
Thesis Co Advisor	Associate Professor SUCHADA SUKRONG, Ph.D. WEERAPONG PRASONGCHEAN, Ph.D.

---

Accepted by the Faculty of Pharmaceutical Sciences, Chulalongkorn  
University in Partial Fulfillment of the Requirement for the Doctor of Philosophy

..... Dean of the Faculty of  
Pharmaceutical Sciences  
(Assistant Professor RUNGPETCH SAKULBUMRUNGSIL,  
Ph.D.)

DISSERTATION COMMITTEE

..... Chairman  
(Associate Professor PARKPOOM TENGAMNUAY, Ph.D.)  
..... Thesis Advisor  
(PHANPHEN WATTANAARSAKIT, Ph.D.)  
..... Thesis Co-Advisor  
(Associate Professor SUCHADA SUKRONG, Ph.D.)  
..... Thesis Co-Advisor  
(WEERAPONG PRASONGCHEAN, Ph.D.)  
..... Examiner  
(Professor GARNPIMOL RITTHIDEJ, Ph.D.)  
..... Examiner  
(Assistant Professor Dusadee Charnvanich, Ph.D.)  
..... External Examiner  
(Kostas I. Papadopoulos, Ph.D.)

วัชรพงษ์ แจ่มสว่าง : องค์ประกอบทางเคมีและฤทธิ์ต้านมะเร็งแบบนอกกายของสารสกัด  
เมล็ดกระเจี๊ยบเขียว เพื่อพัฒนาให้อยู่ในรูปพอลิเมอร์ไมเซลล์. ( CHEMICAL  
COMPOSITION AND *IN VITRO* ANTICANCER ACTIVITY OF OKRA  
(*ALBELMOSCHUS ESCULENTUS*) SEED EXTRACT TO DEVELOP INTO  
POLYMERIC MICELLES ) อ.ที่ปรึกษาหลัก : อ. ภาณุ. ดร.พรรณเพ็ญ วัฒนาอาชากิจ, อ.  
ที่ปรึกษาร่วม : รศ. ภาณุ. ร.ต.อ.หญิง ดร.สุชาติดา สุขหรั่ง,อ. ภก. ดร.วีระพงษ์ ประสงค์  
จีน

วัตถุประสงค์ของงานวิจัยนี้ เพื่อศึกษาองค์ประกอบทางพิษเคมีของสารสกัดเมล็ด  
กระเจี๊ยบเขียวและฤทธิ์ต้านเซลล์มะเร็งแบบนอกกาย สำหรับนำไปใช้ในทางเภสัชกรรม โดยในสาร  
สกัดเมล็ดกระเจี๊ยบเขียวพบสารสำคัญในกลุ่มฟลาโวนอยด์ ซึ่งพบปริมาณของไอโซเคอซิทรินร้อยละ  
 $2.89 \pm 1.64$  การศึกษาฤทธิ์ต้านอนุมูลอิสระของสาร ด้วยวิธี ดีพีพีเอช และ เอบีทีเอส ได้ค่า  
การยับยั้งที่ร้อยละ 50 เท่ากับ 55.80 ไมโครกรัมต่อมิลลิลิตร และ 49.04 ไมโครกรัมต่อมิลลิลิตร  
ตามลำดับ พบว่าสารสกัดเมล็ดกระเจี๊ยบเขียวมีคุณสมบัติต้านเซลล์มะเร็ง ทั้งเซลล์มะเร็งปากมดลูก  
(ฮีลา) มะเร็งตับ (เฮปจีทู) และมะเร็งเต้านม (เอ็มซีเอฟ-7) โดยมีการตอบสนองต่อเซลล์มะเร็งเต้านม  
ชนิดที่สูงสุด นอกจากนี้ยังพบฤทธิ์ในการยับยั้งการเคลื่อนที่ของเซลล์มะเร็ง การยับยั้งการหลั่งวีโอจี  
เอฟ และการเหนี่ยวนำให้เกิดการตายของเซลล์มะเร็งแบบอะพอพโทซิส การพัฒนาระบบนำส่งสาร  
สกัดเมล็ดกระเจี๊ยบเขียวด้วยระบบนำส่งพอลิเมอร์ไมเซลล์โดยใช้ โพลีออกซาเมอร์ 407 เป็นสารก่อ  
ไมเซลล์ พบว่าอัตราส่วนระหว่างสารสกัดเมล็ดกระเจี๊ยบเขียวต่อโพลีออกซาเมอร์ 407 ที่ 1:10 ได้  
อนุภาคนาโนขนาดเล็กที่สุดในช่วง  $190.23 \pm 46.96$  นาโนเมตร และมีประสิทธิภาพในการกักเก็บตัวยา  
สำคัญสูงถึงร้อยละ  $93.43 \pm 2.45$  และการเพิ่มอัตราส่วนของสารก่อไมเซลล์มีผลเพิ่มขนาดอนุภาค  
โดยที่ประสิทธิภาพในการกักเก็บตัวยาสำคัญลดลง

สาขาวิชา เภสัชกรรม

ปีการศึกษา 2561

ลายมือชื่อนิสิต .....

ลายมือชื่อ อ.ที่ปรึกษาหลัก .....

ลายมือชื่อ อ.ที่ปรึกษาร่วม .....

ลายมือชื่อ อ.ที่ปรึกษาร่วม .....

# # 5476219533 : MAJOR PHARMACEUTICS

KEYWORD: Okra, polymeric micelles, anticancer, In Vitro study

Watcharaphong Chaemsawang : CHEMICAL COMPOSITION AND *IN VITRO* ANTICANCER ACTIVITY OF OKRA (*ALBELMOSCHUS ESCULENTUS*) SEED EXTRACT TO DEVELOP INTO POLYMERIC MICELLES . Advisor: PHANPHEN WATTANAARSAKIT, Ph.D. Co-advisor: Assoc. Prof. SUCHADA SUKRONG, Ph.D., WEERAPONG PRASONGCHEAN, Ph.D.

The objective of this research was to study the phytochemical composition of the Okra seed extract and its *in vitro* anticancer activity for future pharmaceutical use. We detected active flavonoids compounds such as isoquercitrin, at an amount of  $2.89 \pm 1.64$  % w/w. Furthermore, antioxidation testing by DPPH assay and ABTS assay, showed values of  $IC_{50} = 55.80$  ug/ml and  $49.04$  ug/ml, respectively. The Okra seed extract's anti-cancer activity was evaluated on cancer cell lines, indicating anticancer properties for certain forms of cancer such as cervical cancer (HeLa), liver cancer (HepG2), and most significantly for breast cancer (MCF-7). The mechanisms studied were anti-migration, anti-invasion, VEGF release inhibition, and cell apoptosis inducers. A polymeric micelles carrier system used poloxamer 407 as the micelle inducer delivering the Okra seed extract was further studies. We found that the optimal ratio between the Okra seed extract and poloxamer 407 to prepare polymeric micelles is the 1:10 ratio at which the entrapment efficiency was  $93.43 \pm 2.45\%$ , and particle size of  $190.23 \pm 46.96$  nanometers. Increasing poloxamer 407 results in larger particle sizes with a decreasing drug entrapment efficiency.

Field of Study: Pharmaceutics

Academic Year: 2018

Student's Signature .....

Advisor's Signature .....

Co-advisor's Signature .....

Co-advisor's Signature .....

## ACKNOWLEDGEMENTS

This research could not have been accomplished without the dedicated encouragement, as well as invaluable counsel and assistance from a number of persons. Firstly, I would like to extend most impressive and deepest gratitude to my dissertation advisor, Phanphen Wattanaarsakit, Ph.D. and my co-advisor, Associate Professor Suchada Sukrong, Ph.D and Weeraphong prasonchaen, Ph.D. for their crucial comments, valuable suggestions and helpful advice.

Special thanks Professor Garnpimol Ritthidej, Ph.D. and Associate Professor Parkpoom Tengamnuy, Ph.D for everything such as encouragement and suggestion. More over thank Konstantinos I. Papadopoulos Ph.D. for comment and suggestion of my dissertation

I wish to express my appreciation to all the members of my dissertation committee, for their kind and beneficial comments and enlightening discussions. I am gratefully acknowledging the special effort by Department of Pharmaceutics and Industrial Pharmacy for their kindness to facilitate in laboratory.

I would like to thank are devoted to Faculty of pharmaceutical science, Burapha university for provided instrument and facilitate in laboratory.

I am thankful to my friends and my lab mates for their encouragement, helping, care and being good listeners along with dissertation study.

Finally, my sincere appreciation eventually dedicates to my family. Unless unconditional love, care, support, and warm encouragement provide, this research would not have been successful.

Watcharaphong Chaemsawang

## TABLE OF CONTENTS

	Page
.....	iii
ABSTRACT (THAI) .....	iii
.....	iv
ABSTRACT (ENGLISH) .....	iv
ACKNOWLEDGEMENTS .....	v
TABLE OF CONTENTS .....	vi
Table .....	viii
Figure .....	ix
List of abbreviations .....	xiii
CHAPTER I .....	1
INTRODUCTION .....	1
CHAPTER II .....	3
LITERATURE REVIEW .....	3
CHAPTER III .....	25
MATERIALS AND METHODS .....	25
Materials .....	25
Method .....	27
CHAPTER IV .....	39
RESULTS AND DISCUSSIONS .....	39
CHAPTER V .....	96
CONCLUSION .....	96

REFERENCES .....	100
VITA.....	159



## Table

	Page
Table 1. Comparison of the biochemical indexes in all experimental groups (Tian et al., 2015).....	5
Table 2. The polysaccharide compositions of the Okra extract (Alba,Laws and Kontogiorgos, 2015).....	5
Table 3. Sample of block copolymers used to prepare polymeric micelles .....	19
Table 4. Types of poloxamer.....	21
Table 5. Solubility of poloxamer in a different solvents at 20 °C.....	22
Table 6. Gradient condition for HPLC analysis of the Okra seed extract. ....	30
Table 7. Methodology for screening anticancer activity each fraction. ....	34
Table 8. Methodology for anticancer screening.....	34
Table 9. Phytochemical screening test.....	40
Table 10. Retention time of HPLC chromatogram .....	43
Table 11. Phytochemical quantitative analysis.....	45
Table 12. The standard of TLC plate with 8 cm elution heights and R <sub>F</sub> values. ....	52
Table 13. FTIR characteristic peaks of the Okra seed extract. ....	55
Table 14. Antioxidation activity of the Okra seed extract.....	59
Table 15 Cell apoptosis. ....	78
Table 16 Characterization of Okra seed extract loaded polymeric micelles.(n=3) .....	85
Table 17 Physical stability of the Okra seed extract loaded polymeric micelle after lyophilization. (n=3) .....	94

## Figure

	Page
Figure 1. Morphology of Okra.....	3
Figure 2. Result of the Okra extract (AEaq) affecting rats induced by ethanol and indomethacin.....	4
Figure 3. Structure of the acidic polysaccharide.....	6
Figure 4. Chemical structure of isoquercitrin.....	7
Figure 5. Incident type of cancers in Thailand men. (years 2010-2015, ratio 1:100,000) 9	9
Figure 6. Incident type of cancers in Thailand women. (years 2010-2015, ratio 1:100,000).....	10
Figure 7. Hallmark of cancer.....	11
Figure 8. Anatomy of the female Breast.....	12
Figure 9. Anatomy of liver organ .....	14
Figure 10 Anatomy of uterus and cervical .....	15
Figure 11. Angiogenesis.....	16
Figure 12. Micelle structure. ....	18
Figure 13. Poloxamer structure formula. ....	21
Figure 14. Thermoreversible property of poloxamer 407.....	23
Figure 15. Complex reaction between flavonoid and aluminum salt.....	31
Figure 16. Chemical reaction of phenol-sulfuric assay .....	32
Figure 17. Cells scratch assay.....	35
Figure 18. Transwell invasion assay.....	36
Figure 19 The Okra seed extraction process.....	39
Figure 20. Chemical reaction of ferric chloride and phenol group. ....	40

Figure 21. Shinoda reaction. ....	41
Figure 22. Sodium hydroxide test .....	41
Figure 23. HPLC chromatogram of the standard Isoquercitrin. ....	42
Figure 24. HPLC chromatogram of the Okra seed extract.....	43
Figure 25. Reaction scheme of the phenol-sulfuric test. ....	46
Figure 26. TLC Chromatogram of Okra seed extract observed under visible light (A) and under UV light at 254 nm (B) and 366 nm (C); tracks: (1)Hexane fraction; (2)DCM fraction; (3)Ethanol fraction; (4)Crude OSE; (5)Isoquercitrin; (6)Quercetin; (7)Rutin; (8)Silibinin; (9)Myricetin . Adsorbent: Silica gel GF .....	48
Figure 27. TLC Chromatogram of Okra seed extract after reacting with ferric chlorides observed under visible light; tracks: (1)Hexane fraction; (2)DCM fraction; (3)Ethanol fraction; (4)Crude OSE; (5)Isoquercitrin; (6)Quercetin; (7)Rutin; (8)Silibinin; (9)Myricetin. Adsorbent: Silica gel GF.....	49
Figure 28. TLC Chromatogram of Okra seed extract after reacting with $AlCl_3$ reagent under visible light (A) and under UV light at 366 nm (B); tracks: (1)Hexane fraction; (2)DCM fraction; (3)Ethanol fraction; (4)Crude OSE; (5)Isoquercitrin; (6)Quercetin; (7)Rutin; (8)Silibinin; (9)Myricetin. Adsorbent: Silica gel GF.....	50
Figure 29. TLC Chromatogram of Okra seed extract after reacting with NP reagent observed under visible light (A) and under UV light at 366 nm (B) tracks: (1)Hexane fraction; (2)DCM fraction; (3)Ethanol fraction; (4)Crude OSE; (5)Isoquercitrin; (6)Quercetin; (7)Rutin; (8)Silibinin; (9)Myricetin. Adsorbent: Silica gel GF.....	51
Figure 30. TLC Chromatogram of Okra seed extract after reacting with DPPH reagent observed under visible light; tracks: (1)Hexane fraction; (2)DCM fraction; (3)Ethanol fraction; (4)Crude OSE; (5)Isoquercitrin; (6)Quercetin; (7)Rutin; (8)Silibinin; (9)Myricetin . Adsorbent: Silica gel GF.....	53
Figure 31. Infrared spectrum of the Okra seed. ....	54
Figure 32. Infrared spectrum of isoquercitrin.....	54
Figure 33. Infrared spectrum of quercetin.....	55
Figure 34. Chemical structure of a flavonoid.....	56

Figure 35. Chemical structure of a flavonoid glycoside .....	56
Figure 36. HPLC chromatogram of a standard quercetin. ....	56
Figure 37. Thermogram of the Okra seed extract.....	57
Figure 38. Cytotoxicity of the Okra seed extract fractions (48hr). ....	61
Figure 39. Cell viability versus concentration, A: HeLa, B: HepG2 and C: MCF-7 .....	62
Figure 40. Synergistic of baicalein and silymarin on HepG2 cell. ....	64
Figure 41. Okra seed extract cytotoxicity of human keratinocyte cell.....	65
Figure 42. Cell migration (HeLa cell).....	67
Figure 43. Cell migration (HepG2 cell).....	69
Figure 44. Cell migration (HepG2 cell).....	70
Figure 45. Cell migration (MCF-7 cell) .....	71
Figure 46. Cell migration (MCF-7 cell) .....	72
Figure 47. Cell invasion inhibition. ....	75
Figure 48. Cell apoptosis.....	77
Figure 49. Cisplatin induce cell death (A: HeLa, B: HepG2 and C: MCF-7).....	79
Figure 50. Anti-vascular endothelial growth factor (HeLa cell).....	80
Figure 51. Anti-vascular endothelial growth factor (HepG2 cell).....	81
Figure 52. Anti-vascular endothelial growth factor (MCF-7 cell).....	82
Figure 53. Critical micelle concentration of poloxamer 407. ....	83
Figure 54. Surface tension and critical micelle concentration. ....	84
Figure 55 Okra seed extract loaded polymeric micelles (50:50).....	87
Figure 56. Okra seed extract loaded polymeric micelles (50:100).....	87
Figure 57. Okra seed extract loaded polymeric micelles (50:200).....	88
Figure 58. Okra seed extract loaded polymeric micelles (50:500).....	88

Figure 59. Okra seed extract loaded polymeric micelles (50:1,000).....	89
Figure 60. Possible location of isoquercitrin in micelles. ....	90
Figure 61. Chromatographic elution of Okra seed extract (A: OSE-micelles, B: OSE)...	91
Figure 62. Cytotoxic activity of Okra seed extract loaded polymeric micelles. ....	92
Figure 63. Stability of Okra seed extract loaded in polymeric micelle. ....	95



## List of abbreviations

% w/v	=	Percent weight by volume
ug	=	Microgram
ug/ml	=	Microgram per milliliter
°C	=	Degree Celsius
7AAD	=	7-Aminoactinomycin D
Abs.	=	Absorbance
ANOVA	=	Analysis of variance
AR	=	Analytical reagents
CO <sub>2</sub>	=	carbon dioxide
Conc.	=	Concentration
DCM	=	Dichloromethane
DSC	=	Differential scanning calorimeter
DMSO	=	Dimethyl sulfoxide
E.E. %	=	Percentage of entrapment efficiency
EtOH	=	Ethanol
EtOAc	=	Ethyl acetate
FTIR	=	Fourier transform infrared spectroscopy
Hacat	=	immortalized human keratinocytes cell
HeLa	=	Cervical cancer cell
HepG2	=	Hepatocellular carcinoma cell

Hex	=	Hexane
HPLC	=	High performance liquid chromatography
Hr.	=	Hour
MCF-7	=	Breast cancer cell
Min.	=	Minute
ml	=	Milliliter
mm	=	Millimeter
MW.	=	Molecular weight
nm	=	Nanometer
OSE	=	Okra seed extract (crude)
OSE-EtOH	=	Okra seed ethanol fraction
OSE-DCM	=	Okra seed dichloromethane fraction
OSE-Hex	=	Okra seed hexane fraction
PDI	=	Poly disperse index
UV-vis	=	Ultraviolet visible spectroscopy
ZP	=	Zeta potential

## CHAPTER I

### INTRODUCTION

Cancer is a non-communicable disease with a high incidence for mortality rates (Dela Cruz, Tanoue and Matthay, 2011, Khazaei, Salehiniya and Mohammadian-Hafshejani, 2015, Roswall and Weiderpass, 2015). At present, incidences of cancer among the Thai population have increased. The five most important kinds in the country are breast cancer, colorectal cancer, liver cancer, lung cancer and cervical cancer, accounting for 62.01% of all cancer cases (Thai Ministry of Public Health, 2013-2017). This study focused on three types of cancer, namely breast cancer, cervical cancer and liver cancer since breast cancer and cervical cancer are the two leading causes of cancer in women, accounting for 24.69% and 8.23%, respectively, of all cases in 2015. Meanwhile, liver cancer is the third most common cancer among the Thai population, accounting for 10.99% of all cases and a high-mortality disease (Sia et al., 2017). Based on the above information, cancer appears to be a disease that poses a public health problem in the country. The data presented shows that incidences of cancer among Thai and foreign populations are increasing continuously. Therefore, there is an ever increasing research activity for the development of drugs and products to treat or prevent cancer. One group of extracts that has been very interesting is natural extracts, especially due to the active substances in a group of antioxidants.

*Albemoschus esculentus* (L.) Moench (Okra) is a flowering plant in the family Malvaceae. Okra is planted in tropical regions around the world, such as Southeast Asia, Africa and the Mediterranean. Okra is edible in many areas. In folk medicine, it is also commonly used to treat gum disease. A great list of clinical studies regarding the use of Okra in various conditions such as its use as an anti-inflammatory treatment, as a dietary supplement for the body when under stress (Xia et al., 2015), nervous system relief, and Alzheimer's protection (Karim et al., 2014, Mairuae et al., 2015). Various phytochemistry reports have confirmed the presence of substances of the flavonoid type. Okra seed also display antioxidant activity (Gates, 2013, Xia et al., 2015, Esan et al., 2017), which is higher than in the pods. A substance commonly mentioned in the Okra seed extract is Isoquercitrin. Isoquercitrin possesses many pharmacological activities (Valentová et al., 2014). Isoquercitrin has shown inhibition of urinary bladder (Chen et al., 2016), and pancreatic cancer progress (Chen et al., 2015), as well as colon cancer suppression (Amado et al., 2014). Despite the above

numerous mentions, there is a paucity of reports regarding the anticancer effects of Okra seeds. Hence, this research was focused on studying the composition and activity of Okra seed extract on cancer cell lines in order to develop products for future cancer prevention. Solubility issues pertaining to flavonoid compounds necessitate a delivery system to increase cellular uptake and cytoplasm accessibility. One of the most promising delivery systems is the polymeric micelles, due to the easiness and low cost of preparation (Chen et al., 2011, Lu and Park, 2013, Xu, Ling and Zhang, 2013). Polymeric micelle is a polymer block with both hydrophobic and hydrophilic properties. Polymers can be induced by self-assembly when dissolved into the appropriate medium and is more concentrated than the critical micelle concentration (CMC). The polymeric micelle formed consists of the core part formed by the incorporation of the hydrophobic part and is surrounded by a hydrophilic part. Examples of polymeric micelles are the ones used for delivery of the *Juglans mandshurica* Maxim extract using poloxamer 188 mixed with lecithin to deliver it to breast cancer cells (Jin et al., 2016) or the use of polymeric micelle to increase the solubility and stability of nevirapin (Jindal and Mehta, 2015) and clozapine (Singla et al., 2018). Another example is Cisplatin (CDDP)-crosslinked, glutathione-sensitive, tumor-targeting micelles based on carboxymethyl chitosan designed for synergistic cisplatin-doxorubicin (DOX) combination chemotherapy (Zheng et al., 2017b).

In this research, the chemical and functional components of Okra seed extract were investigated as was their delivery in the form of polymeric micelles.

#### Objective

The aim of the present study was

- 1) to elucidate the phytochemical composition of the Okra seed extract and
- 2) study the anticancer activity of its flavonoid-rich fraction, delivered in its native form as well as
- 3) in the form of a polymeric micelle with enhanced solubility, in three carcinoma cell lines.

## CHAPTER II

### LITERATURE REVIEW

Okra (*Albermoschus esculentus*) is a flowering plant species belonging to the family Malvaceae. In terms of botanical characteristics, Okra is classified as a dicotyledon growing up to one-two meters. Its leaves are palmately lobed and are 10-20 centimeters in length, and the flowers are four-eight centimeters in size, polypetalous with five white or yellow petals. The fruit is a pentagonal capsule with a locule in the interior, which is divided into five pods; each containing a lot of seed. Furthermore, Okra is grown in the tropical areas of the world; for example, South East Asia, Africa, and the Mediterranean. Its fruits are usually consumed as food in many areas.



Figure 1. Morphology of Okra

(<https://worldoffloweringplants.com/planting-growing-harvesting-okra-plants/>)

In terms of traditional medicine, it is believed that consuming Okra will heal peptic ulcers. A study by Joshi et al. (Joshi et al., 2011) conducted on rats consuming Okra extracted by water (AEaq) at 1g/kg and induced by ethanol and indomethacin when compared to cimetidine found that the extract of Okra had the competency to decrease the peptic ulcer lesion, which had increased in size on the gastric wall mucus (figure 2).

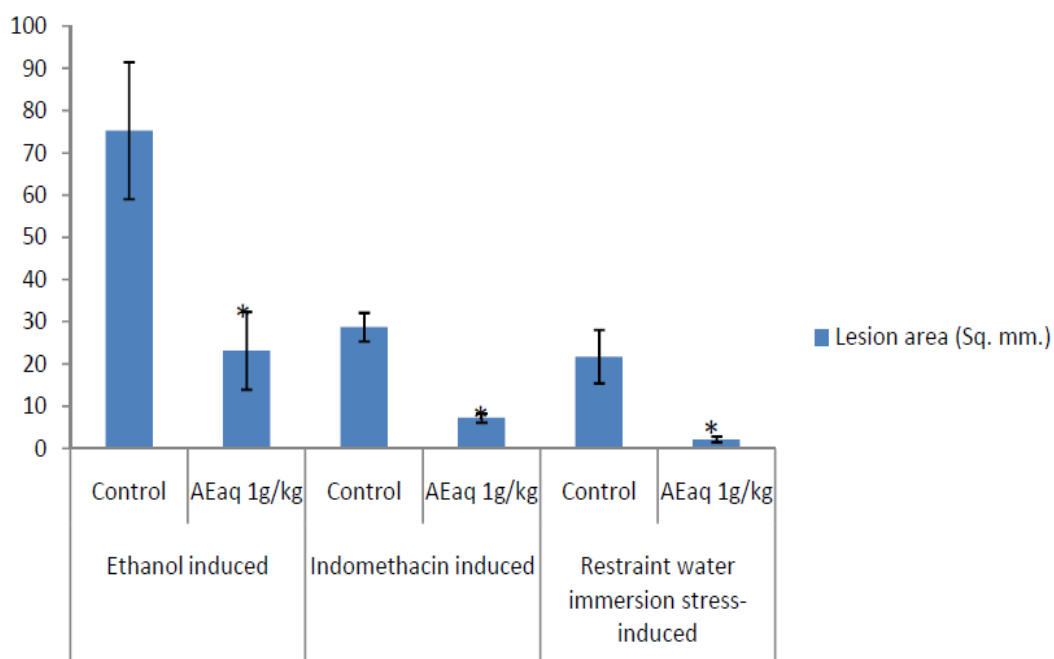


Figure 2. Result of the Okra extract (AEaq) affecting rats induced by ethanol and indomethacin.

Other research found that the Okra extract was able to resist the adherence of *Helicobacter pylori* (*H. pylori*) in the tube (Lengsfeld et al., 2004, Messing et al., 2014). *H. pylori* is a cause of peptic ulcers. Apart from the study on the pharmacological activities of Okra, according to a study on the hypoglycemic action and anti-hyperlipidemic action (Liu et al., 2017) by Fan et al. (Fan et al., 2014), after the induction of hyperglycemia in rats for three months, when they received the Okra extracted by ethanol, the volume of the glucose and fat decreased when compared to the control group. These results conformed to the research by Tian et al. (Tian et al., 2015) that induced diabetes in rats with streptozocin. As the rats consumed the Okra extract, it was found that the extract could reduce the amount of glucose and fat in the blood.

Table 1. Comparison of the biochemical indexes in all experimental groups (Tian et al., 2015)

Group	Control	GDM group	Intervention group
HbA1c (mmol/L)	5.04±0.85	13.03±2.67	7.17±1.28
TG (mmol/L)	0.66±0.16	3.35±0.28	1.21±0.23
TC (mmol/L)	2.15±0.11	6.13±0.23	2.63±0.34
FBG (mmol/L)	6.67±0.88	9.80±1.02	6.87±0.49
HDL (mmol/L)	1.00±0.15	0.82±0.19	0.98±0.14
LDL (mmol/L)	0.30±0.06	1.46±0.28	0.62±0.16

In addition, it was discovered that ingredients including 90% of fresh Okra fruit and 7% of carbohydrate found in soluble fiber with the quality of soluble cellulose having contact with water would result in the extract becoming mucus. Based on the study of polysaccharides extracted from the Okra fruit, the extract belonged in the acidic polysaccharide group. Moreover, it mainly contained sugar and galacturonic acid (Sengkhampan et al., 2009, Sengkhampan et al., 2010, Kpodo et al., 2017).

Table 2. The polysaccharide compositions of the Okra extract (Alba, Laws and Kontogiorgos, 2015)

	OP2	OP6
Yield (g pectin/100 g dry okra pods)	13.3 ± 0.3	15.7 ± 0.2
Total sugars <sup>a</sup>	70.0 ± 3.7	81.8 ± 6.4
D-GalA <sup>a</sup>	46.8 ± 2.1 (55.0) <sup>b</sup>	56.9 ± 6.9 (51.6) <sup>b</sup>
Methoxyl (-OCH <sub>3</sub> ) <sup>a</sup>	3.3 ± 0.1	2.5 ± 0.1
Degree of methylation (DM%)	40.0 ± 1.6	24.6 ± 1.0
Acetyl (-COCH <sub>3</sub> ) <sup>a</sup>	6.0 ± 0.6	5.2 ± 0.4
Degree of acetylation (DA%)	52.2 ± 5.5	37.6 ± 3.0
D-Gal <sup>a</sup>	17.0 ± 3.3 (21.7) <sup>b</sup>	26.1 ± 1.5 (25.7) <sup>b</sup>
L-Rha <sup>a</sup>	7.1 ± 2.0 (10.1) <sup>b</sup>	12.1 ± 0.9 (13.2) <sup>b</sup>
L-Ara <sup>a</sup>	4.5 ± 3.1 (7.1) <sup>b</sup>	6.0 ± 3.3 (7.3) <sup>b</sup>
D-Glc <sup>a</sup>	2.4 ± 0.5 (3.1) <sup>b</sup>	2.2 ± 0.1 (2.2) <sup>b</sup>
D-Xyl <sup>a</sup>	2.0 ± 0.7 (3.0) <sup>b</sup>	n/a
Protein <sup>a</sup>	4.3 ± 0.0	6.3 ± 0.1

<sup>a</sup> All values are expressed as % on wet basis of pectin powder.

<sup>b</sup> Values in brackets are mol%.

OP2: Extraction to pH2 and OP6: Extraction to pH6.

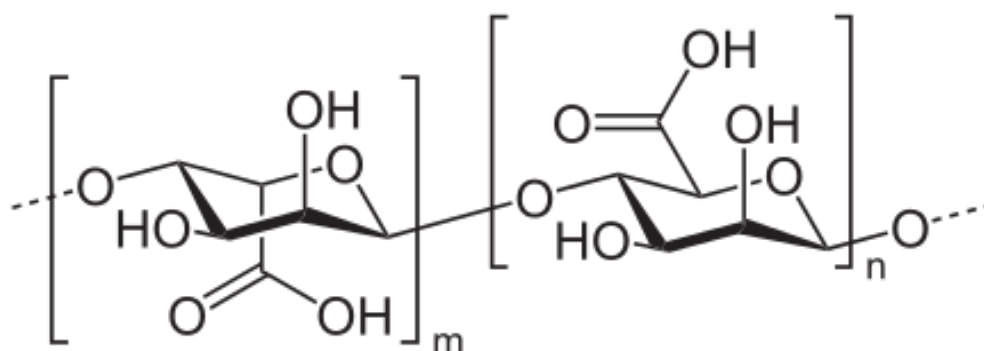


Figure 3. Structure of the acidic polysaccharide.

Nevertheless, a few studies examined the effect of polysaccharides extracted from Okra; for example, the study on the viscosity of the Okra skin extract and the study on the adhesive ability (Sengkhamparn et al., 2010, Kontogiorgos et al., 2012, Ghori et al., 2017) which resulted in some further research and development. From a report on the use of mucus extracted from Okra for the development of the application of Propranolol Hydrochloride in the large intestine, the study compared three types of cellulose: cellulose from tamarind kernel, chitosan, and Okra (Newton, Indana and Kumar, 2015)

As for the anti-cancer effects, Vayssade et al. (Vayssade et al., 2010) researched the use of the Okra seed extract and found an antiproliferative effect and apoptosis on B16F10 skin cancer cells in a tube. Based on their study, Monte et al. (Monte et al., 2014) found that lectin extracted from Okra similarly had an antiproliferative effect towards MCF-7 breast cancer cells in agreement with Okra's phytochemical properties containing many types of flavonoids. Substances in the flavonoid group have antioxidant (Gates, 2013, Xia et al., 2015, Esan et al., 2017) and anticancer properties (de Sousa Ferreira Soares et al., 2012, Chen et al., 2013, Venturelli et al., 2016, Wang et al., 2017, Zang et al., 2017). Several plant seeds display phytochemical and pharmaceutical properties with anti-cancer effects, such as legume seeds' effect on advanced colorectal cancer (Lima et al., 2016) and from the multiple protective effect of peptides released from *Olea europaea* and *Prunus persica* seeds against oxidative damage and cancer cell proliferation (Hernández-Corroto, Marina and García, 2018). However, the Okra plant has as yet not received sufficient attention apart from the reports confirming that the Okra seed contains more major flavonoid substances than fruit. Consequently, this current research study aims to study the composition and effect of the Okra seed extract toward cancer cells as a development pathway for future cancer prevention applications.

One of the important flavonoids is isoquercitrin, which has been found to display several pharmaceutical effects (Valentová et al., 2014); for instance, an antiproliferative effect in bladder cancers (Chen et al., 2016) antiproliferative effect in pancreatic cancer (Chen et al., 2015), antiproliferative effect in colorectal cancer (Amado et al., 2014) and suppressing VEGFR2-mediated signaling in zebrafish (Lin, Wu and Dong, 2012) Nonetheless, substances belonging in the flavonoid group have solubility issues necessitating the development of a transfer system to enhance its target delivery efficiency.. One of the interesting delivery systems is the polymeric micelle as it only requires simple preparation and is not expensive and can thus be easily translated to industrial applications.

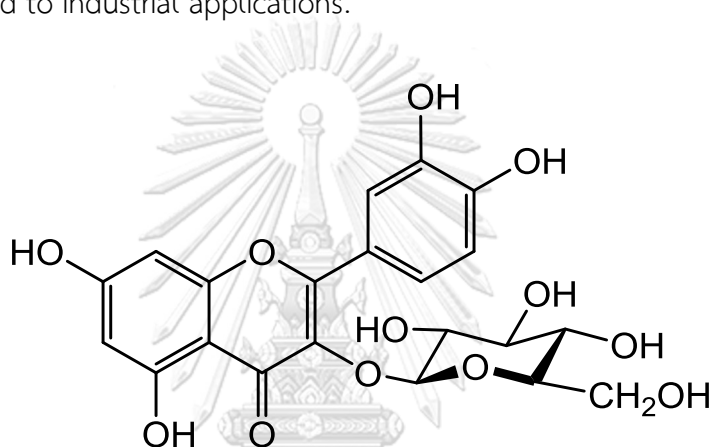


Figure 4. Chemical structure of isoquercitrin

Isoquercitrin is a substance found in flavonoid glycosides, and possesses antioxidant activities, it has therefore been discussed in cardiovascular disease prevention; such as, myocardial ischemia, cerebral hypoxia, and ischemic disease. Furthermore, it is known to display anti-inflammatory, anticancer, and/or antiviral activities. However, isoquercitrin is rarely found in plants. The creation of isoquercitrin in nature is to synthesize it from rutin with the hesperidinase enzyme, but this enzyme is only found in small quantities in nature resulting in a minimal quantities of isoquercitrin (Wang et al., 2015a, Wang et al., 2015b). On the other hand, isoquercitrin has several other effects than rutin; for example, being anti-inflammatory. It was found that this substance is able to reduce the building of prostaglandin better than rutin. (Chanh et al., 1986).

The molar mass of isoquercitrin is 464.38 g/mol and displays the physical characteristics of a yellow powder with conjugated double bonds in its structure that can absorption UV light at maximum wave lengths of 257 and 352 nm; isoquercitrin can dissolve at 95 mg/l, and logP = 0.76. It was initially discovered in the *Cercis*

*Canadensis* L. (eastern redbud) extract (Valentová et al., 2014). Nowadays, it has been found in many plants; for instance, *Soulieana* Crepin flowers (Yang et al., 2013), *Eucommia ulmoides* Oliv. Leaves (Dai et al., 2013), *Crataegus pinnatifida* Bge. (Chinese hawberry) fruits (Jurikova et al., 2012), *Crataegus azarolus* L. (azarole) leaves (Belkhir et al., 2013), flowering shoots of *Caragana arborescens* Lam. (Siberian peashrub; (Olennikov et al., 2012)), leaves of *Arbutus unedo* L. (strawberry tree; (Males et al., 2006)), in various *Allium* species (Vlase et al., 2012), in extracts from amaranth leaves, flowers, stems and seed (Kraujalis and Venskutonis, 2013). Safety studies on humans have not been conducted yet. However, in a Wistar rat 52-week chronic toxicity study, has already been completed. The rats were divided into a control group and an experimental group in which the groups received food mixed with concentrated isoquercitrin at 0.04%, 0.2%, 1%, and 5% w/w, respectively resulting in no deaths. For the biotransformation of isoquercitrin, it was realized that the substance could perform hydrolysis through the gastrointestinal tract. With regards to the experiment with the Wistar rats, 36%, 7%, 96% and 100% of the substance could be dissolved in the duodenum, the jejunum, the ileum, and the colon respectively. Nevertheless, when studied in the Caco-2 cells, there was no change as the cells had no enzyme that was related to biotransformation. Moreover, the findings demonstrated that isoquercitrin could be metabolized by the liver cells with UDP-glucuronosyltransferases (UGTs) and sulfotransferases (SULTs). Isoquercitrin is hydrolyzed through the gastrointestinal tract *in vivo* while *in vitro* in the rat liver and breast cells it is re-secreted via receptor multidrug resistance-associated protein 2 (MRP2) or breast cancer resistance protein (BCRP). Additionally, in the rat it leads to the stimulation of CYP1A1, CYP1A2, and CYP2B1/2 possibly via quercetin, which is one of the metabolites of isoquercitrin.

Isoquercitrin isolated from *Aster yomena*, which has been used as a traditional medicinal herb showed in the study of Yun et al. (Yun et al., 2015), that it possessed fungicidal effects on *Candida albicans* via inducing membrane disturbance. Although its effect is not as proficient as amphotericin B, isoquercitrin has a lower toxic effect towards red blood cells. This is because a concentration of isoquercitrin at 80 µg/ml is required to induce hemolysis of 16% of blood cells compared to only 20 µg/ml of concentrated amphotericin for the same toxicity. Moreover, an amphotericin B concentration at 80 µg/ml will cause 100% hemolysis.

## Cancer

Cancer is the number one cause of death of people around the world. Based on the World Health Organization (WHO)'s information in 2015, there were a total of 8.8 million deaths from cancer, which was more than the total number of deaths from AIDS, tuberculosis, and malaria. The top five types of cancer that cause death in the world are lung cancer (1.69 million people), liver cancer (788,000 people), colorectal cancer (754,000 people), and breast cancer (571,000 people). In Thailand, the statistics of new cancer patients from the National Cancer Institute of the 15 Hospital-based Cancer Registry of Thailand for the years 2010-2012 (Cancer in Thailand Vol VIII, 2010-2015) demonstrated that the top five types of cancer found in Thai males were liver cancer, lung cancer, colorectal cancer, prostate cancer, and leukemia whereas for Thai females, they were breast cancer, cervical cancer, liver cancer, colorectal cancer, and lung cancer. According to the report of the Strategy and Planning Division in 2011, the death toll resulting from cancer in Thailand was approximately 61,082, which comprised 35,437 males and 25,645 females. This is regarded as the major reason for deaths and the number has tended to increase. For Thai males, the top five cancer mortality diagnoses were liver cancer, lung cancer, colorectal cancer, oral and oropharyngeal cancers, and leukemia. For Thai females, the top five cancers cancer mortality diagnoses were liver cancer, lung cancer, breast cancer, and cervical cancer, and colorectal cancer. (figure 5-6)

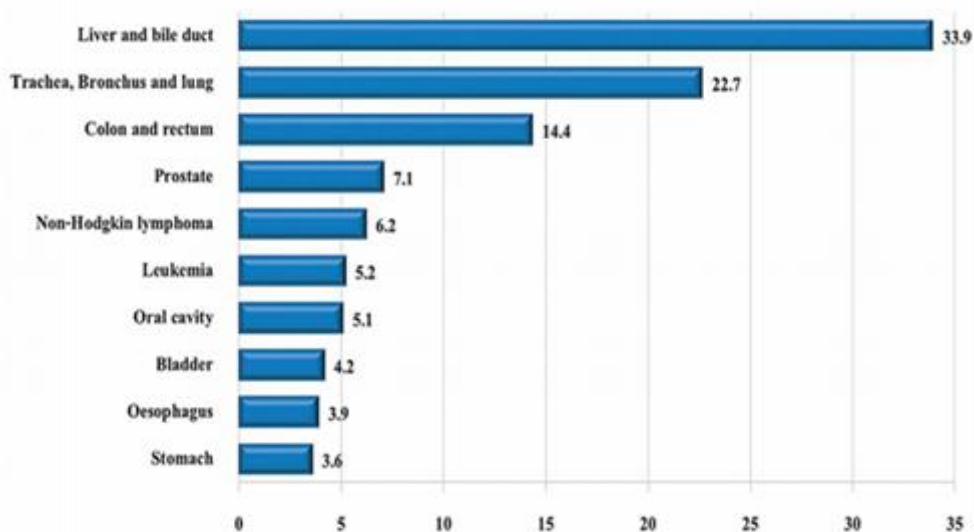


Figure 5. Incident type of cancers in Thailand men. (years 2010-2015, ratio 1:100,000)

(<http://publine.xiahepublishing.com/journals/10.14218/JCTH.2015.00025.pdf>)

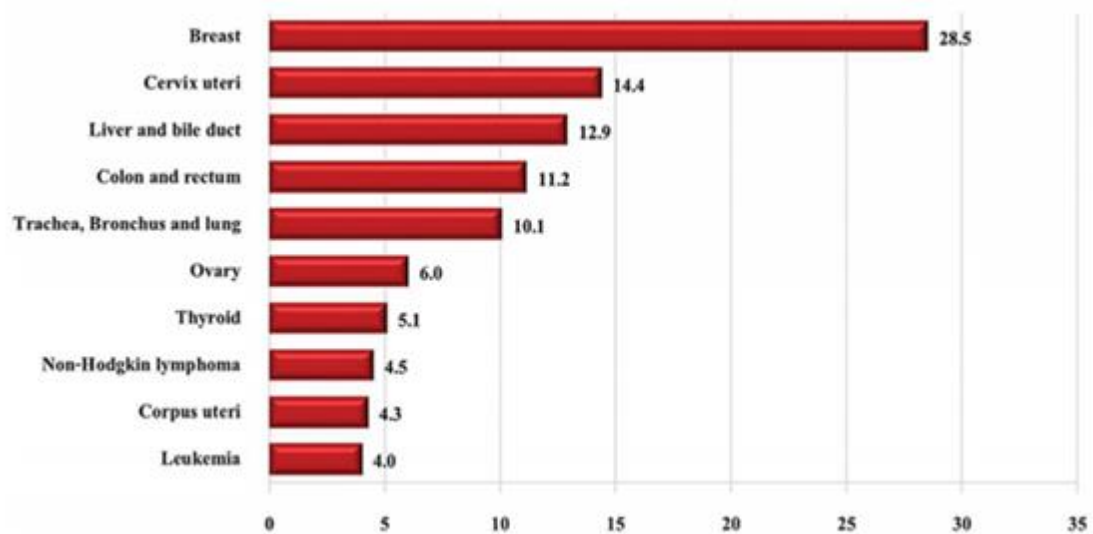


Figure 6. Incident type of cancers in Thailand women. (years 2010-2015, ratio 1:100,000)

(<http://publine.xiahepublishing.com/journals/10.14218/JCTH.2015.00025.pdf>)

All cancers begin in cells. Our bodies have more than 100,000,000,000 (one hundred million million) cells. Sometimes cells lose the capacity to produce or understand signals that control cell growth. If any of these signals are lost or missing or faulty, then uncontrollable growth can occur. Cells may then start to grow and multiply too much and form a lump called a tumor. A primary tumor is where the cancer starts. Some cancers are called leukemias or lymphomas as they start in the blood and the lymphglands respectively. Others start in the bone marrow. Sometimes solid tumors are formed. Tumors may grow and spread to the other organs while the benign one will grow but not spread to other areas. The ability to spread to other tissues in the body could occur to be one way or another; for example, growing directly to nearby tissues or moving to cells that are further away from the tumor.

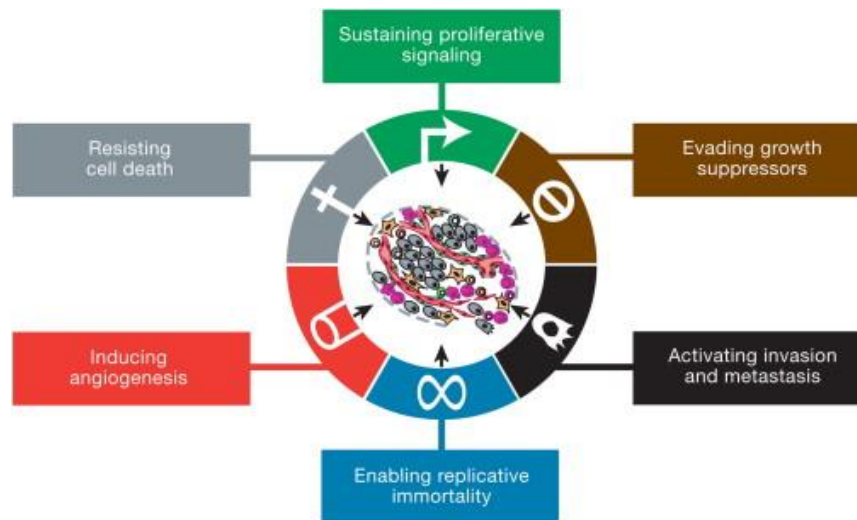


Figure 7. Hallmark of cancer

(<https://www.cell.com/action/showPdf?pii=S0092-8674%2811%2900127-9>)

Furthermore, the tumor can grow and disturb the operation of other systems in the body; such as, the digestive system, nervous system, and circulatory system. In addition, it can release hormones that change the normal functions, thus, resulting in causing damage to the body. The mechanism of cancer stems from the change of normal cells to be cancerous. There are various reasons for this change: heredity of certain genes that are associated with cancer, random mutations or gene rearrangements and chemical inductions; such as, polycyclic aromatic hydrocarbons (PAHs) and an aromatic amine. Moreover, there are physical factors; such as, rays from infection of oncogenic viruses, which can be divided into DNA and RNA viruses. Behavioral factors such as smoking, obesity and lack of exercise are important contributors of cancer risk.

## Breast

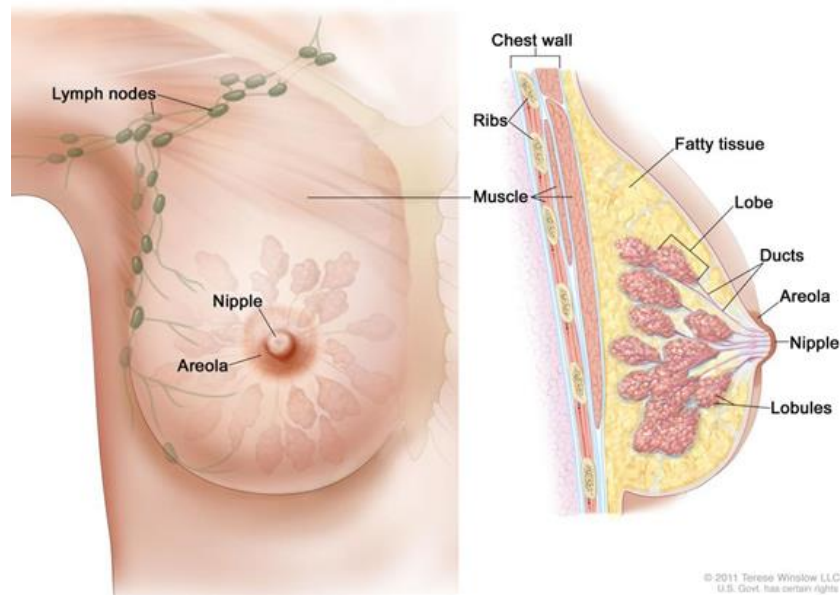


Figure 8. Anatomy of the female Breast

(<https://nbcf.org.au/about-national-breast-cancer-foundation/about-breast-cancer/what-you-need-to-know/breast-anatomy-cancer-starts/>)

The breast is composed of alveolar and duct forming lobes. Each lobe is separated from each other, as the connective tissue blocks them while the septum is composed of veins, lacteals, and nerves. Each lobe can be divided into 20-30 lobules, and a lobule contains a lactiferous duct that branches out as a small ductile. The tip of the ductile is inflated, which is called alveoli. However, each lobe contains 10-100 alveoli (figure8). Inside the alveolus, there are two layers of cells. The inner layer is alveolar cells that have the duty to produce milk when it has been alerted by the prolactin hormone. The outer layer is the myoepithelial cells, which are muscle cells circling the alveolus and easing themselves to let the milk flow inside the tube after being stimulated by the oxytocin hormones. The milk produced inside the alveolar cells will be collected in the alveoli. When the myoepithelial cells shrink and squeeze the milk to flow on the ductile, and it will be collected at the lactiferous duct, which will be opened at the tilt. The ducts passing under the inflated tilt are called the lactiferous sinus, and the milk is collected there. The tube will be minimized and will wait for the tilt to open the exit. There are 15-20 ducts that connect to the exit.

## Breast cancer

This cancer originates from the abnormal distribution of cells in the breast, which usually occurs in the ducts and tissues of the alveolar. Cancer cells will spread to other tissues or other parts of the body starting from the nearby lymph nodes before entering other organs; for example, the heart, bones, brain, and lung. The process of cancer begins from the mutation and over division of cells then the cells overgrow and cause the abnormality of the cells' division. Risk factors relating to breast cancer such as aged over 50, health history indicates that the patients used to have breast cancer in one of the breasts, in member of the family had breast cancer, mutation of the gene BRCA1 or BRCA2 related to the increase of risk of breast cancer or receive estrogen hormones.



## Liver

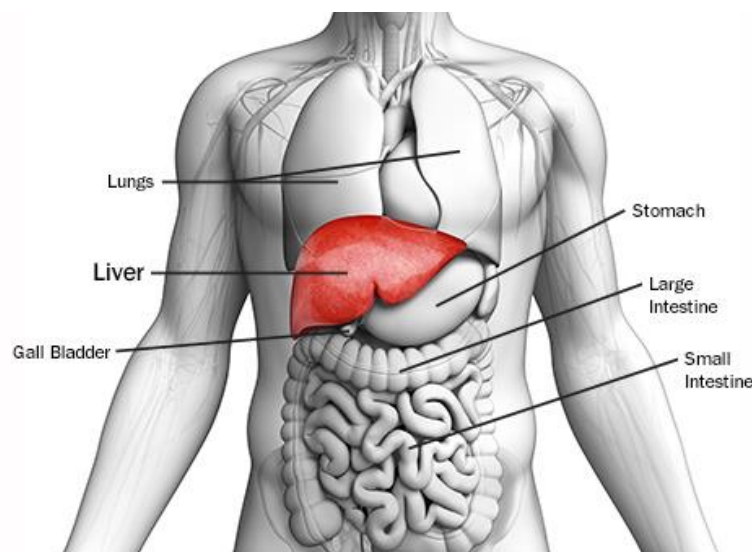


Figure 9. Anatomy of liver organ

(<https://www.webmd.com/cancer/ss/slideshow-liver-cancer-guide>)

The liver is the largest organ of the body which is located under the bottom right ribs or under the right lung. The shape of the liver is similar to a pyramid, and it is divided into the left side and right side. The liver receives blood from two sources that are the hepatic artery delivering oxygen to it, and the portal vein that delivers nutrients from the intestines.

## Liver cancer

This type of cancer grows in liver cells and is also called primary liver cancer, which can be divided into three types. The title comes from the type of development.

1. Hepatocellular carcinoma (HCC): This type of liver cancer has been mostly found due to the fact that the cancer cells originate in the hepatocytes. The types of growth are various. Some cells spread by invading the liver. Some start from one cell and spread to other parts of the liver until developing to the disease.

2. Bile duct cancer: This type stems from the bile in the liver. As the bile is a small thin tube, cancer can spread through the gall bladder and small intestine.

3. Angiosarcomas: This type begins from the endothelial cell at the liver and grows rapidly.

Other cancers that start at other organs and spread to the liver will be called secondary (metastatic) liver cancer, which is more predominant than primary

liver cancer, as the cancer comes from the intestines, anus, lung, and breast spreading to the liver. The characteristics of the cancer cells depend on its origin.

The major risk to liver cancer is chronic hepatitis B virus infection, which multiplies the risk to Hepatocellular Carcinoma from five to 98-fold compared to those people who have never been infected. The other factors that result in the disease are the cell distribution of the hepatitis B Virus (HBsAg), liver function test; alanine aminotransferase test (ALT), age, gender, history of alcohol consumption, consumption of food with aflatoxin, family members having Hepatocellular Carcinoma, and hepatitis B virus infection in the blood (HBV DNA), including other infections associated with hepatitis B virus; for example, Hepatitis C, Hepatitis D, and HIV infection.

Uterus and cervical

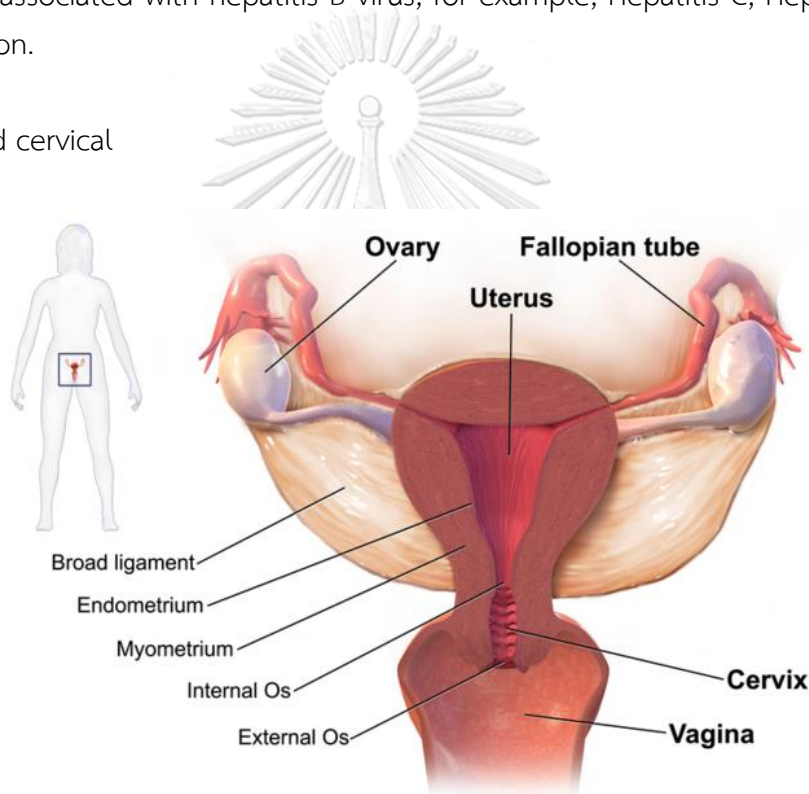


Figure 10 Anatomy of uterus and cervical

(<https://courses.lumenlearning.com/boundless-ap/chapter/the-female-reproductive-system/>)

The uterus is an organ that is composed of muscles as its thick wall. The organ is the location for raising a baby during pregnancy. Its length is 7.62 cm and the shape is similar to a pear or rose apple with a diameter of around 6.35-7.62 cm; the top is a diameter of 2.54 cm. During pregnancy, the uterus will expand. It consists of

two parts: the body and cervix, and the joint of the two parts is called the isthmus. The cervix is a lower part of uterus usually 2-3 cm long. The cervical canal is a passage through which sperm after sexual intercourse. Anatomy of cervical canal is a line with single layer of column epithelial cell. Infection with human papillomavirus can cause change morphology of epithelial, which lead to cancer of the cervix.

### Cervical cancer

Cervical cancer is a type of cancer that occurs at the uterine cervix. It stems from the abnormality of cell growth spreading to nearby tissues. At first, there are no signs. The frequent symptom found is unusual bleeding, pelvic pain, or pain during sexual intercourse, but sometimes there is no sign until the cancer invades many areas. Most treatments require surgery in the initial stage and use chemotherapy/radiation in a later stage.

The causes of cervical cancer consist of many factors; for example, sexual intercourse at a young age, having many children, and have a medical history of venereal disease. From the statistics and research, cervical cancer is associated with 70% of the cases of (HPV),

### Angiogenesis

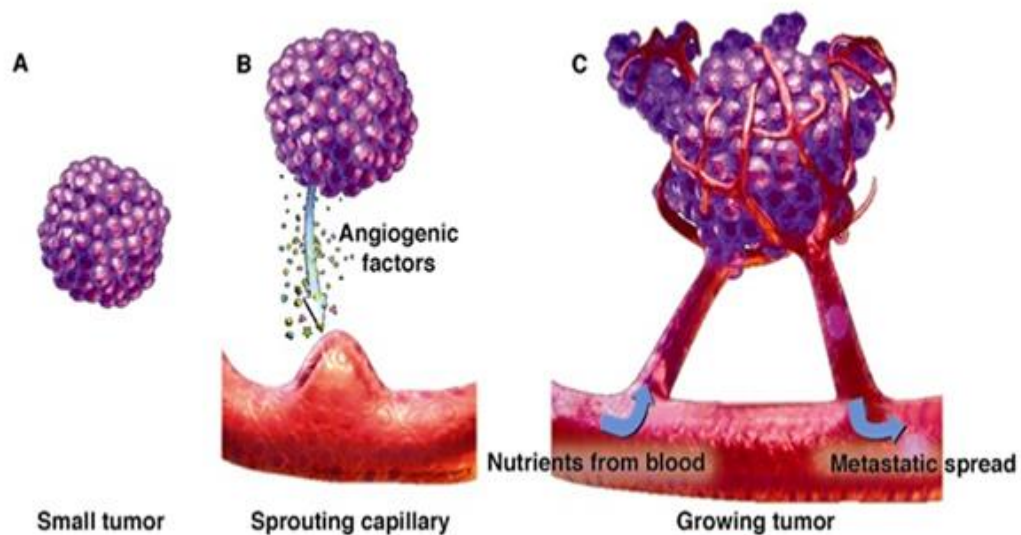


Figure 11. Angiogenesis

(<https://peoplebeatingcancer.org/toxicnon-toxic-anti-angiogenesis-drugs-and-cancer/>)

Angiogenesis is the process of growing new blood vessels in the body. Normally, angiogenesis will occur when the body needs a new capillary in the area that lacks it, in an injured area to replace a lost one, or when the body needs it in special circumstances. The process is stimulated by a growth factor such as vascular endothelial growth factor (VEGF). This growth factor will divide the existing blood vessels into new ones to carry nutrients in order to nurture the cells. In the cancer cells, angiogenesis can often be specifically found because the mechanism of cancers is cell division, resulting in an increased need for nutrients. Moreover, it requires the circulatory system to eliminate waste resulting from the metabolism in the cells. As was found, the cancer cells create more VEGF when there is a lack of cancer cells with a diameter of more than  $2\text{ mm}^2$ . The result is that, after the release of the growth factor, the blood vessels will nurture the cancer cells more. Frequently, the cancer cells can diffuse to other organs through the blood circulation system when there are the vessels that nurture the cancer tumour. In consequence, the other approach of cancer treatment is to resist the angiogenesis by cutting off the transport of nutrients to the cancer cells and delay their growth. Additionally, this method reduces the chance of diffusion to other organs. The resistance methods are, for example, the use of antibodies to block the growth factor such as VEGF in order to avoid stimulating the creation of new blood vessels, the use of medications such as Bevacizumab (Avastin®) and Sunitinib (Sutent®), or the development of substances that can reduce VEGF in the cancer cells by using flavonoids.

### Micelle

The micelle is a nanoparticle of the amphiphilic molecule in the aqueous solution, which consists of two parts. In water, the outer part is always in contact with the solvent while the other part creates the hydraulic tails in the interior. The amphiphilic molecule is a single particle with its surface facing water and air. When adding the amphiphilic molecule in water at a concentration level, it is called a critical micelle concentration (CMC) that makes the molecules form into shapes. The concentration of the micelle depends on two factors, which are the CMC and temperature. The size and shape of a micelle depend on the type of compound and the concentration. Furthermore, the micelle's part that is attached to water will

cause hollows on the interior while the part that dislikes water will be the outer shell, which is called an inverse micelle.

The amphiphilic molecule is mostly used to reduce surface tension and polymer. The surfactants can be divided into four types, which are anionic: carboxylates, sulfonates, and sulfates; cationic head groups: amines, quaternary ammonium halide, and pyridine groups; nonionic: polysorbates and sorbitan, and zwitterionic surfactants: lectins and cephalins.

Polymeric micelles are amphiphilic block copolymers. These polymers can carry their self (self-assembly) when using the suitable medium and the concentration is more intense than the CMC. The amphiphilic molecules are spontaneously self-assembled into supramolecular core/shell structures, and water insoluble drugs can be loaded into the hydrophobic cores. Most of them are circular particles with a size of 10-100 nanometers. When comparing micelles from polymers and micelles from a surfactant, it was found that the polymeric micelles had greater thermodynamic and kinetic durability than the micelles from the surfactants.

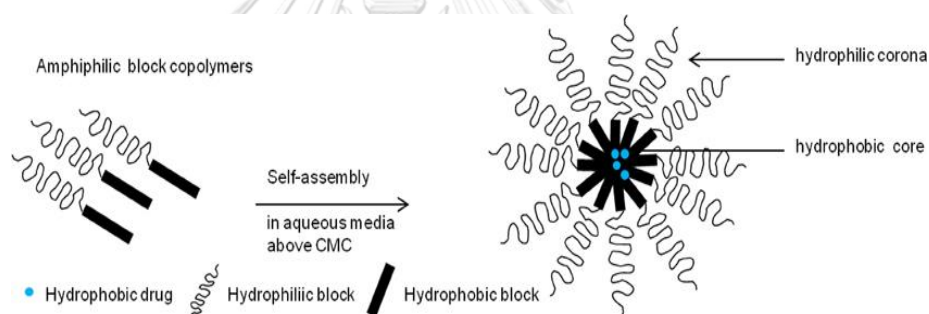


Figure 12. Micelle structure.

([https://www.researchgate.net/publication/262055716\\_Multifunctional\\_polymeric\\_micelles\\_for\\_delivery\\_of\\_drugs\\_and\\_siRNA](https://www.researchgate.net/publication/262055716_Multifunctional_polymeric_micelles_for_delivery_of_drugs_and_siRNA))

The ability of the polymeric micelles relates to the solubility of the medicine due to the interaction of the water insoluble part. Apart from the ability to increase the solubility of medicine, the use of amphiphilic block copolymers will enhance the consistency of medicine in blood that affects the efficiency of the treatment. Generally, polymeric micelles have the appropriate size to avoid the excretion system in the body (>50kDa), and they can penetrate the cell's wall (<200 nm). The selected polymeric in the preparation of polymeric micelles should have degradability to the body's tissues. It is mostly applied to prepare polymeric micelles, both block copolymer (di, tri, or tetra) and graft copolymer, which have a hydrophilic segment and water insoluble part. It is composed of a major polymer;

such as, lines and connecting polymer. For the hydrophilic segment, there is polyethylene glycol (PEG), poly (N-vinyl-2-pyrrolidone (PVP), poly (ethylene oxide) (PEO), polyelectrolyte, and chitosan. For the water insoluble segment, there is poly (L-amino acid): poly(L-aspartate) and poly(L-glutamate); polyester group: poly (glycolic acid), poly (D-lactic acid), poly (D, L-lactic acid), a copolymer of lactide/glycolide, and poly-  $\gamma$  -caprolactone.

Table 3. Sample of block copolymers used to prepare polymeric micelles

Type of polymer	Structure	example
Block co polymer	AAAAAABBBBBB (di-block copolymer)	Poly(styrene)-b-poly(ethylene oxide)
	AAAABBBBBAAAA (tri-block copolymer)	Poly(ethylene)-b-poly(propylene oxide) b-poly(ethylene)
Graft co polymer	AAAAAAAAAAAA B B B B B B B B B B B B	M-phthaloylchitosan-g-polycaprolacton

A= Hydrophilic unit; B=hydrophobic unit

#### Preparation of a polymeric micelle

##### 1. Direct dissolution

For dissolving polymer and medicine in the solution, this method needs a soluble polymer and medicine. The medicine's molecule will aggregate and be entrapped in the micelles due to the temperature and mixture force. However, the disadvantage is the micelle can entrap medicine in a small proportion.

##### 2. Dialysis

The preparation requires mixing the polymer in the solution. The selected solution must be soluble to medicine and polymer, then mix the medicine and polymer in the dialysis package and dip the solution for the hydrophilic segment of the polymer to dissolve the organic substance in the package. When the organic substance exits the dialysis package, the water will be replaced while the micelles will carry the medicine.

### 3. Thin film hydration

This method is suitable for a copolymer that is able to be slightly dissolved in water. This preparation will mix polymer in the organic solution and wait for the evaporation to produce a thin film. Then water and sound waves are added to reduce the size and produce the micelles. The advantage is it can entrap medicines in large quantities, but the disadvantage is using it with only a low HLB polymer.

### 4. Freeze-drying

Medicine and polymer are dissolved in the solution that is mixed with water and an organic solution; such as, water/tert-butanol then the water is evaporated until receiving the powdered mixture of water and polymer. The production of the micelles is after adding the water or buffer in the powdered medicine; however, one problem is the organic solvent remains in the powder.

### 5. Microphase separation

Medicine and polymer are dissolved in a volatile water-miscible solvent; such as, tetrahydrofuran (THF). The solvent is placed drop by drop in the water under the magnetic stirring machine whereby the micelles will be formed. Pressure will be used to evaporate the organic solvent. The problem is the organic solution may remain.

### 6. Oil in water emulsion

Organic-water solvent; such as, dichloromethane or chloroform are added in the water that contains the copolymer. Then, it is stirred slowly until causing the emulsion solvent. After evaporation, the products will be the micelles. The problem of this solvent is evaporation. Mix the medicine and polymer in the organic solution or the mixture of the organic solvent before rapidly adding water. Evaporate the organic solution slowly for two to 24 hours until it produces micelles.

## Poloxamer

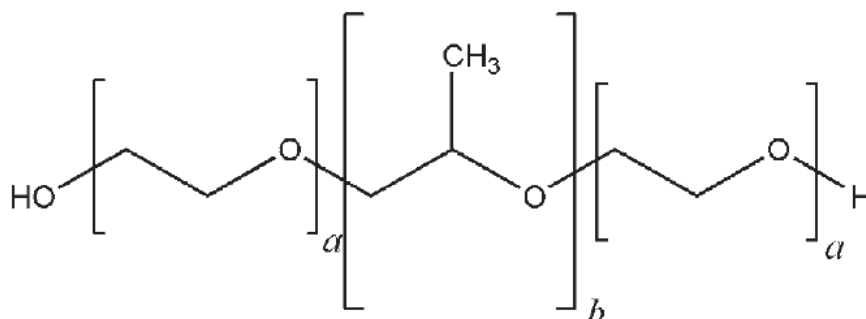


Figure 13. Poloxamer structure formula.

### Nonproprietary Names

BP: Poloxamers

PhEur: Poloxamers

USP-NF: Poloxamer

### Synonyms

Lutrol; Monolan; Pluronic; poloxalkol; poloxamera; polyethylene-propylene glycol copolymer; polyoxyethylene-polyoxypropylene copolymer; Supronic; Synperonic  
Chemical Name and CAS Registry Number a-Hydro-o-hydroxypoly(oxyethylene) poly(oxypropylene) poly-(oxyethylene) block copolymer [9003-11-6]

Simple formula:  $\text{HO}(\text{C}_2\text{H}_4\text{O})_a(\text{C}_3\text{H}_6\text{O})_b(\text{C}_2\text{H}_4\text{O})_a$

Table 4. Types of poloxamer.

Poloxamer	Physical form	a	b	Average molecule weight
poloxamer 124	Liquid	12	20	2090-2360
poloxamer 188	Solid	80	27	7680-9510
poloxamer 237	Solid	64	37	6840-8830
poloxamer 338	Solid	141	44	12700-17400
poloxamer 407	Solid	101	56	9840-14600

### Pharmaceutical benefits

Poloxamers are polyoxyethylene–polyoxypropylene nonionic copolymers. They contain two segments, which are the polyoxyethylene hydraulic segment and polyoxypropylene non-hydraulic segment. The entire structure is similar, but the difference is the molecular mass.

Table 5. Solubility of poloxamer in a different solvents at 20 °C.

Solubility at 20 °C for various types of poloxamer in different solvents.					
Type	Solvent				
	Ethanol 95%	Propan-2-ol	Propylene glycol	Water	Xylene
poloxamer 124	Freely soluble	Freely soluble	Freely soluble	Freely soluble	Freely soluble
poloxamer 188	Freely soluble	-	-	Freely soluble	-
poloxamer 237	Freely soluble	Sparingly soluble	-	Freely soluble	Sparingly soluble
poloxamer 338	Freely soluble	-	Sparingly soluble	Freely soluble	-
poloxamer 407	Freely soluble	Freely soluble	-	Freely soluble	-

### Poloxamer 407

Its composition includes ethylene oxide (EO) and propylene oxide (PO). The arrangement of the polymer is a triblock (EO x -PO y -EO x). The formula is as follows: HO[CH<sub>2</sub>-CH<sub>2</sub>O] x [CH(CH<sub>3</sub>)-CH<sub>2</sub>O] y [CH<sub>2</sub>-CH<sub>2</sub>O] x OH. Nowadays, the registered trademark is called Pluronic F127® (BASF laboratories, Wyandotte, USA) and Synperonic F127® (ICI laboratories, Wilton, UK). The mass of molecules is approximately 9,840 – 14,600 kDa. The Foods and Drugs Organization (FDA) of the USA suggests using the pharmaceutical products type IV, inhalation, oral solution, suspension, ophthalmic, and topical formulations.

The solution of poloxamer 407 has the ability as a gel that can transform into a liquid when receiving heat (thermoreversible). It will melt when the temperature rises and changes its status as a compound called sol-gel transition temperature. In other words, if the surrounding temperature is higher than the

solution, it will change to a liquid gel, but if the temperature is lower, the substance will return to its original form. Thus, the mechanism depends on the temperature. When the temperature continues to increase, polypropylene oxide will turn to the non-polar side and polyethylene oxide will turn to the polar side and become a gel. The shape of the micelles depends on the solution used (figure14).

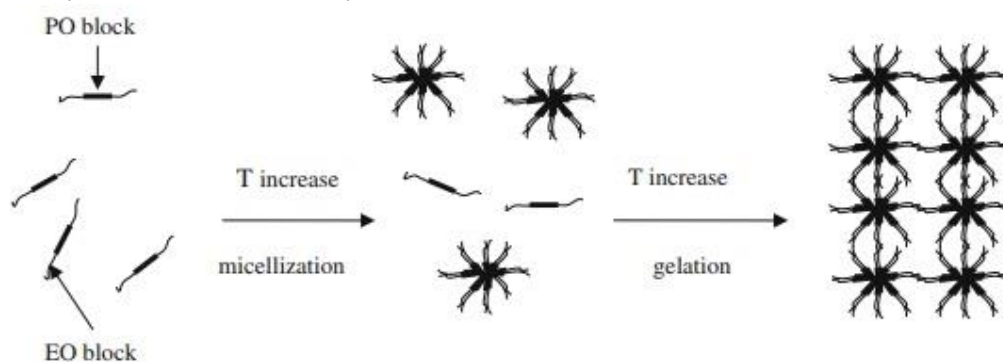


Figure 14. Thermoreversible property of poloxamer 407.

Due to its aforementioned qualifications, various usages exist; example, in the medical industry; as a degradable polymer that attaches to the body's tissues, it is not toxic and can be eliminated from the body. On the other hand, a report found that poloxamer 407 may interact with other compounds; such as, solvents and other polymers. Therefore, it always requires caution in usage.

Pharmaceutical benefits

Antitumor drugs delivery

Poloxamer block copolymers for overcoming drug resistance in cancer were studied where a compound mixed with poloxamer 407 and D- $\alpha$ -Tocopheryl polyethylene glycol 1000 succinate (TPGS) was used to produce micelles as a means to boost the efficiency of the treatment by increasing the concentration of medicine to the cancer cells and resisting P-glycoprotein (P-gp) (Kabanov, Batrakova and Alakhov, 2002). Explained the new method in applying Pluronics® in the treatment of multidrug-resistant cancer, and they discovered that Pluronics® was able to interact with multidrug-resistant cancer. The cancer cell would be severely allergic owing to the compounds of the anticancer medicine, especially anthracycline antibiotics.

Amiji et al. (Amiji et al., 2002) examined the intratumoral administration of paclitaxel in an in situ gelling poloxamer 407 formulation and reported significant

enhancement in the anti-tumor efficacy. The initial tumor growth rate was delayed by 67% and the tumor volume doubling time was increased by 72% relative to saline control. In addition, more than 91% of the tumor-bearing animals that received paclitaxel in poloxamer 407 gel survived on day 15 post-administration as compared to 58% in the control group. The results of this study show significant benefit of paclitaxel for solid tumor when administered locally in an in situ gelling poloxamer 407 formulation. Moreover, they demonstrated that Poloxamer 407 solution undergoes a reversible sol-gel transition when the temperature is raised to above 21°C. In vitro paclitaxel release from poloxamer 407 gels was very slow (only 6.1% after 6 hr) probably due to the poor aqueous solubility of the drug. In another report, enhanced in vitro cytotoxicity and anti-tumor activity of vorinostat-loaded poloxamer micelles with prolonged release and reduced hepatic and renal toxicities were reported (Mohamed et al., 2017). In other studies, Pluronic® mixed micelles were efficient nanocarriers for benzoporphyrin derivatives applied to photodynamic therapy in cancer cells (Pellosi et al., 2016), while others used targeted Pluronic® P123/F127 mixed micelles (PMM) delivering niclosamide (NCL) as a repositioning strategy to treat multidrug resistant non-small lung cancer cell lines (Russo et al., 2016).

## CHAPTER III

### MATERIALS AND METHODS

#### Materials

1. Standard material
  - Isoquercitrin (90%), Lot.no BCBT7495, Sigma.
  - Quercetrin (95%), Lot.no STBH046, Sigma.
  - Rutin (94%), Lot.no BCBV4040, Sigma.
  - Gallic acid (97.5%), Lot.no SLB4564, Sigma.
  - Glucose (98%), Lot.no MO13176, Sigma.
  - Cisplatin, Lot.no LRAA8271, Sigma.
  - Caffeine, Lot.no 061M0052V, Sigma.
2. Cell culture reagent
  - Dulbecco's Modified Eagle Medium (DMEM), Biowest, Franch.
  - Roswell Park Memorial Institute (RPMI) 1640, Biowest, Franch.
  - Fetal bovine serum (FBS), Gibco, Thermofisher, US.
  - Glutamax, Gibco, Thermofisher, US.
  - Antibiotic-antimycotic, Gibco, Thermofisher, US.
  - Trypsin, Gibco, Thermofisher, US.
  - Prestobblue reagent, Thermofisher, US.
  - Matrigel matrix: Lot.no 7121011, corning.
  - Crystal violet biological stain, Lot.no MKCB9878, Sigma.
  - Dimethyl sulfoxide (DMSO), Lot.no 1596C189, Armesco.
  - AnnexinV-7AAD cocktail, Lot.no 3045559, Merck Millipore.
  - VEGF Elisa kit, Lot.no GR3197296-1, Abcam.
3. Chemical reagent
  - Folin-Ciocalteu reagent, OC546658, Merck millipore.
  - Poloxamer 407 suitable for cell culture Lot.no. SLBM9355V, Sigma.
  - DPPH: Lot.no 3041739, Merck millipore.
  - ABTS: Lot.no 3118667, Merck millipore.
  - Acetonitrile HPLC grade, Honey well.
  - Methanol HPLC grade, Honey well.
  - Hexane AR grade, Honey well.

- Dichloromethane HPLC grade, Honey well.
- 95%ethanol.
- NaOH.
- Ferric chloride, Lot.no BCBP2118V, Sigma.
- Hydrochloric acid, Lot.no MMBB4057, Honey well.
- $\alpha$  naphthol blue.
- Gelatin, Lot.no 56H0130, Sigma.
- 90% Phenol Merck Millipore.
- Aluminium chloride, Lot.no 1854491, Fisher scientific.
- Sodium carbonate, Lot.no A1017792626, Merck millipore.
- Potassium acetate.
- Acetic acid.
- Potassium persulfate, Lot.no BCB0478V, Sigma.

#### 4. Analytical instrument

- HPLC shimadzu, Diode array detector SPD-M20A, Auto sampler SIL-20A HT, Communication CBM-20Alite, Column oven CTO-10AS VP, Degassing Unit DGU-20A 5R,  
Liquid Chromatography LC-20A.
- HPLC column C18, Length 250mm, particle size 5 $\mu$ m, Kinetex, Phenomenex.
- Fourier transform infared (FTIR), Thermo scientific, Nicolet iS5, US.
- Freeze dryer: LCC-1-7382020, Labconco, US.
- Microplate reader, carioStar, BMG Labtech, Germany.
- Flow cytometry, Guava easycyte HT system, Merck Millipore.
- UV visible spectrophotometry, U-2900, Hitachi, Japan.
- Inverted microscope, Olympus IX51, Japan.
- Dunouy ring tensiometer, Krüss, Germany.
- Differential scanning calorimeter, Model DSC 822e, Mettler Toledo., Germany.
- Photon correlation spectrometer (Zetasizer Nano ZS), Malvern Instruments, UK.
- 24-well plate, 96 well plate, corning, US.
- 8.0  $\mu$ m 24-well cell culture insert, Falcon, US.

## Method

### 1. Extraction of Okra seed

Okra pods were purchased from the Pathom Mongkol market in Nakhon Pathom province, Thailand. The seeds were separated from its fruit before maceration with 95% ethanol for 24 hrs. before filtering through Whatman No. 4 filter paper. The extracted solution was evaporated by solvent evaporator at 50 °C and then lyophilization until it was dry. The dry Okra seed extract was stored at -20°C and protect from light. Isoquercitrin content was determined in the extract every 6 months.

### 2. Separation of Okra seed extraction

The separation was carried out using liquid partitioning method. The compounds in the extract become separated by their polarity into three groups; non-polar, semi-polar and polar group.

Group 1: OSE-Hex, The Okra seed extract (OSE) was partitioned with hexane:ethanol:water in ratio 50:45:5. The hexane layer was evaporated and lyophilized to collect the non-polar fraction.

Group 2: OSE-DCM, the ethanol layer was further partitioned with dichloromethane:ethanol:water in ratio 50:30:20. The dichloromethane layer was evaporated and lyophilized to collect the semi-polar fraction.

Group 3: OSE-EtOH, the ethanol from OSE-DCM was evaporated and lyophilized to collect the polar fraction.

### 3. Basic phytochemical composition test

To study basic phytochemical compositions of the crude and all of the extract fractions (crude, OSE-Hex, OSE-DCM, and OSE-EtOH), the following tests were conducted to find compounds such as phenolic, flavonoid, glycoside, alkaloid, tannin, and saponin.

#### 3.1 Ferric chloride test

To test a phenolic compound; for examples, flavonoid, tannin, and coumarin; the chemical reaction between phenolic group and ferric chloride produces a complex compound which leads to a dark-blue precipitate. The method is to add one-two drops of the ferric chloride reagent in the tube containing the extract. If the extract contains a phenolic compound, it will cause a dark-blue or black precipitate.

### 3.2 Shinoda test

The reaction to test the structure of the gamma-benzopyrone ring of the flavonoid with the reduction reaction of magnesium and HCl showed a positive change regarding the color of the flavonoid compound changing to red or reddish-purple. The extract was dissolved in 95% of ethanol and 2 ml of the dissolved extract was added in the magnesium ribbon.

### 3.3 Sodium hydroxide test

The sample extract was dropped on the filter paper two to three times. In decreasing 10% of NaOH, the flavonoid would change to yellow. Halcon, and under the wavelength of 365 nm, green, blue and yellow fluorescence could be seen.

### 3.4 Molisch test

To examine if the extract is composed of glycosides or not, the test checked glycosides that links to the structure. A positive result demonstrates a ring around the joints with HCl, but when the quantity of the glycoside is high, the sulfuric layer should become entirely purple. The extract was dissolved in 95% of ethanol and used only 2 ml of the dissolved extract. Five percent of  $\alpha$  naphthol blue was dropped four-five times and shaken to mix them. Then 1-2 ml of the intensive sulfuric solvent was added to the laboratory tube, and the change between the liquid layers could be seen.

### 3.5 Gelatin solution test

This test examines the presence of tannins, a non-crystallized substance displaying colloidal dispersion. The gelatin could produce a complex compound with tannin and cause precipitation without solubility. Two percent of gelatin solution was added two to three times on the sample extract to see if it would precipitate.

### 3.6 Dragendorff's test

Alkaloids are organic compounds, where their base effect stems from the nitrogen that stays in the molecules. Alkaloids can be precipitated in some agents; such as, Dragendorff's reagent. Dragendorff's reagent was dropped on the extract. In the presence of an alkaloid, a reddish-brown precipitation will persist.

### 3.7 Foam test

Saponin is a substance that produces bubbles with the shape of an hexagon consistently. Saponin toxicity will cause hemolysis. The foam test starts by shaking the extract with water. If saponin is present, stable hexagonal shape bubbles will appear.

## 4. Characterization of the Okra seed extract

### 4.1 Thin layer chromatography

The Okra seed extract and the standard were marked on the thin layer chromatography (TLC) using the mobile phase (ethyl acetate: methanol: formic acid; 7:2.5:0.5) to make a segment then the reagent was sprayed on the extract. It was then examined under UV wavelengths of 254 nm and 365 nm to confirm the fingerprint of the extract.

Prepared as follows:

#### 4.1.1. NP/PEG reagent spray

Prepare the 1% diphenylboryloxyethylamine (NP) in methanol and the 5% PEG 4000 in ethanol, then spray TLC with the NP reagent and then spray with the PEG reagent to increase sensitivity.

#### 4.1.2. Ferric chloride reagent

Prepare the 5% ferric chlorides in ethanol, and then spray this on TLC to detect the substance in the phenolic compounds.

#### 4.1.3. Aluminium chloride reagent

Spray the 1% aluminium chloride ( $\text{AlCl}_3$ ) on TLC to detect the flavonoid compounds under the wavelength of 366 nm

#### 4.1.4. DPPH spray reagent

Dissolve DPPH in methanol until the concentration is 0.2%, then spray it on TLC. With the extract that contains antioxidant, a white circle around the substance will appear under the visible light.

#### 4.2 High performance liquid chromatography

HPLC-DAD was used to analyze isoquercitrin content in the Okra seed extract (Seal, 2016). The analysis was carried out with HPLC column 250 mm (Kinetex) and gradient injection using the mobile phase of 1% of acetic acid (solvent A): acetonitrile (solvent B), flow rate 0.7 mL/min at wavelength 353 nm; Linearity, accuracy, limit of detection (LOD), and limit of quantification (LOQ) were applied to ensure the validity of the analysis method

Table 6. Gradient condition for HPLC analysis of the Okra seed extract.

Time(min)	Pump A: 1%Acetic acid	Pump B: Acetonitrile
0	90	10
28	60	40
39	40	60
50	10	90
55	90	10

#### 4.3 Fourier transform infrared spectroscopy

The reason for using the Fourier transform infrared spectroscopy (FTIR) was our substance's glutinous nature. The ATR probe is applied to test the IR spectrum as one of the general quality controls of the extract in accordance with pharmacopeia standards, using the IR spectrum fingerprint to resist the other extracts in order to receive the same type of substance at a wavelength between 500 to 4,000 cm<sup>-1</sup>.

#### 4.4 Differential scanning calorimetry

The thermal properties of the extract were determined by differential scanning calorimetry (DSC). The DSC scans of the Okra seed extract using an empty aluminum pan served as reference. Dry nitrogen gas was used as the purge gas through a DSC cell at a flow rate of 40 mL/min and heated at a rate of 10 °K/min from -10 to 300 °C.

### 5. Quantitative analysis of the phytochemical composition

#### 5.1 Total phenolic content

Total phenolic contents (TP) in different seed extracts of Okra seeds were determined using a modified Folin-Ciocalteu (FC) colorimetric method (Stankovic, 2011, Fernandes et al., 2017, Mendez-Lagunas et al., 2017). In short, 25 µL of the extract was mixed with 75 µL deionized water in 96 well-plates, then 1:1 FC reagent

was added and incubated in the dark for 6 minutes. Following this, 100  $\mu\text{l}$  of 7.5%  $\text{Na}_2\text{CO}_3$  was added and the solution was incubated in the dark for another 90 min. The phenolic content is then measured using a microplate reader at 765 nm wavelength carried out using a standard solution of gallic acid, reported as gallic acid equivalents (GAE)/gram dry weight extract.

### 5.2. Total flavonoid content

The test uses the  $\text{AlCl}_3$  reaction with the ketone (C-4) at ring C and -OH group, or C-5 at the ring (Stankovic et al., 2011, Sharma et al., 2015)

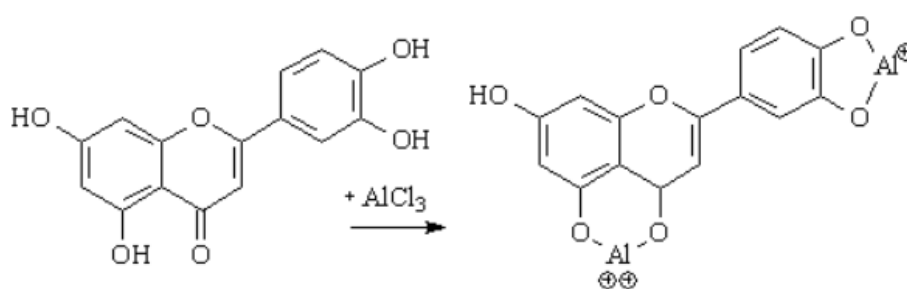


Figure 15. Complex reaction between flavonoid and aluminum salt.

The total flavonoid content (TF) was determined spectro-photometrically. A sample extract of 20  $\mu\text{l}$  was mixed with 60  $\mu\text{l}$  ethanol in 96 well-plates. Then, 4  $\mu\text{l}$  of 10%  $\text{AlCl}_3$  and 4  $\mu\text{l}$  of 1M potassium acetate were added with 112  $\mu\text{l}$  deionized water. The solution was incubated in the dark for 45 minutes. The total flavonoid content was measured afterwards using a microplate reader at 415 nm wavelength. A calibration curve is prepared using a standard solution of quercetin, reported as quercetin equivalents (QE)/gram dry weight extract.

### 5.3. Total sugar content

The total polysaccharide (TPS) content was determined with phenol–sulfuric acid method modified from the method of Masuko et al. (Masuko et al., 2005) . In brief, 600  $\mu\text{l}$  of extract were mixed with 100  $\mu\text{l}$  of 5% phenol solution. Then, 3 ml of concentrated sulfuric was added and left for 10 minutes. Following this step, the solution was shaken well and left for 30 minutes. The TPS content was measured using UV-spectrophotometry at 490 nm wavelength compared with a standard curve obtained from the glucose standard.

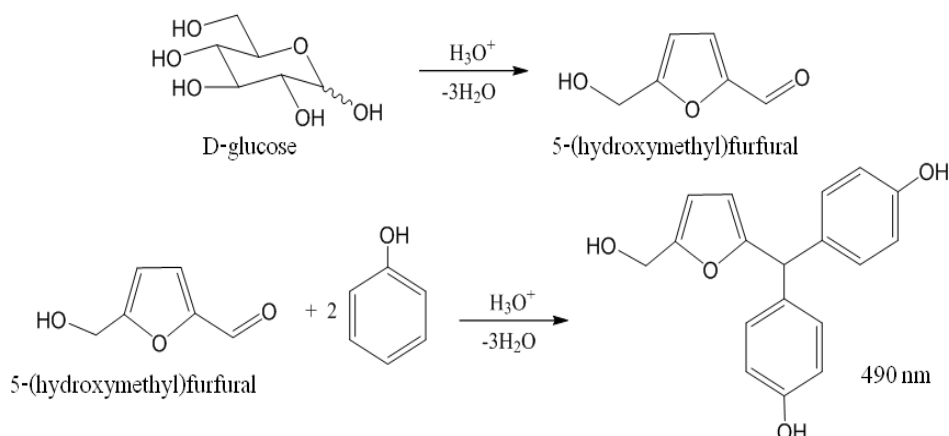


Figure 16. Chemical reaction of phenol-sulfuric assay

#### 5.4 2, 2-diphenyl-1-picrylhydrazyl (DPPH) assay

The assay is initiated with the preparation of the 0.1 mM DPPH solution. Proceed by dissolving 1.97 mg of DPPH in 50 ml methanol, then test the antioxidation by using a pipette. Add 100  $\mu$ l of the sample solution into 96 well plates and add DPPH to the 100  $\mu$ l. Incubate in the darkness for 30 minutes at room temperature before testing with the microplate reader with a wavelength of 520 nm. If the extract contains antioxidation, the purple colour will change to yellow.

%Inhibition was calculated following the equation =  $\left( \frac{\text{Abs}_{\text{Control}} - \text{Abs}_{\text{sample}}}{\text{Abs}_{\text{control}}} \right)$ .

#### 5.5 2,2'-azino-bis(3-ethylbenzothiazoline-6-sulphonic acid) (ABTS) assay

Prepare the 14 mM ABTS solution by dissolving exactly 360.23 mg of ABTS in the water and adjust the volume until 50 ml. Dissolve potassium persulfate 66.23 mg in water and adjust the volume until it reaches 50 ml in order to prepare the potassium persulfate solution with the concentration 4.9 mM. Mix the two solutions at the ratio of 1:1, then incubate under the darkness for 16 hours until it produces the  $\text{ABTS}^+$  radicals when the solution becomes green. Dilute the solution with methanol at the ratio of 1:50. Measure the absorbance to determine if it remains at 0.1 - 0.7. After determining the concentration of the  $\text{ABTS}^+$  solution, add 100  $\mu$ l of the seed extract into 96 well plates, then add 100  $\mu$ l of the  $\text{ABTS}^+$  solution before incubating for 6 minutes at room temperature. Then, use the microplate reader with a wavelength of 734 nm to determine antioxidation activity.

%Inhibition was calculated following the equation =  $\left( \frac{\text{Abs}_{\text{Control}} - \text{Abs}_{\text{sample}}}{\text{Abs}_{\text{control}}} \right)$ .

## 6. *In vitro* study

### 6.1 Cell culture study

The cancer cells were cultured under a temperature of 37°C and 5% CO<sub>2</sub>. The culture medium was changed every three days and trypsinized with 0.25% trypsin and 0.04% EDTA solution.

Breast cancer cells (MCF-7), were cultured using DMEM culture medium, 10% of fetal bovine serum, 1% of antibiotic-antimycotic, 1% glutamax.

Hepatocellular carcinoma (HepG2) cells, were cultured using RPMI1640 culture medium, 10% of fetal bovine serum, 1% of antibiotic-antimycotic, 1% glutamax.

Cervical cancer (HeLa) cells, were cultured using DMEM culture medium, 10% of fetal bovine serum, 1% of antibiotic-antimycotic.

Human keratinocytes, were cultured using DMEM culture medium, 10% of fetal bovine serum, 1% of antibiotic-antimycotic.

### 6.2 Anticancer activity

All of the extract fractions (OSE-Hex, OSE-DCM and OSE-EtOH) and crude extract would be tested for their anticancer effect at different concentration levels in order to evaluate which composition was most active.. Cisplatin was used as the positive control, and analyzed with the PrestoBlue assay. When resazurin penetrates a living cell, it will be changed by the enzyme's reductase in the mitochondria and become pink (resorufin) which is soluble outside the cell (Zhang, Du and Zhang, 2004, Wang et al., 2011).

The experiment can be summarized into two steps as follows:

6.2.1 Conduct the partition to divide the 100 mg of the Okra seed extract (crude) before evaporation and lyophilization. In every fraction, add the cell culture medium (final conc. 1% DMSO in medium) in equal quantities to test if any extract of all fractions has the anticancer activity. Up to 10,000 cells were seeded in each well plate and tested with the extract for 24 and 48 hours, respectively. The anticancer activity was compared for every fraction and the ones with the highest activities were selected for further testing.

Table 7. Methodology for screening anticancer activity each fraction.

Treatment	Drying the Extracts		Adjusting the final volume	
Crude	→	OSE-Hex	→	Anticancer test
	→	OSE-DCM	→	Anticancer test
	→	OSE-EtOH	→	Anticancer test
Crude			→	Anticancer test
Control group (Blank)	→			Anticancer test
Control group (Cisplatin)	→			Anticancer test

### 6.2.2 Study for the dose dependent for anticancer effect

The crude extract (OSE) and OSE-EtOH fraction containing the highest activity from Section 6.2.1 were selected for further evaluation of the most appropriate concentrations to exert the effect for the remaining experiments and compared to pure isoquercitrin on 10,000 cells incubated for 48 hours.

Table 8. Methodology for anticancer screening.

Treatment	48 Hours
Okra seed extract (crude)	Anticancer test
OSE-EtOH	Anticancer test
Isoquercitrin	Anticancer test
Control group (Blank)	Anticancer test
Control group (Cisplatin)	Anticancer test

### 6.3 Migration and invasion assay

#### 6.3.1 Cell scratch assay

Cell scratch assay examines the resistance of a cancer cell's movement by using the crude from the fraction that contains the highest anticancer effect in regard to Section 6.2. Cells at  $1 \times 10^4$  were plated onto 24-well culture plates in complete medium. When the cells had grown to a nearly confluent cell monolayer, a linear wound was made by scratching the center of well with a yellow pipette tip (200  $\mu$ l) followed by washing with PBS. The monolayers were then incubated with complete medium of different concentrations of the Okra seed extract at 37 °C for 24, 48 and 72 hours. The monolayers were photographed at 0 hours and 24 hours after scratching using an inverted microscope (Olympus, Tokyo, Japan) to capture the size of the scratch. The experiments were performed in triplicate for each treatment group. (Li et al., 2012). The gap distance of the wound was measured using the Image J program.

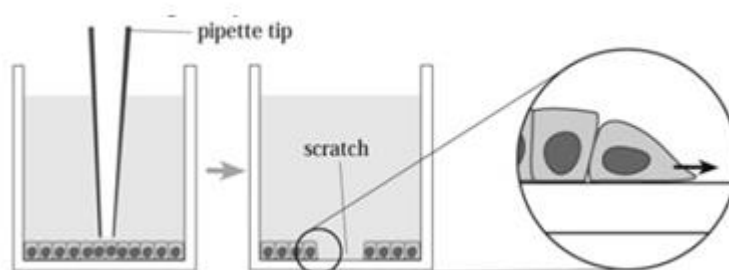


Figure 17. Cells scratch assay.

#### 6.3.2 Transwell invasion assay

This assay studies the movement resistance through small holes in a vertical way. The Boyden chamber migration test was used to study for cell invasion. The 8.0  $\mu$ m PET filters 24-well cell culture inserts (Falcon, USA) were coated with Matrigel (Corning) and incubated for 1 h at 25 °C to form a thin layer on the filter surface. The complete medium was added to the lower compartment of the chamber. After that, the wells on the upper chamber were seeded with  $2 \times 10^4$  cell/well and okra seed extract was added at different concentrations ranging from 25 to 500  $\mu$ g/ml in low (1%) FBS medium. After 48 hours, non-invasive cells were wiped in the upper chamber using a cotton bud, lower and upper chamber were washed three times with PBS pH 7.4, then fixed with 3% glutaraldehyde in PBS and stained with 0.5% crystal violet in PBS. Later, the cells were lysed by using 10 %

acetic acid and the quantity of cells was analyzed by using a micro-plate reader at a wave length of 590 nm.(Li et al., 2012, Xia et al., 2018)

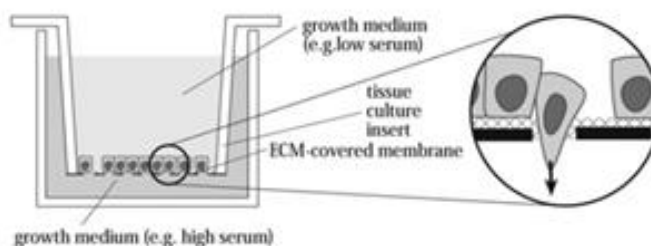


Figure 18. Transwell invasion assay.

#### 6.4 Cytokine assay

Cancer cells were seeded on 12-well plates and incubated for 24 h at 37°C in 5% CO<sub>2</sub>. After that the old medium was washed and okra seed extract was added at different concentrations ranging from 25 to 1,000 µg/ml in medium and incubated for 24 and 48 hours. After that, the supernatant was collected and centrifuged to analyze the quantity of vascular endothelial growth factor (VEGF) by using a sandwich Elisa (VEGF Elisa kit, Abcam, ab100662). The obtained supernatant was placed in a 96-well plate kit according to the company protocol by adding 100 µl of cell culture supernatant into appropriate wells. Cover Wells were covered and incubated for 2.5 hours at room temperature. The solution was discarded and washed 4 times with 1X Wash Solution. 100 µl of 1X Biotinylated VEGF Detection Antibody was added to each well and incubated for 1 hour at room temperature shaken gently. Then the solution was discarded and the wash was repeated 4 times with 1X Wash Solution before adding 100 µl of 1X HRP-Streptavidin solution to each well and incubating for 45 minutes at room temperature. The wash was repeated another 4 times with 1X Wash Solution and 100 µl of TMB One-Step Substrate Reagent was added to each well and Incubated for 30 minutes at room temperature in the dark. After that 50 µl of Stop Solution was added to each well. Finally VEGF was analyzed by using the micro-plate reader at a wave length of 450 nm (Wang et al., 2017, Zang et al., 2017).

#### 6.5 Apoptosis

The cells were cultured in a 6-well cell culture plate at a seeding density of  $1 \times 10^6$  cells/well incubated for 24 hours at 37 °C in 5% CO<sub>2</sub> before treated with the extract. The cells were cultured in a 6-well cell culture plate at a seeding density of

$1 \times 10^6$  cells/well. After the cells were treated with different doses of the Okra seed extract for 48 h, the cells were trypsinized and a single cell suspension was prepared. Then, the cells were stained using Annexin V and 7AAD (Guava Nexin Reagent, Merck Millipore), which were then analyzed by flow cytometry (Guava, Merck Millipore) (Wang and Zhan-Sheng, 2018, Zhang et al., 2018).

## **7. Preparation of the polymeric micelle particles loading the Okra seed extract**

### **7.1 Preparation of the polymeric micelle particles**

For the preparation of the polymeric micelle particles, the thin film hydration technique (Jin et al., 2016, Tima et al., 2017) was used where poloxamer 407 and extract were dissolved in 10 ml of absolute ethanol. After that the solution was put in a round bottom flask and placed in the solvent evaporator for dehydration at 50 °C 100 rpm/min. When the film was dry, deionized water 10 ml was added to produce the micelle particles. After that the micelles were reduced in size by 15-minute sonication. Then, they were filtered through a 0.45 µm syringe filter to eliminate the insoluble extract. The proportion between poloxamer 407 and the Okra seed extract was then compared to select the best formula for the efficiency testing.

### **7.2 Characterization of polymeric micelle**

#### **7.2.1 Physical evaluation**

Evaluate the physical qualification of the particles, review the color, precipitation, and isolation.

#### **7.2.2 Evaluation of the size and ion on the surface of the particle**

Use light scattering to measure the size and zeta-potential, using a Malvern nanosizer to evaluate the particles.

### 7.3 Entrapment efficiency

Assess the quantity of the extract entrapped in the micelle, use the UV-visible spectrometer to analyze the total flavonoid. Bring the particles that were filtered through the 0.45 membrane and add the organic solvent to dissolve the poloxamer 407 and release the entrapped extract. Measure the light absorption with the UV-visible spectrometer at lambda 353 nm.

% Entrapment efficiency was calculated following the equation

$$\left( \frac{\text{Amount extract in micelles} - \text{Amount free extract dissolve DI}}{\text{Initial extract}} \right) \times 100.$$

### 7.4 Anticancer activity of the Okra seed extract loaded in polymeric micelles

Select the best formula from the test data from Sections 7.2 and 7.3 for consideration. Next, test the anticancer effect, the same way as in Sections 7.2 and 7.5 and compare the blank polymeric micelle and the extract that contain in the polymeric micelles. The OSE loaded micelles and blank micelles were compared to each other after dilution with cell culture medium to a concentration comparable with Okra seed extracts of 500 ug/ml.

## 8. Stability test

Prepare the best formula of the polymeric micelles for the lyophilization process, then store in a temperature of 40°C and 4°C for three months. After that, analyze the drug content that remains and the size of the particles comparing to the first day (day 0). Random test every month.

## 9. Statistics analysis

The whole data were demonstrated as mean values  $\pm$  standard deviation (SD), and the statistics for the data analysis is one-way ANOVA and tukey multiple comparison tests with reliability or  $\alpha = 0.05$ .

## CHAPTER IV

### RESULTS AND DISCUSSIONS

#### 1. Preparation of extracts from Okra seed extract

When Okra seeds were macerated with ethanol for 24 hours the extract turned transparent yellow. After solvent evaporation and lyophilization, the extract becomes light yellow crystals. Its physical characteristics are a low melting point, sticky at room temperature, and becomes solid at low temperature. The % Yield crude extract after lyophilization is approximately  $4.27 \pm 0.45$  %.

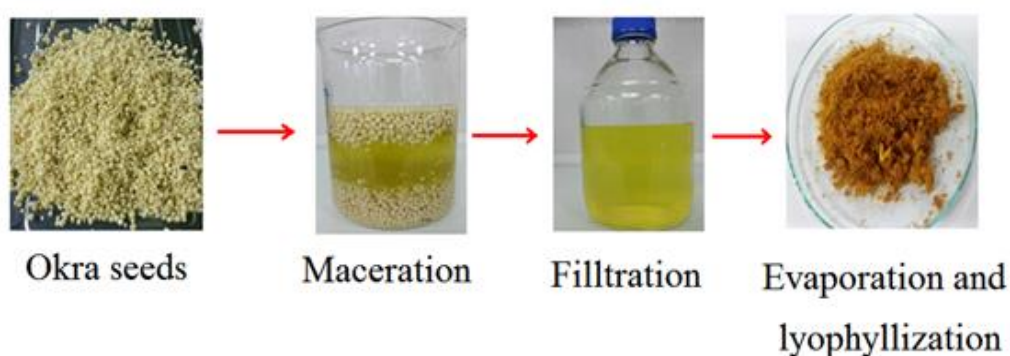


Figure 19 The Okra seed extraction process

The Okra seed extract that has been processed through partition were separated and existed in the ethanol fraction without residue in the hexane and dichloromethane fractions.

## 2. Phytochemical screening

The aim of the present study was to elucidate the phytochemical composition of the Okra seed extract. Moreover, regarding the evaluation of isoquercitrin in the Okra seed, we could not substantiate the presence of it in the hexane and dichloromethane fractions as the partition process did not separate the extract into these two fractions, as they did not contain any of it. For the ethanol fraction and the crude Okra seed extract, using ferric chloride, we observed the same result, i.e. a phenolic compound such as flavonoid or tannin, resulting in dark-blue precipitates as shown in figure20.

Table 9. Phytochemical screening test

	OSE-Hex fraction	OSE-DCM fraction	OSE-EtOH fraction	Okra seed extract
FeCl <sub>3</sub> test – Phenolic	-	-	+	+
Shinoda test - Flavonoids	-	-	+	+
Sodium hydroxide test - Flavonoids	-	-	+	+
Molisch test - Glycosides	-	-	+	+
Dragendorff test - Alkaloids	-	-	-	-
Foam test – Saponins	-	-	-	-
Gelatine test – Tannins	-	-	-	-

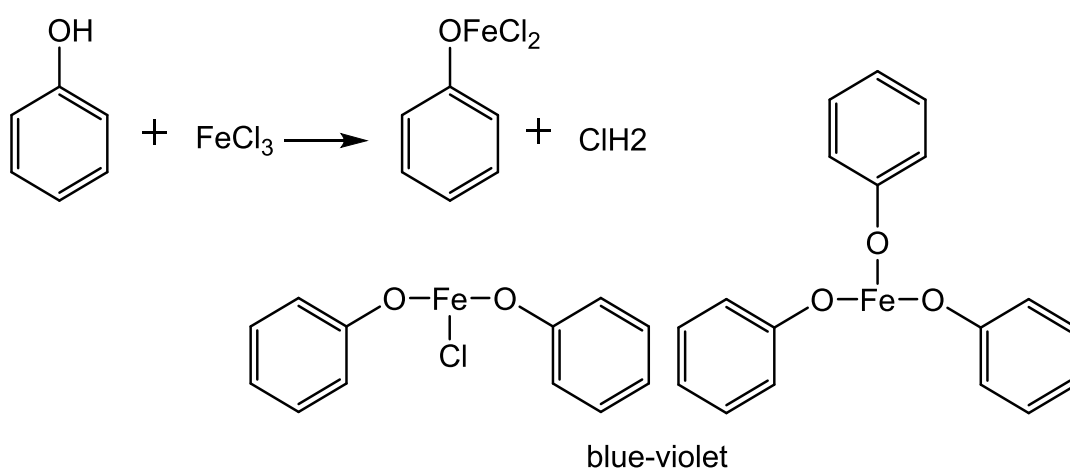


Figure 20. Chemical reaction of ferric chloride and phenol group.

In the same experiment, the crude OSE and the OSE ethanol fraction also produced dark blue precipitate. The next experiment was to test for substances in the flavonoid group. The experiment consisted of two methods: 1. The Shinoda Test using the reduction mechanism of magnesium of a gamma-benzopyrone ring in the flavone structure to produce a red compound (figure21).

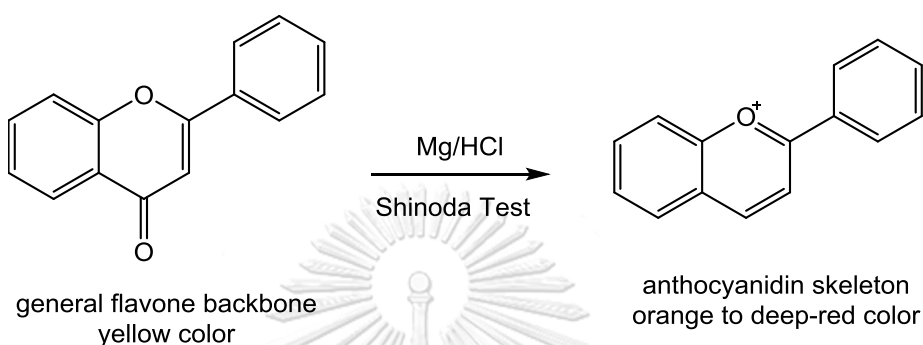


Figure 21. Shinoda reaction.

In the experiment, it was found that only the crude and ethanol fraction give positive results, which was confirmed by Sodium hydroxide test: after dropping the 10% sodium hydroxide and the compound, change to dark yellow (figure22B). Examined under the wavelength of 365 nm, the OSE and OSE ethanol will glow (figure22C).

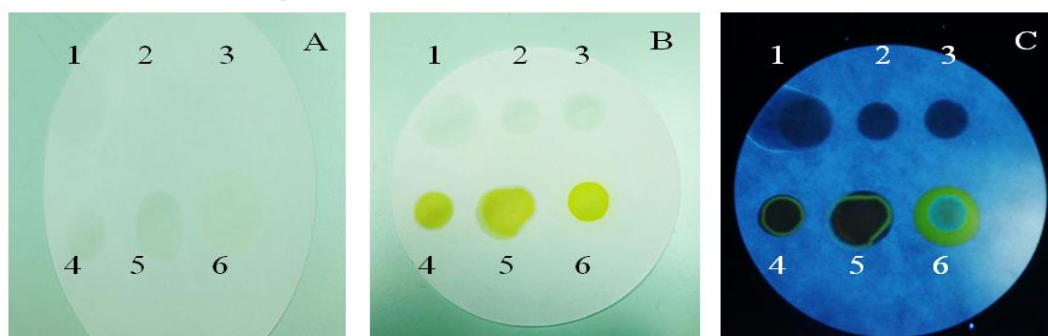


Figure 22. Sodium hydroxide test

(A: Before dropping sodium hydroxide, B: After dropping sodium hydroxide under invisible light, C: After dropping sodium hydroxide under 365 nm; No. 1: Blank, 2: OSE-Hex, 3: OSE-DCM, 4: OSE-EtOH, 5: OSE, 6: Quercetin)

Our experiments confirmed the presence of flavonoid substances in the Okra seed extract. This is in accordance with previous studies confirming the presence of isoquercitrin, which belongs to the flavonoid glycosides, in the Okra seed. A subsequent experiment using the Molisch test was conducted to test the presence of sugars or glycosides in order to confirm the existence of isoquercitrin in the extract. We could confirmed that OSE and OSE-ethanol contain glycosides. However, the results do not indicate the existence of alkaloids, saponins, or tannins in any of the fractions or the Okra seed extract (crude).

### 3. Characterization of the Okra seed extract

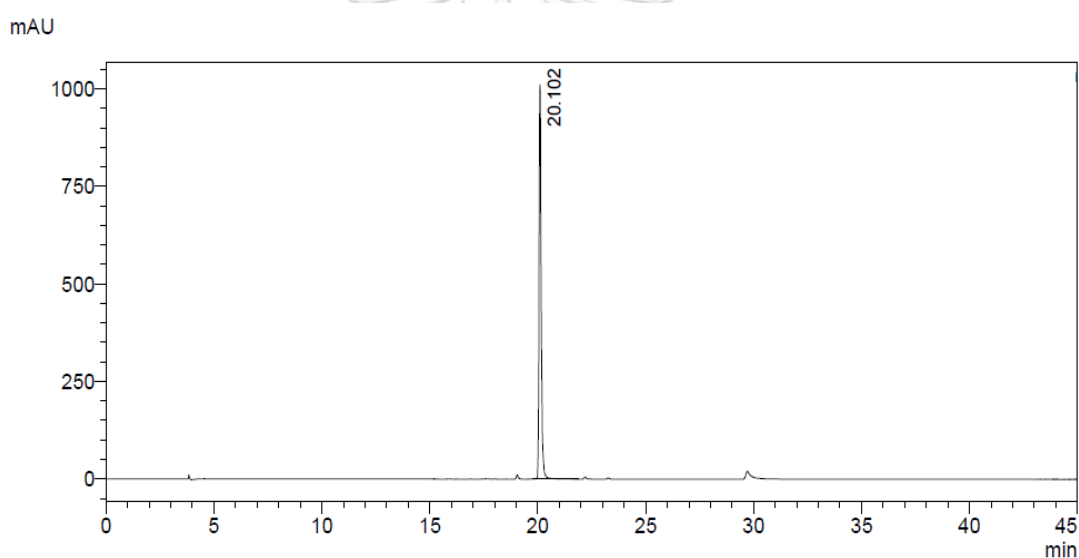


Figure 23. HPLC chromatogram of the standard Isoquercitrin.

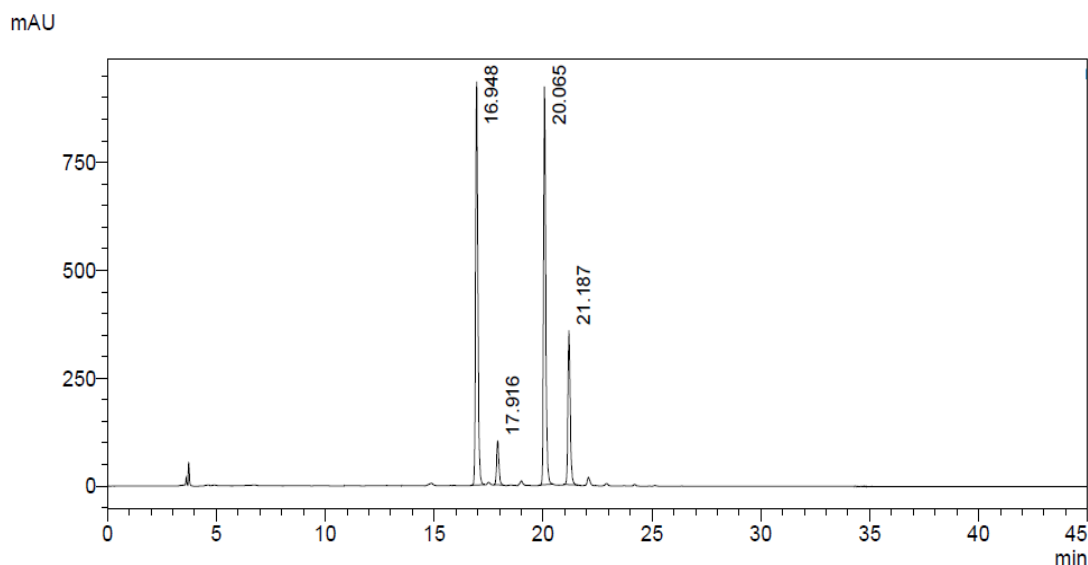


Figure 24. HPLC chromatogram of the Okra seed extract.

The analysis of the Okra seed extract compositions with HPLC at the wavelength of 353 nm, revealed that the Okra seed extract has four main compositions (figure24) as follows:

Table 10. Retention time of HPLC chromatogram

Peak no.	Retention time (min)
No. 1	16.948
No. 2	17.916
No. 3	20.065
No. 4	21.187
Std. Isoquercitrin	20.102

In accordance to previous reports (Mérída-Ortega et al., 2016, Venturelli et al., 2016), the Okra seed extract contains isoquercitrin as the main component. Isoquercitrin has a retention time of 20.102 (figure23) and this was evident in the chromatogram of the Okra seed extract with a peak at the same position, confirming that the Okra seed extract truly contains isoquercitrin. After the partition process and analysis of the isoquercitrin quantity, only the ethanol fraction contains isoquercitrin while none was found in the hexane and dichloromethane fractions (data not

shown). The linearity of standard isoquercitrin resulted in  $R^2 = 0.9996$  and showed that LOQ = 100 ng/ml and LOD = 40 ng/ml, which is low enough for the analysis of its quantity. According to the results, the quantity of isoquercitrin in the Okra seed extract is  $2.89 \pm 1.64\%$  of the extract's weight, while the ethanol fraction contains  $2.68 \pm 1.92\%$ . This might be because of the decomposition of the extract due to the fact that the partition process used heat for lyophilization. In 24 hours, the extract became solid again. The heat and the humidity of the solution might have decomposed some major compounds, especially the compounds of flavonoids that are not stable. There is a chance of hydrolysis or being easily oxidized if there is any catalysis. The quantitative analysis of isoquercitrin provides results in accordance with the analyses of total phenolic or total flavonoid content. As in the analyses of total phenolic or total flavonoid, the standard curve of gallic acid and quercetin were made, respectively to compare the quantity of phenol and flavonoids. With regard to the result, the total phenolic content in the crude is  $56.66 \pm 1.88$  mg GAE/g extract and the total flavonoid content is  $44.07 \pm 7.03$  mg QE/g extract, which is higher than the extraction by partition, in which the phenolic of the ethanol fraction remains merely  $46.51 \pm 5.61$  mg GAE/g extract and the flavonoid remains just  $41.71 \pm 10.88$  mg QE/g extract, obviously a lower number than in the crude.

Table 11. Phytochemical quantitative analysis

	OSE-Hex fraction	OSE-DCM fraction	OSE-EtOH fraction	Okra seed extract
Total Phenolic (TP) content	-	-	46.51 ± 5.61 mg GAE/g extract	56.66 ± 1.88 mg GAE/g extract
Total Flavonoid (TF) content	-	-	41.71 ± 10.88 mg QE/g extract	44.07 ± 7.03 mg QE/g extract
Total polysaccharide (TPS) content	-	-	31.74 ± 1.23%	36.73 ± 2.41%
Isoquercitrin content	-	-	2.68 ± 1.92%	2.89 ± 1.64%

Values represent the total phenolic content, total flavonoid content, total polysaccharide content and isoquercitrin content, value= mean ± SD (n=3).

Furthermore, with reference to glycoside testing, the extract contained sugar in its structure, in agreement with previous reports stating that isoquercitrin is a flavonoid glycoside. Therefore, the experiment to measure the sugar content in the form of flavonoid glycosides depends on the chemical reaction with sugar, such as glucose reacting to intensive acid resulting in 5-(hydroxymethyl) furfural. Examination of the quantity of 5 -(hydroxymethyl) furfural by the phenol method was conducted to find the compound with the colour and quality to be measured by UV-visible with the wavelength of 490 nm (figure25).

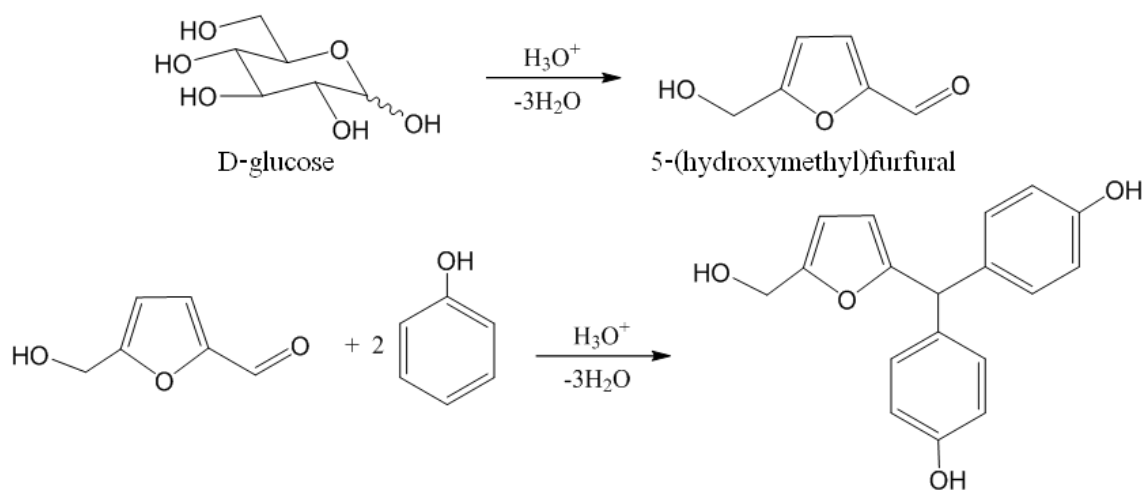


Figure 25. Reaction scheme of the phenol-sulfuric test.

In the experiment, the standard curve of glucose was created to compare the quantity of sugar found in the extract. As seen in table 11, it is demonstrated that the Okra seed extract and the ethanol fraction contain sugars at  $36.73 \pm 2.41\%$  and  $31.74 \pm 1.23\%$ , respectively. As previously mentioned, the information could basically conclude that the Okra seed extract contains major compositions of flavonoid glycoside and flavonoid groups.

In the experiment to examine the characteristics of the Okra seed's fingerprint by TLC, this method will ensure the results of HPLC indicate how many types of major compositions are present in the extract. Comparing with the standard compounds, which are isoquercitrin, quercetin, rutin, silibinin, and myricetin, it was found that the TLC chromatogram of the extract contains four major constituents while isoquercitrin is one of them, indicated by  $R_f = 0.687$ , which matches the standard isoquercitrin, while the other three constituents could not be indicated (figure26). However, the  $R_f$  of the other standard are as follows: isoquercitrin= 0.687, quercetin = 0.875, myricetin = 0.850, and rutin = 0.462 (Table 12). The TLC results are in agreement with the HPLC results. It is obvious that the chromatogram from the HPLC device reveals the four major compounds. After spraying ferric chloride on TLC, there will be dark-brown, sometimes almost black, spots, demonstrating the quality of the substance of the phenolic compounds. By spraying the TLC sheet with  $AlCl_3$  or NP/PEG reagent, the two solutions provide a similar result, as the fluorescent reaction occurs under a wavelength of 365 nm. This presents the compositions of

the flavonoid compounds (figure 26- 29). The TLC sheet sprayed by  $\text{AlCl}_3$  produced the fluorescent reaction of the flavonoid compounds as the substance became yellow-blue. It also depends on the type of flavonoid. On the other hand, this method has the disadvantage of having the sensitivity that is lower than that of the NP/PEG reagent. The TLC sprayed by the NP/PEG reagent has brighter orange spots than the sheet sprayed with  $\text{AlCl}_3$ . Nonetheless, comparing the two methods, the composition of the Okra seed extract with the two methods are not different.



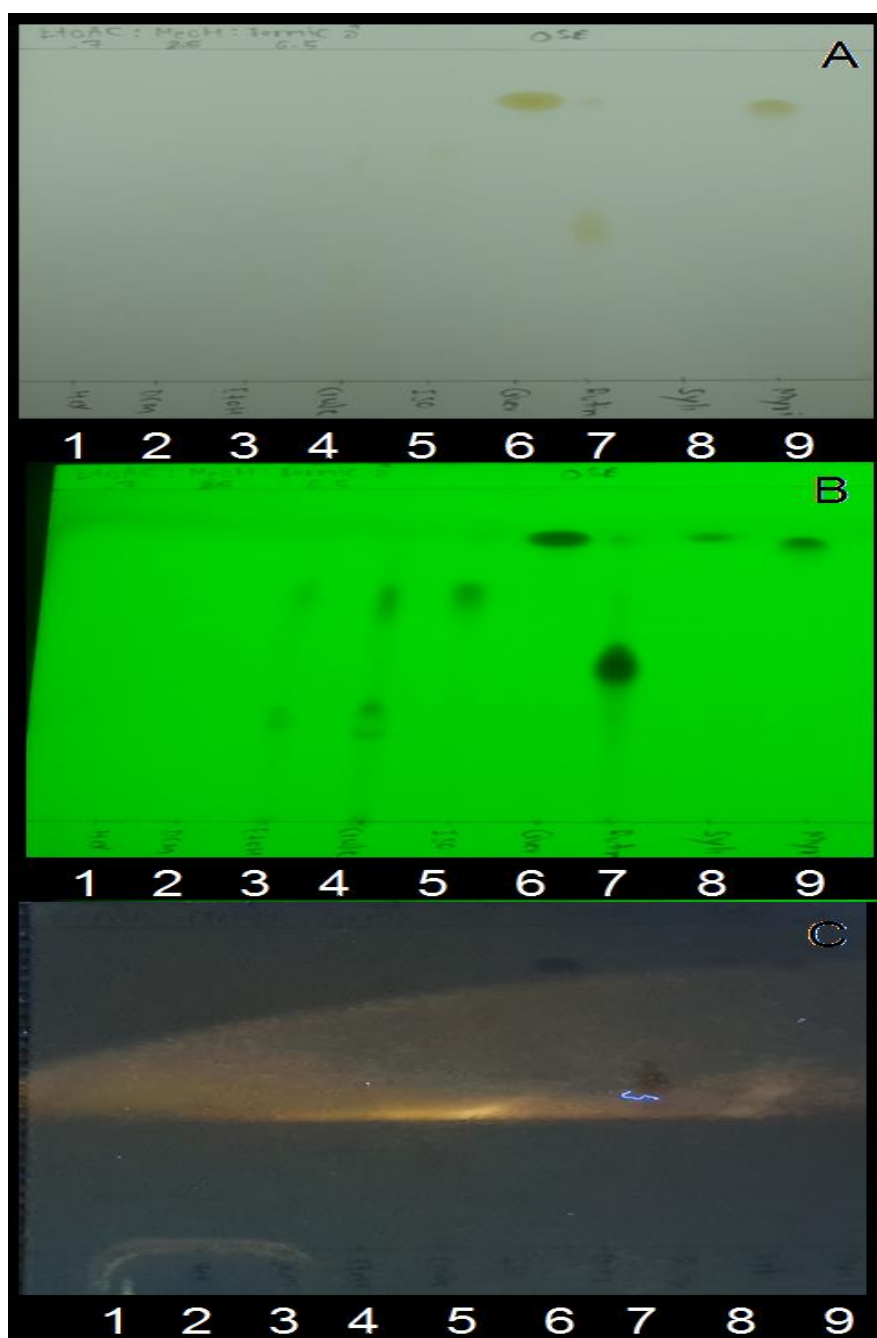


Figure 26. TLC Chromatogram of Okra seed extract observed under visible light (A) and under UV light at 254 nm (B) and 366 nm (C); tracks: (1)Hexane fraction; (2)DCM fraction; (3)Ethanol fraction; (4)Crude OSE; (5)Isoquercitrin; (6)Quercetin; (7)Rutin; (8)Silibinin; (9)Myricetin . Adsorbent: Silica gel GF

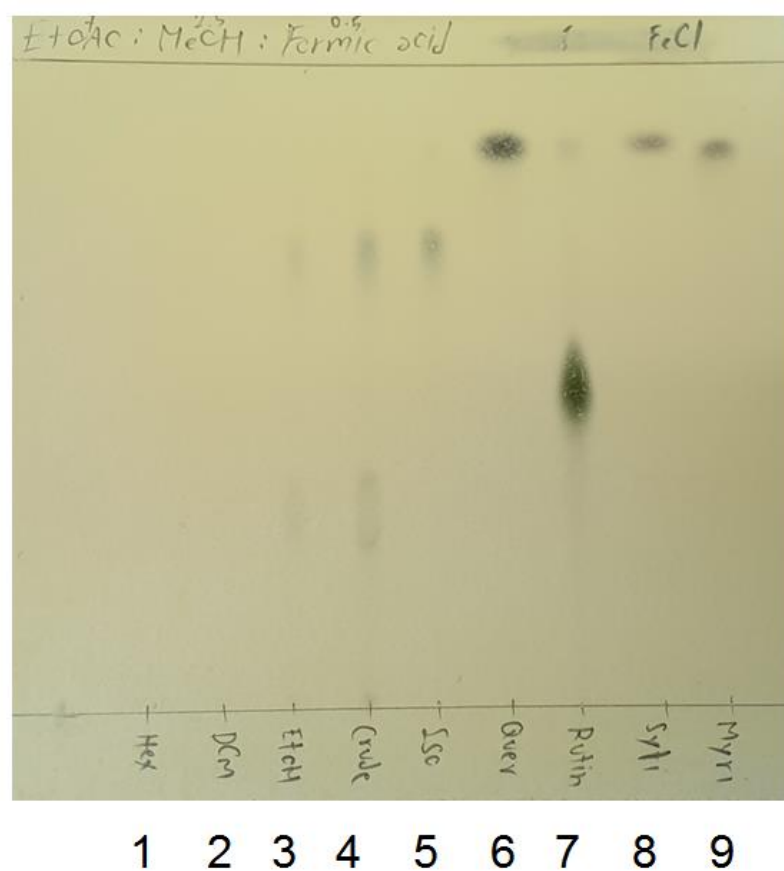


Figure 27. TLC Chromatogram of Okra seed extract after reacting with ferric chlorides observed under visible light; tracks: (1)Hexane fraction; (2)DCM fraction; (3)Ethanol fraction; (4)Crude OSE; (5)Isoquercitrin; (6)Quercetin; (7)Rutin; (8)Silibinin; (9)Myricetin. Adsorbent: Silica gel GF.

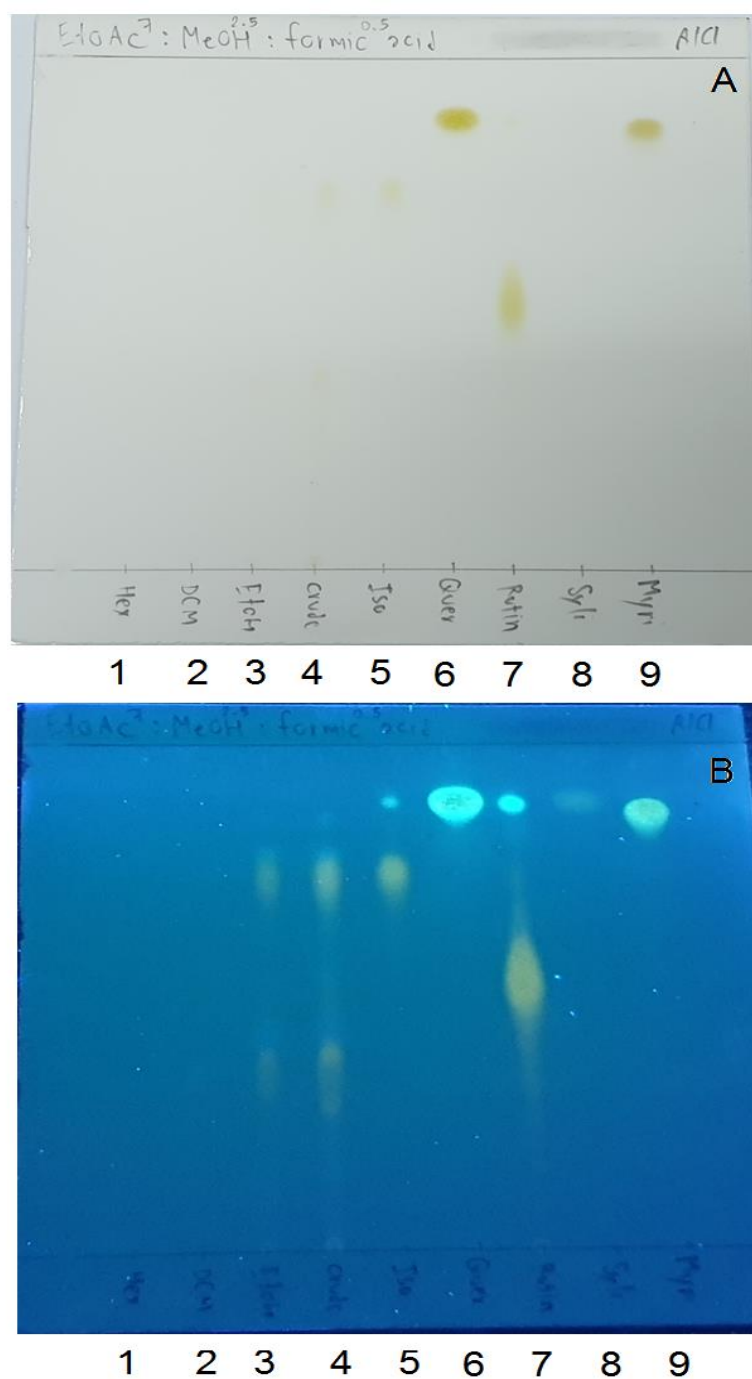


Figure 28. TLC Chromatogram of Okra seed extract after reacting with  $\text{AlCl}_3$  reagent under visible light (A) and under UV light at 366 nm (B); tracks: (1) Hexane fraction; (2) DCM fraction; (3) Ethanol fraction; (4) Crude OSE; (5) Isoquercitrin; (6) Quercetin; (7) Rutin; (8) Silibinin; (9) Myricetin. Adsorbent: Silica gel GF.

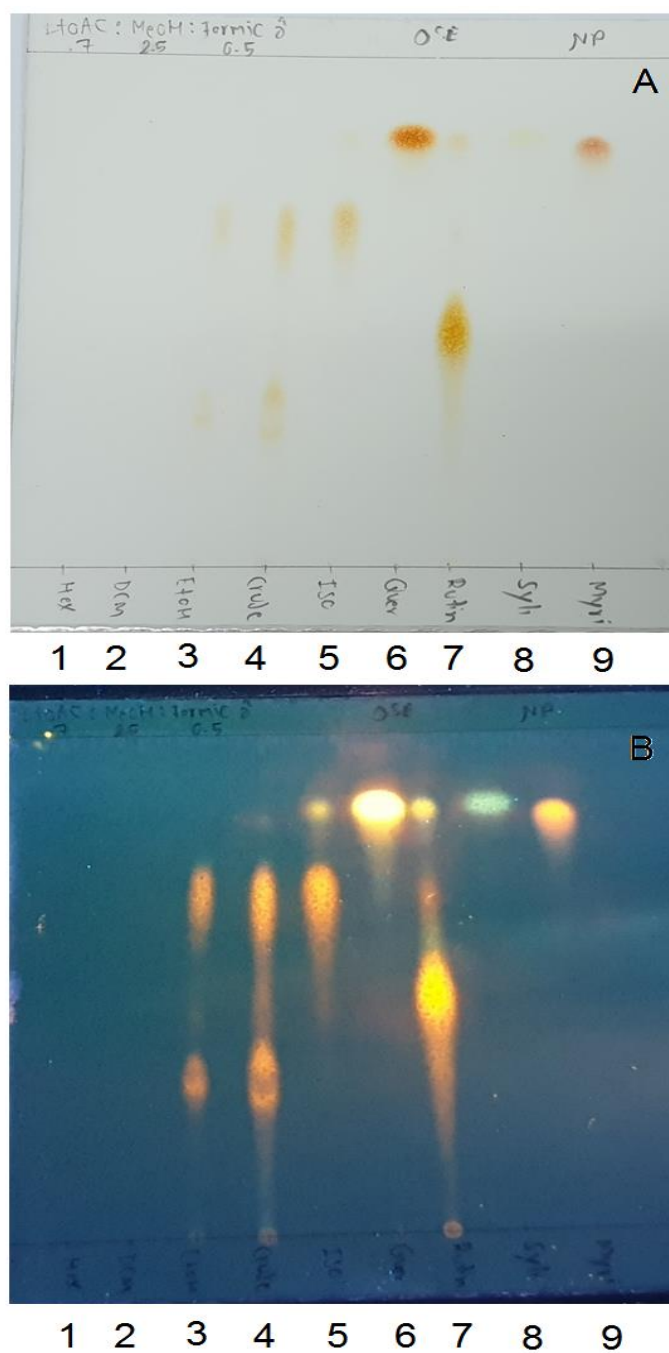


Figure 29. TLC Chromatogram of Okra seed extract after reacting with NP reagent observed under visible light (A) and under UV light at 366 nm (B) tracks: (1)Hexane fraction; (2)DCM fraction; (3)Ethanol fraction; (4)Crude OSE; (5)Isoquercitrin; (6)Quercetin; (7)Rutin; (8)Silibinin; (9)Myricetin. Adsorbent: Silica gel GF

Table 12. The standard of TLC plate with 8 cm elution heights and  $R_f$  values.

Sample	Height (cm)	$R_f$	Remark
Ethanol fraction Spot 1	1	0.125	Unknown
Ethanol fraction Spot 2	2.2	0.275	Unknown
Ethanol fraction Spot 3	2.7	0.338	Unknown
Ethanol fraction Spot 4	5.5	0.687	Isoquercitrin
Crude Spot 1	1	0.125	Unknown
Crude Spot 2	2.2	0.275	Unknown
Crude Spot 3	2.7	0.338	Unknown
Crude Spot 4	5.5	0.687	Isoquercitrin
Isoquercitrin Spot 1	5.5	0.687	Isoquercitrin
Isoquercitrin Spot 2	7	0.875	(impurity of quercetin)
Quercetin	7	0.875	Quercetin
Rutin Spot 1	3.7	0.462	Rutin
Rutin Spot 2	7	0.875	(impurity of quercetin)
Silibinin	7	0.875	Silibinin
Myricetin	6.8	0.850	Myricetin

Following this, sprayed TLC Chromatography with DPPH reagent was conducted to test the antioxidation activity. If the substance contains an antioxidant, white spots appear, and the background of silica will change from white to purple. According to the test, the Okra seed extract and the Okra seed ethanol fraction gave same positive results other standard flavonoids (Figure 30). Hence, it is expected that the Okra seed extract displays an anti-cancer effect due to its antioxidative activity, as for example, Ascorbic acid (Cimmino, Neel and Aifantis, 2018, Kim et al., 2018), astaxanthin (Shanmugapriya, Kim and Kang, 2019), or many other flavonoid-type compounds with similar antioxidative properties (Farombi, Akinmoladun and Owumi,

2019). For example flavonoid compounds such as rutin (ben Sghaier et al., 2016, Nafees et al., 2018), belonging in the flavonoid glycosides display anti-cancer effects towards colorectal cancer and lung cancer, or luteolin (Ahmed et al., 2019), able to cause apoptosis in breast cancer cells.

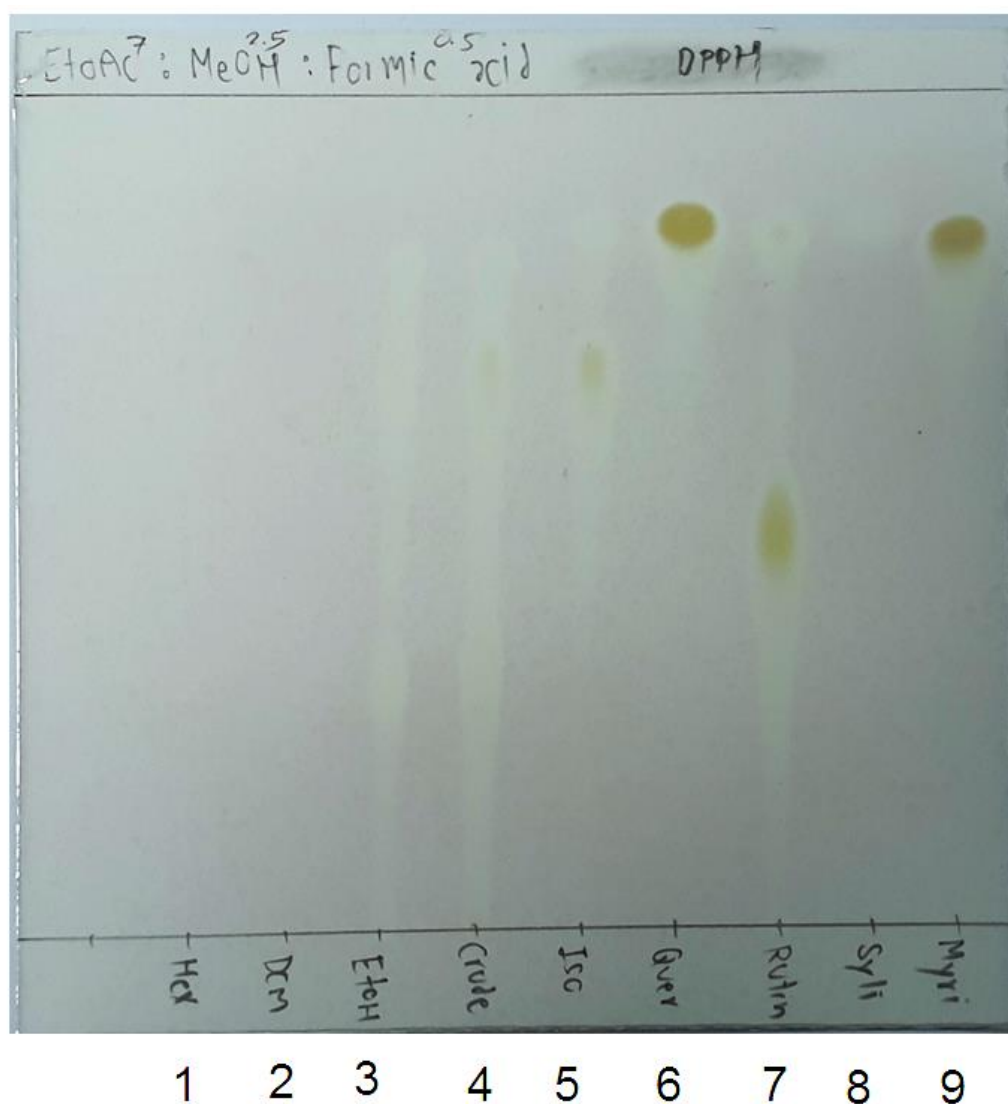


Figure 30. TLC Chromatogram of Okra seed extract after reacting with DPPH reagent observed under visible light; tracks: (1)Hexane fraction; (2)DCM fraction; (3)Ethanol fraction; (4)Crude OSE; (5)Isoquercitrin; (6)Quercetin; (7)Rutin; (8)Silibinin; (9)Myricetin . Adsorbent: Silica gel GF

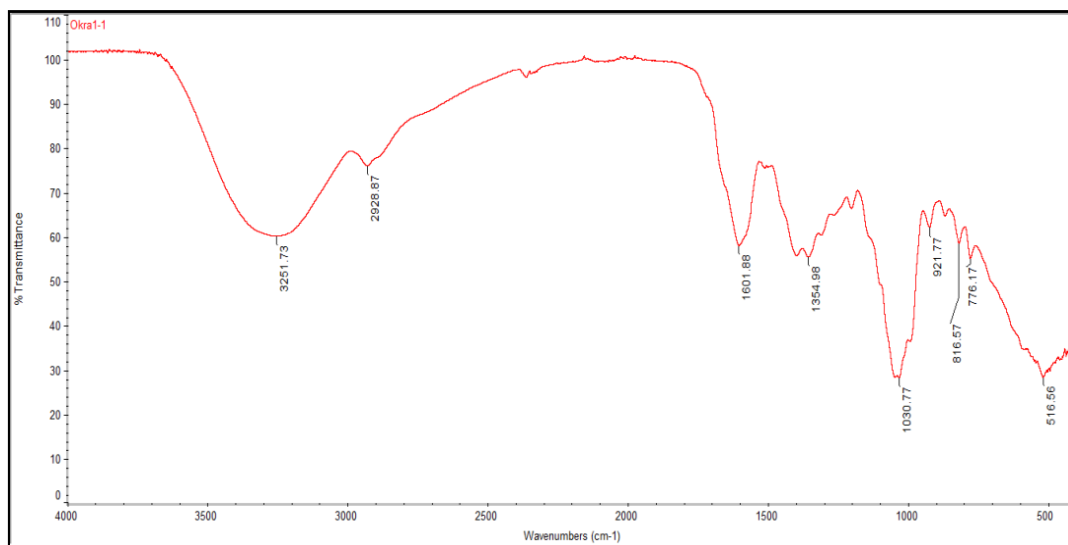


Figure 31. Infrared spectrum of the Okra seed.

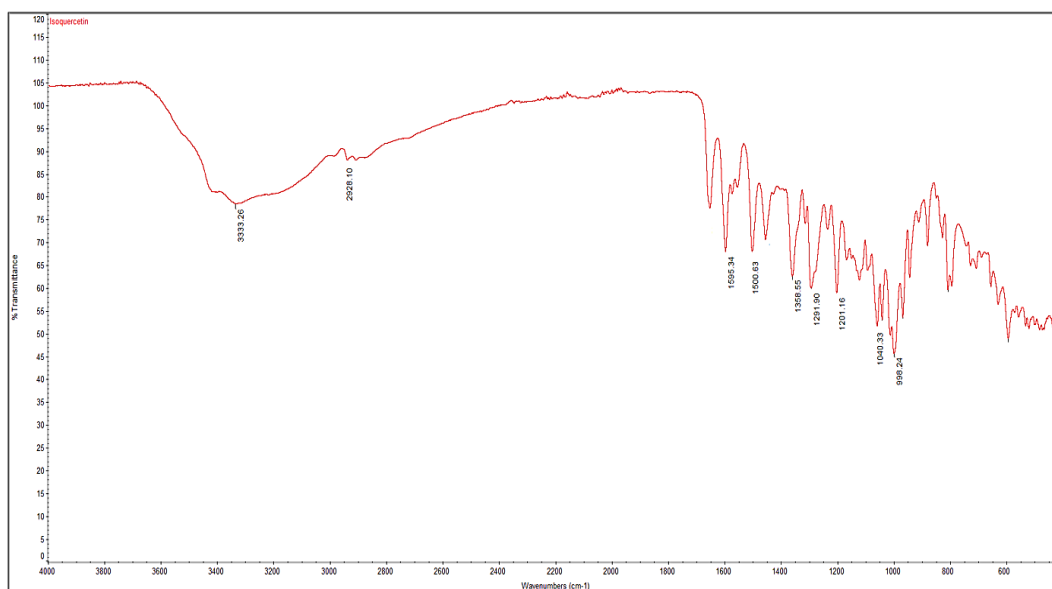


Figure 32. Infrared spectrum of isoquercitrin.

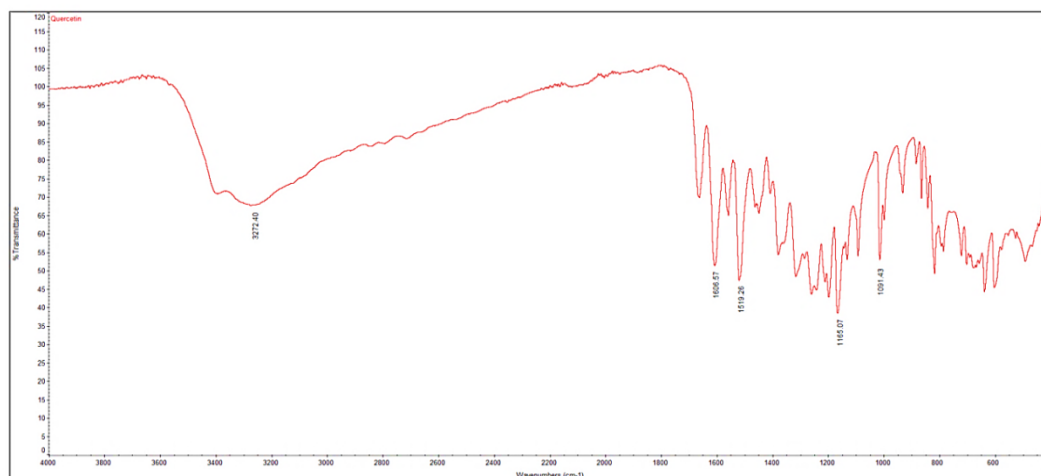


Figure 33. Infrared spectrum of quercetin.

Table 13. FTIR characteristic peaks of the Okra seed extract.

Absorption <sup>-1</sup>	Appearance	Group
1030.77	Strong	C-O stretching
1354.98	Medium	O-H bending (Phenol)
1601.88	Strong	C=O stretching
2000-2500	Weak	Overtone of aromatic compound
2928.87	Weak	sp <sup>3</sup> C-H stretching
3251.73	Strong	O-H stretching

The spectral characteristics of the Okra seed extract analysed with FTIR fingerprint are shown in figure 31. The spectrum characteristics represent clear positions, which conform to the flavonoid structure that is visible the peak of the spectrum. Examples are the functional groups such as aromatic ring (2000-1650), carbonyl groups (1601.88), and hydroxyl groups (3251.73). The spectrum characteristics were slightly contaminated by other substance groups; therefore, the peak position is very Strong detected (table 13). After processing the results, the structure of the flavonoid and flavonoid glycoside appeared (figures 34 – 35).

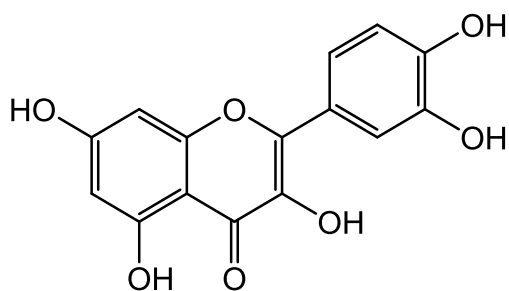


Figure 34. Chemical structure of a flavonoid

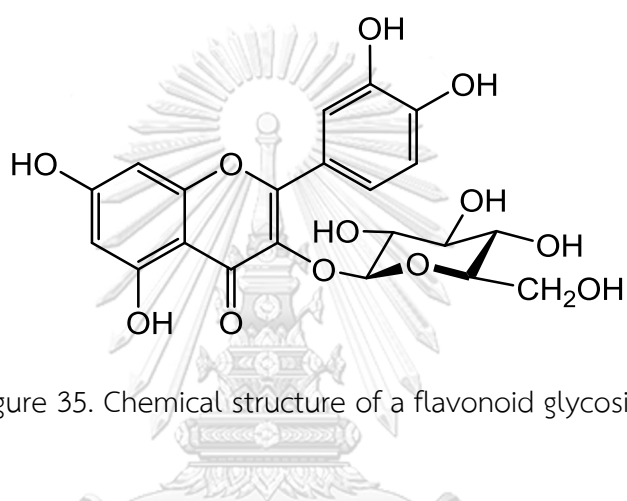


Figure 35. Chemical structure of a flavonoid glycoside

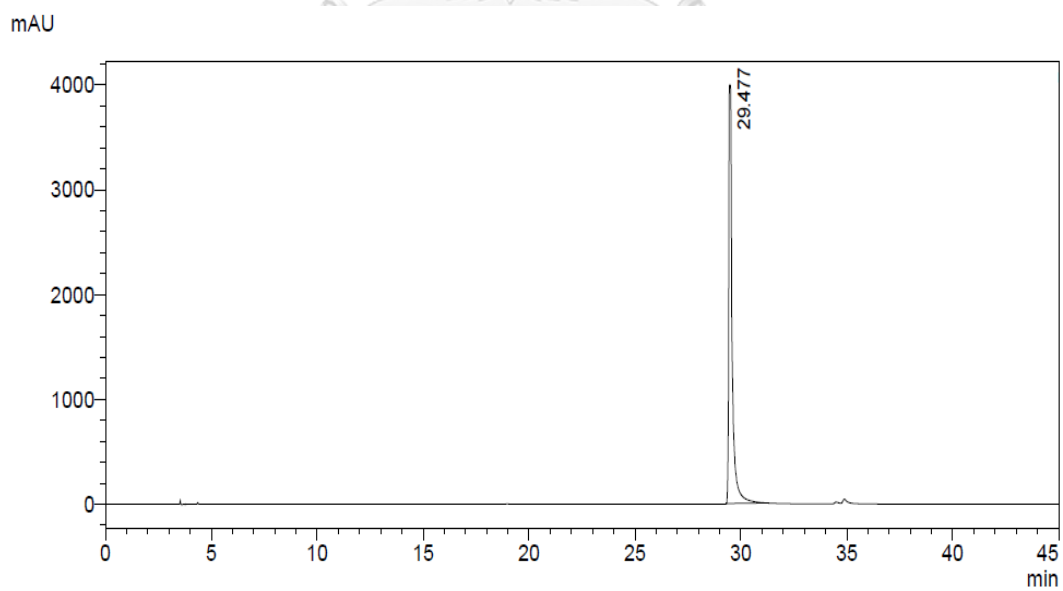


Figure 36. HPLC chromatogram of a standard quercetin.

The FTIR spectrum of the Okra seed extract is similar to the spectrum of standard quercetin and isoquercitrin. Although the two substances are different, as quercetin is a flavonoid and isoquercitrin is a flavonoid glycoside, their spectra share similarities due to having the same core structure, resulting in the lack of difference in the functional group's vibration. Nonetheless, considered in pair with the HPLC chromatogram of the Okra seed extract (figure24) and the aforementioned experiments, it is anticipated that the four compounds in the Okra seed extract are regarded as one type of flavonoid glycoside. Owing to the experiment by HPLC of standard quercetin, the retention time of quercetin is between 29 to 30 minutes because is more nonpolar than the substances in the flavonoid glycoside types and contains none of the sugar in the structure. In the final stage of the experiment, the moment that the mobile phase of HPLC increased more than the movement of isoquercitrin occurred (figure23).

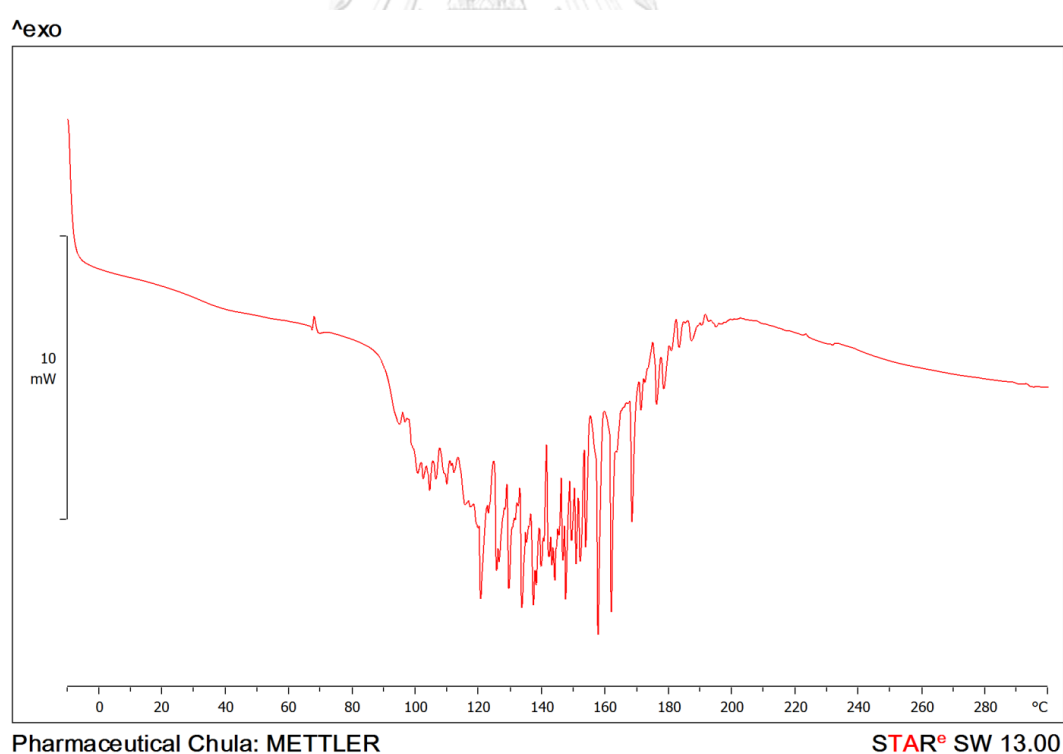


Figure 37. Thermogram of the Okra seed extract.

Analysis of the thermal properties of Okra seed extract using DSC instrument could not find a melting point clearly. However, the baseline of thermogram displayed thermal absorption, which continued to increase, when increasing the temperature from 0°C. This means the substance has a melting point, when the temperature is higher. This conformed to the physical characteristics of the extract that Okra seed extract becoming glue at room temperature. When the temperature increased to approximately 90°C, it apparently absorbed the heat. The peak endothermic was being in a mess, which demonstrated the degradation of the substance. Based on this information, it is useful for designing a product related to heat that might result in degradation, such as evaporation or sterilization.

#### **4. Antioxidant activity**

From the aforementioned, it was found that the Okra seed extract has the antioxidation effect. The purpose of this study is to find the antioxidation of the extract using two approaches, which are DPPH and ABTS. Subsequently, it was found that in the hexane and dichloromethane fractions, IC<sub>50</sub> could not be analysed and found due to the effect value being very rare, though the quantity of the extract had been added. However, in the ethanol fraction and crude, the IC<sub>50</sub> of antioxidation could be found by DPPH and ABTS. In the ethanol fraction, IC<sub>50</sub> tested by DPPH and ABTS is 48.35 ug/ml and 43.76 ug/ml respectively, and in the crude, IC<sub>50</sub> is 55.80 ug/ml and 49.04 ug/ml, respectively (table 14). These results are in accordance with the total phenolic content, the total flavonoid, and the isoquercitrin content. In other words, the ethanol fraction has fewer effects and quantity than the crude, which might be the result from the decomposition or loss during partition.

Table 14. Antioxidation activity of the Okra seed extract.

	OSE-Hex fraction	OSE-DCM fraction	OSE-EtOH fraction	Okra seed extract	Ascorbic acid
DPPH assay (IC <sub>50</sub> ) $\mu\text{g/ml}$	-	-	56.65 $\pm$ 8.80	48.59 $\pm$ 5.57	4.09 $\pm$ 0.11
ABTS assay (IC <sub>50</sub> ) $\mu\text{g/ml}$	-	-	49.04 $\pm$ 0.43	43.76 $\pm$ 0.12	3.59 $\pm$ 0.09

Values represent IC<sub>50</sub>. Value= mean  $\pm$  SD (n=3).

## 5. Cytotoxicity test

One hundred (100) mg crude OSE was partitioned using a solvent to obtain OSE-Hex, OSE-DCM, and OSE-EtOH. The extract was then dissolved in complete medium containing 1% DMSO to clear solution and diluted with the complete media 100-fold. The cytotoxicity test of cancer cells uses a PrestoBlue assay test method by seeding cells in 96-well plates and incubating for 24 hours. The tests are performed at 24 and 48 hours and measured with a microplate reader at excitation/emission 560/590 nm. Each OSE fraction was compared to the crude Okra seed extract. The most effective OSE part in the cytotoxicity assay was then further compared to standard isoquercitrin equivalent to isoquercitrin found in the 1,000  $\mu\text{g}$  current Okra seed extract. When the cytotoxic effect of the OSE and its various fractions was tested on the three cancer cell lines, we observed no effects of the Hexane (OSE-Hex) and Dichloromethane (OSE-DCM) fractions compared to controls after 24 hours or 48 hours. However, in the present study, the onset of the Okra seed extract's cytotoxic effect appeared at 48 hours indicating a possibly chronically toxic effect (figure38). The crude OSE displayed the highest anticancer activity after 48 hours, and followed by the Okra in the ethanol fraction also at 48 hours. Among the three cancer cell lines, the breast cancer cell displayed the highest sensitivity, with cell viabilities of 62.11 $\pm$  2.81 % for the crude OSE and 77.89 $\pm$ 4.65 % OSE-EtOH. The cell line with the next highest sensitivity was liver cancer cell HepG2 displaying viabilities for the crude

OSE and OSE-EtOH of  $77.41 \pm 4.11\%$  and  $83.08 \pm 6.95\%$  respectively. It was hypothesized that synergistic effects of the components of the Okra seed were present. When we used the Okra seed extract in the partition by hexane, dichloromethane, and ethanol, respectively, the components in the Okra seed are divided according to the polarity of the solvent. In other words, the non-polar substance would be separated with hexane, while the semi-polar substance would be separated with dichloromethane. These substances in two layers might be behind a synergistic effect with the main components (Batra and Sharma, 2013, Vemuri et al., 2017, Zheng et al., 2017a). Moreover, the drying process of our extract required heat, humidity, and light which may have compromised the different components. Earlier studies have shown that flavonoid compounds display little stability as Yan Hu and others (Hu et al., 2018) found that the flavonoid extracted from the orange peel was unstable when kept at a temperature of  $4^{\circ}\text{C}$ . Among 4 types of flavonoids including narirutin, hesperidin, nobiletin, and tangeretin, were decreased significantly compared to day 0. Besides, Biesaga (Biesaga, 2011) also found that the difference in extraction affects the quantity and degradation of the substances of flavonoids. Isoquercitrin, the main compound of the Okra seed extract, could degrade and hydrolyze easily, pH alterations or metal ions could also degrade the extract. Moreover, the higher the temperature, the higher the chance of hydrolysis.

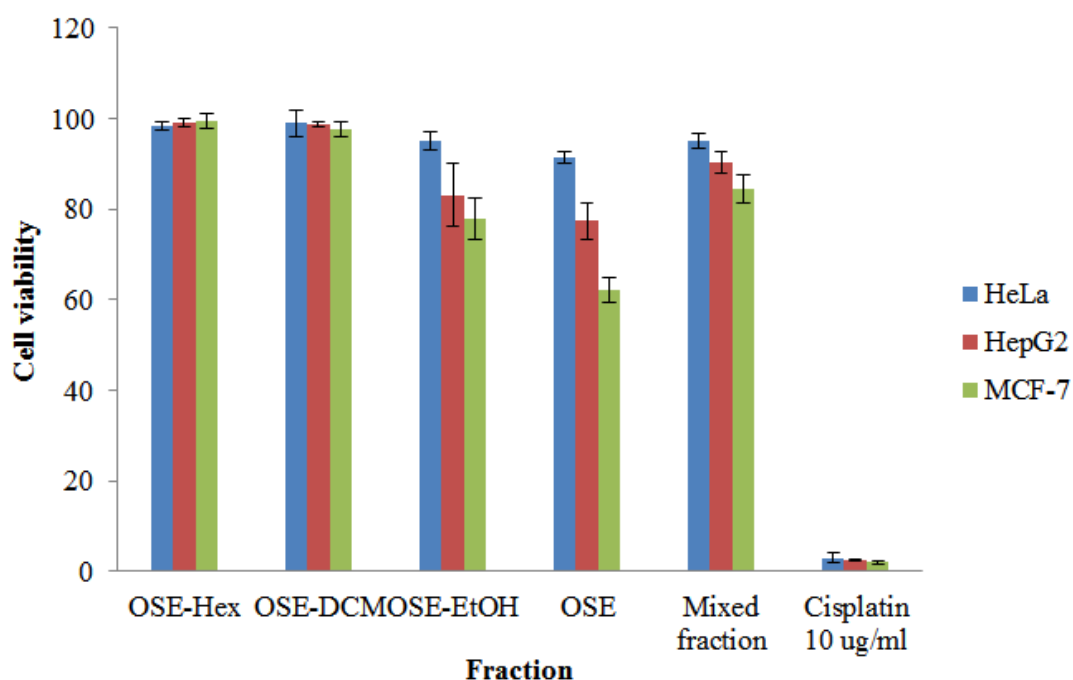


Figure 38. Cytotoxicity of the Okra seed extract fractions (48hr).

Cells were left untreated or were treated with various fractions of the Okra seed extract for 48 hr. Cell viability was determined by presto blue assay. Values shown are relative cell viability compared to control cells and plots are mean  $\pm$  SD (n=3).

\*P < 0.05 versus non treated controls.

In summary, the direct delivery of Okra seed extract followed by the OSE-EtOH fraction had the highest cytotoxic effect on the breast cancer cell line (MCF-7), followed by the hepatocellular carcinoma (HepG2) and cervical carcinoma (HeLa) cell lines in that order. It would thus be preferable to select the crude OSE for future studies.

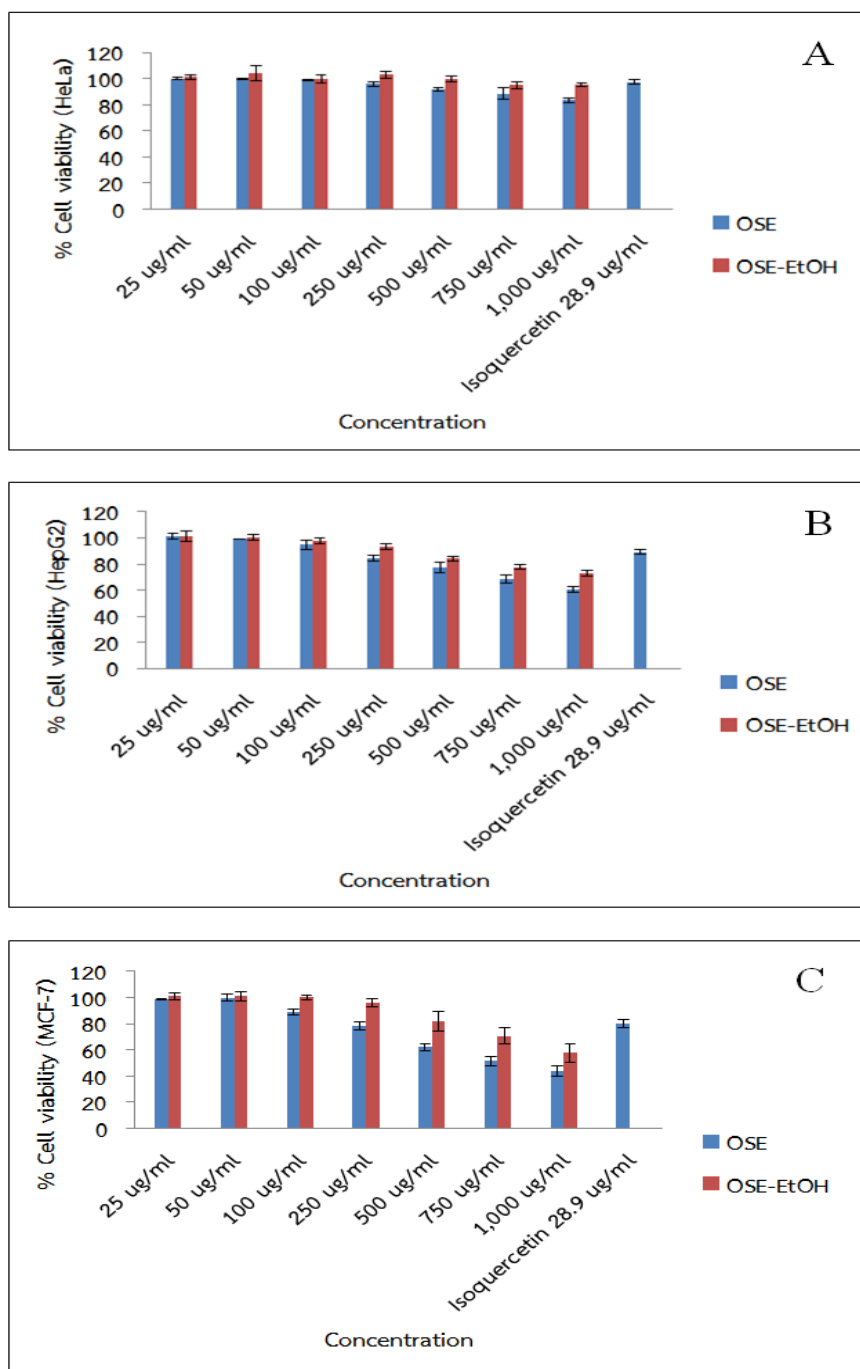


Figure 39. Cell viability versus concentration, A: HeLa, B: HepG2 and C: MCF-7 Cells were left untreated or were treated with various fractions of the Okra seed extract for 48 hr. Cell viability was determined by presto blue assay. Values shown are relative cell viability compared to control cells and plots are mean  $\pm$  SD (n=3).

\*P < 0.05 versus non treated controls.

In our experiments, the 3 types of cancer cells responded to the Okra seed extract differently. Breast cancer cells responded to the Okra seed extract the most, while HeLa cervical cancer cells responded to the Okra seed extract the least. Earlier reports observed similar findings towards HeLa (Ahmed et al., 2014). In the work of Jarial and others (Jarial et al., 2018) who tested the anticancer activity of *Cheilanthes tenuifolia* containing rutin and quercitrin where HeLa responded to the extract less than HepG2. This was similar to the research of Lingrong Wen (Wen et al., 2014), who tested the effect of flavonoid in *Litchi chinensis Sonn* and provided a different response towards the cancer cells HepG2 and HeLa. Moreover, the work of Muhammad Maqsood and others (Maqsood et al., 2018) experimented with the anticancer activity of *Withania coagulans*, belonging to the Solanaceae family. The total flavonoid content in *Withania coagulans* is  $394.34 \pm 1.26$  ug/g. It was revealed that the extract could resist HeLa less than breast cancer MCF-7 and brain cancer (RG2), though the response towards methotrexate was better than breast cancer. However, what is interesting is the concentration of isoquercitrin is 28.9 ug/ml. An equivalent quantity of the isoquercitrin was found in 1,000 ug of the Okra seed extract, when compared with the single isoquercitrin, which is the main composition of Okra seed extract. The Okra seed extract provided better efficiency for cancer resistance than the isoquercitrin. The Okra seed extract at 250 ug/ml of concentration began to have anticancer activity close to isoquercitrin. When we calculated the quantity of isoquercitrin in the Okra seed extract, just 7.2 ug/ml was measured. We thus hypothesized that, apart from isoquercitrin, other substances with an effect are present and operative providing a synergistic effect. This is in congruence with previous research with baicalein and silymarin (Chen et al., 2009), also flavonoids. The use of two 2 types of flavonoids could destroy cancer cells better than a single substance. As for the use of baicalein alone and silymarin alone at 6.75 ug/ml and 100 ug/ml, respectively, cell viabilities at approximately 70-80% was observed. However, mixing the 2 substances at the equal concentrations reduced cell viability to lower than 20% (figure40). It is probable that there are at least 4 compounds found in Okra seed extract behind the hypothesized synergistic effect.

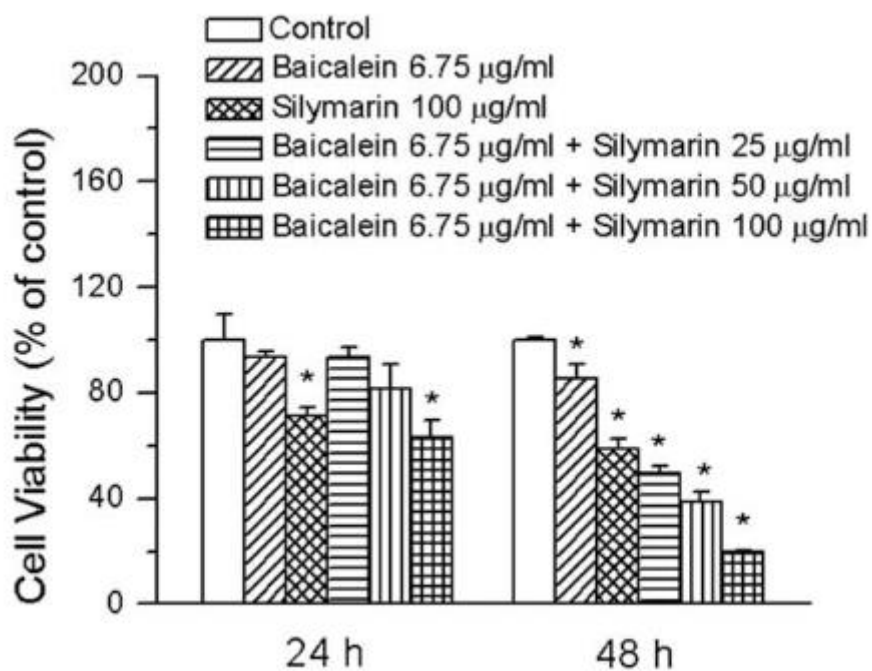


Figure 40. Synergistic of baicalein and silymarin on HepG2 cell.  
(Chen et al., 2009)

We used the Okra seed extract in normal human keratinocyte cells (HaCaT) but observed no effects on cell division (figure41).

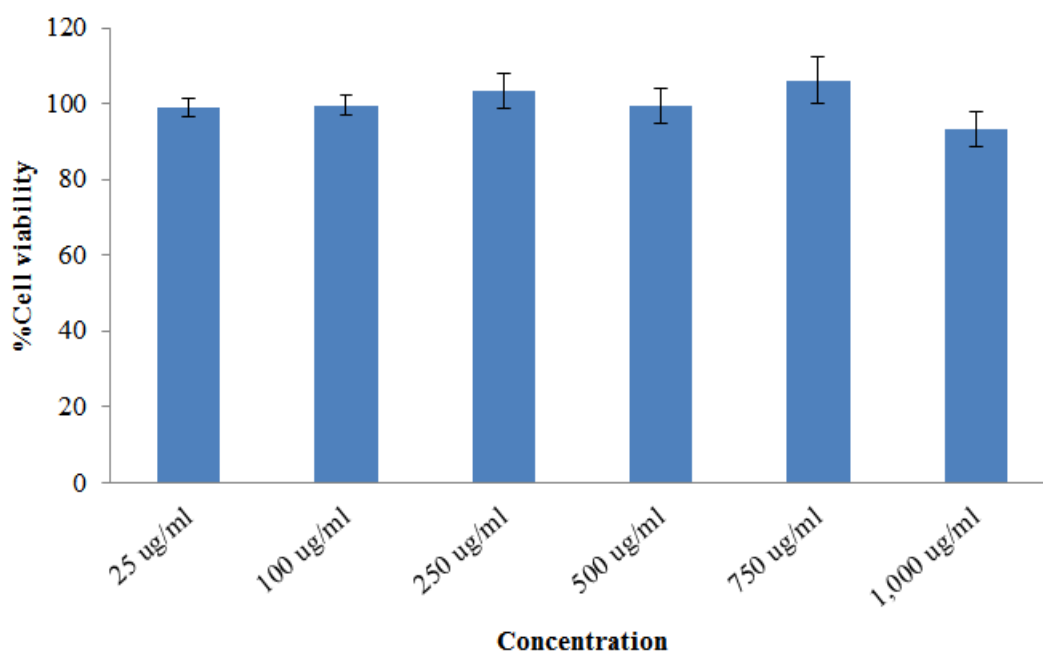


Figure 41. Okra seed extract cytotoxicity of human keratinocyte cell.

Cells were left untreated or were treated with various fractions of the Okra seed extract for 48 hr. Cell viability was determined by presto blue assay. Values shown are relative cell viability compared to control cells and plots are mean  $\pm$  SD (n=3).

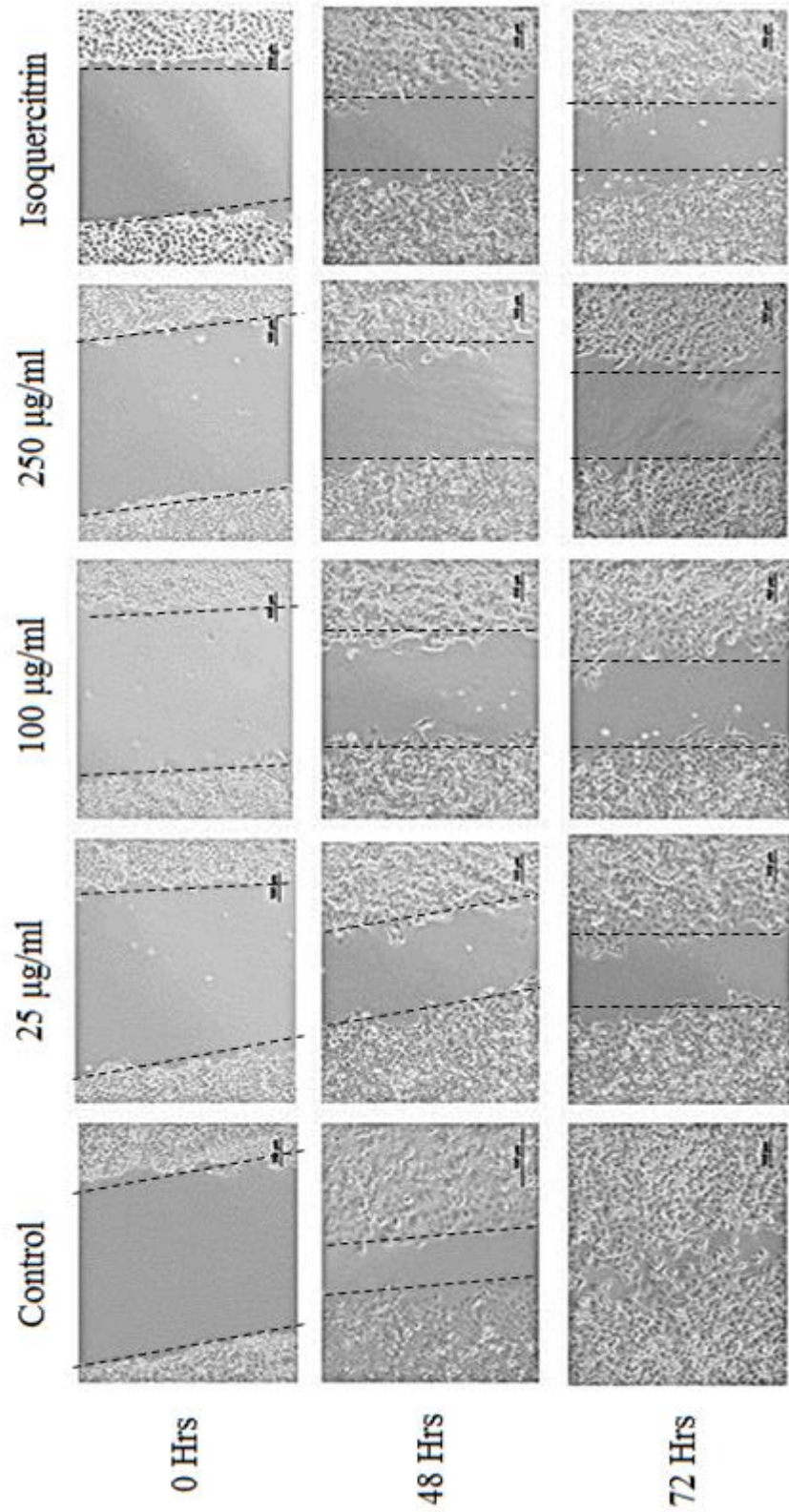
\*P < 0.05 versus non treated controls.

In a previous report of burns in rats (Bhatia et al., 2016), the 0.06%-isoquercitrin cream was more efficient in inducing wound healing than silver sulfadiazine cream and the lowest isoquercitrin concentration being close to the effect of silver sulfadiazine cream. In other words, isoquercitrin's healing effect showed when using 100 ug/ml but in our experiments we applied 1,000 ug/ml of Okra seed extract it was found isoquercitrin 28.9 ug/ml.

## 6. Anti-cells migration assay

Anti-migration and anti-invasion studies elucidate other mechanisms of cancer cell biology. Cancer cells will metastasize to ensure continued expansion and this occurs often by using blood or lymph vessels and the circulatory as well as the lymphatic system(Kibe et al., 2019). Cancer cells reach the vessels via migration and invasion. Cell migration was tested by observing how the extract could cancer cells prevent from moving.





———— = 100 µm

Figure 42. Cell migration (HeLa cell).

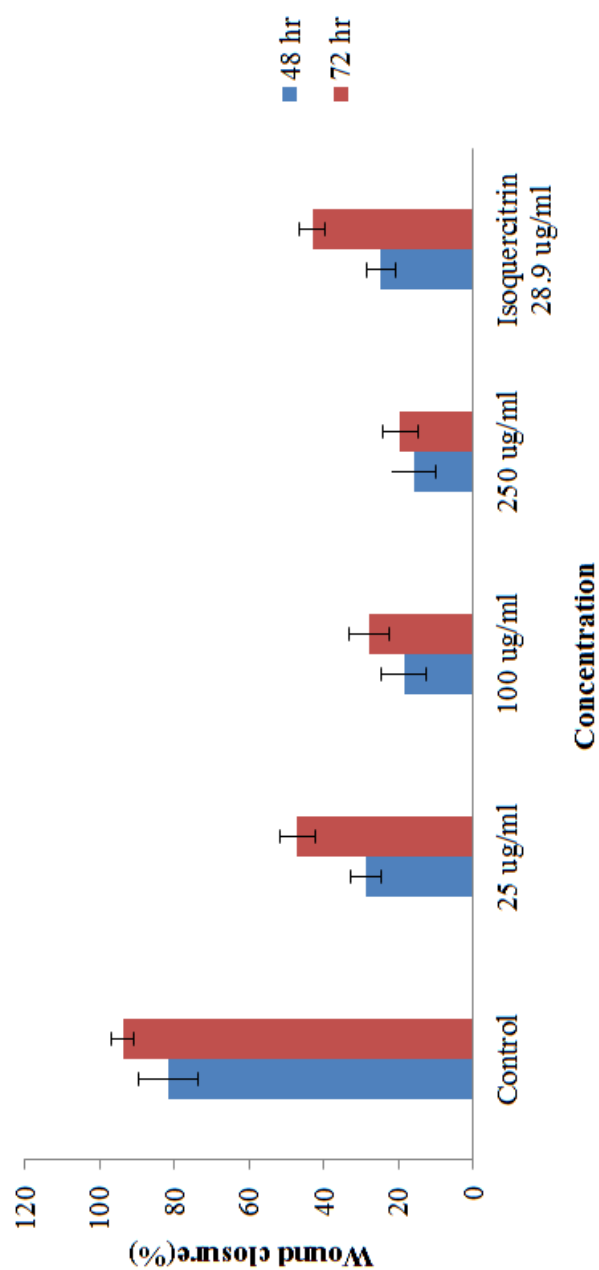
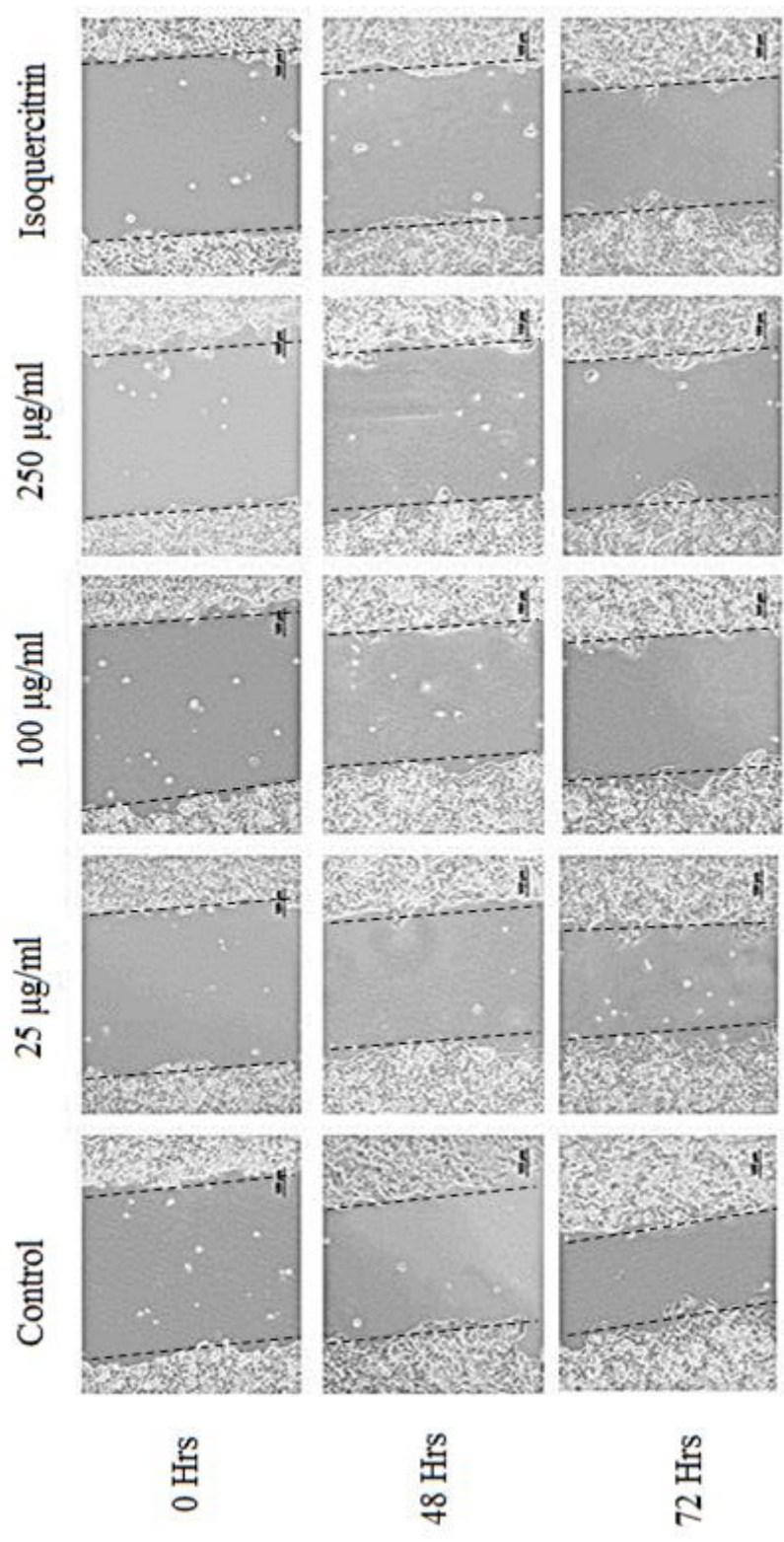


Figure 42 Cell migration (HeLa cell).

Cell scratch assay on HeLa cell line was observed by inverted microscope and analyzed with Image J program. Values represent gap distance compared to control cells and plots are mean  $\pm$  SD (n=3). \*P < 0.05 versus non treated controls.



— = 100 µm

Figure 43. Cell migration (HepG2 cell)

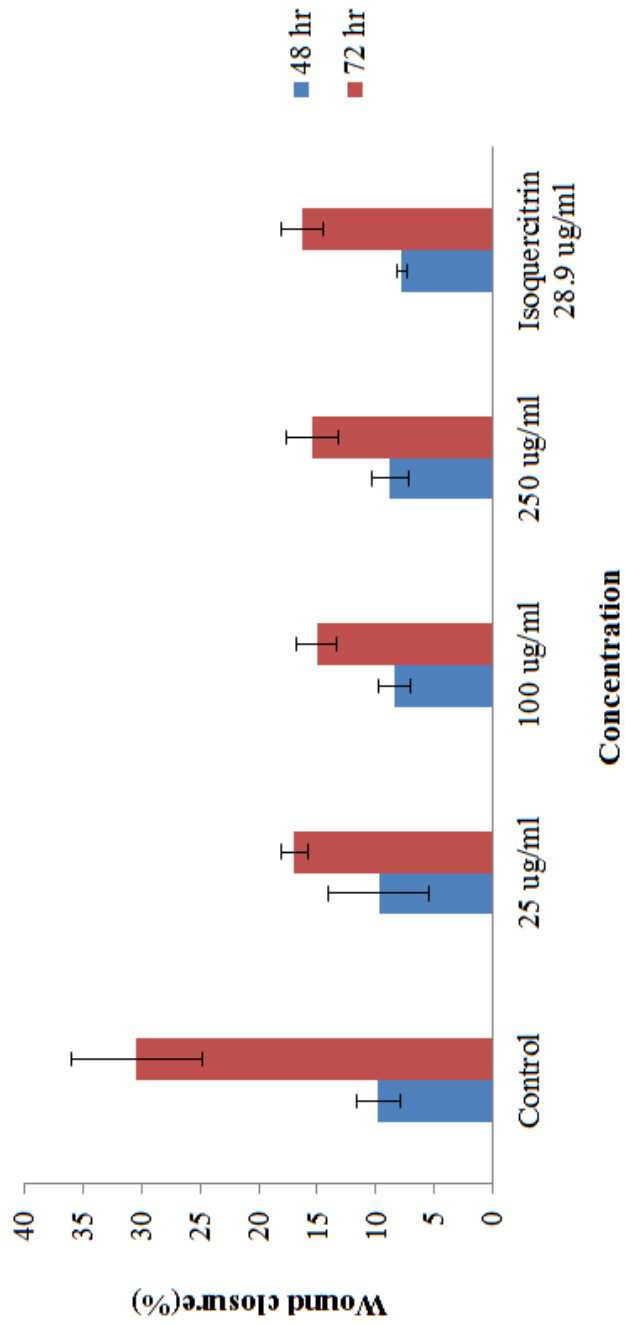
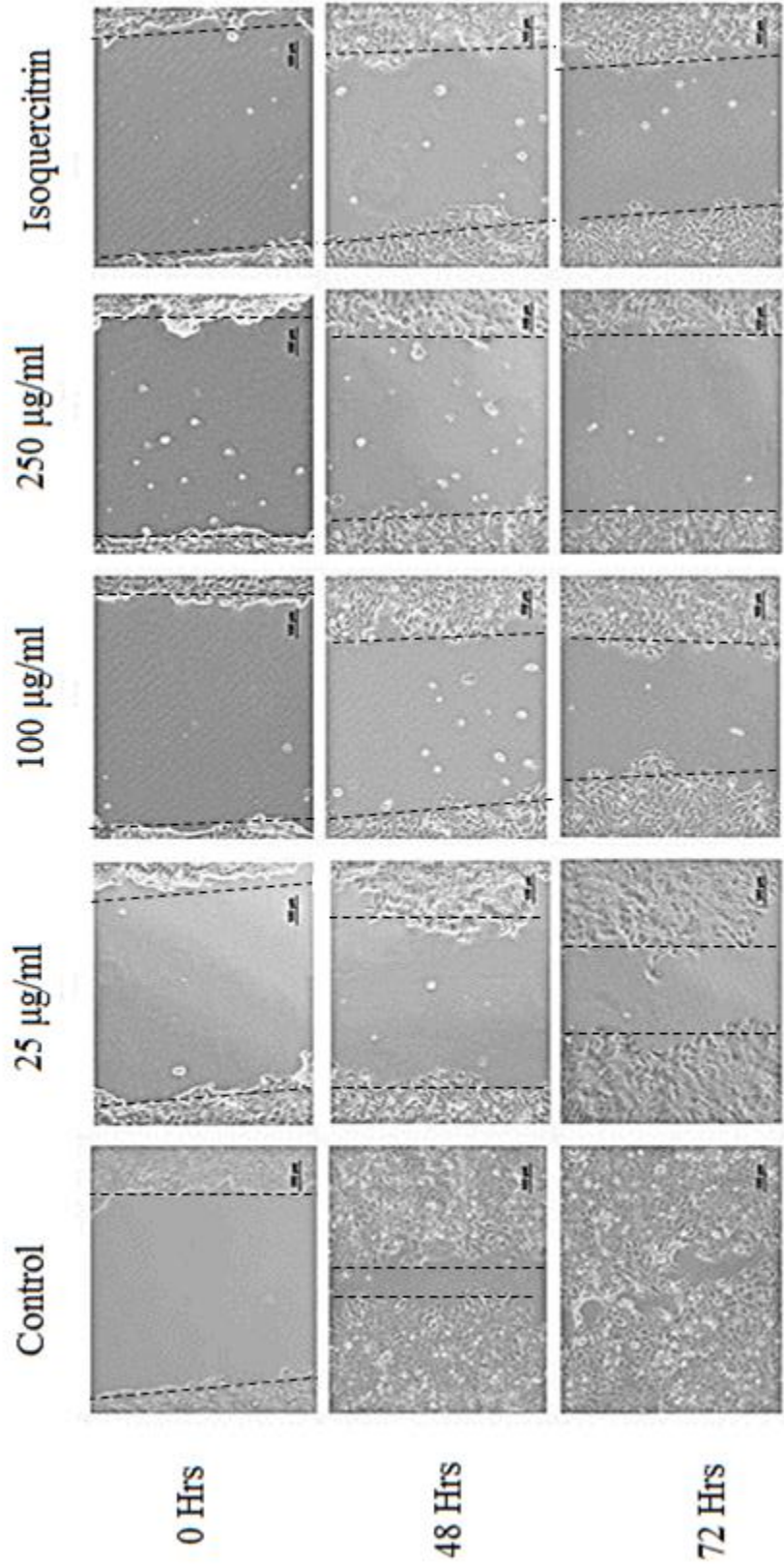


Figure 44. Cell migration (HepG2 cell)

Cell scratch assay on HepG2 cell line was observed by inverted microscope and analyzed with Image J program.

Values represent gap distance compared to control cells and plots are mean  $\pm$  SD (n=3). \*p < 0.05 versus non treated controls.



— = 100  $\mu\text{m}$

Figure 45. Cell migration (MCF-7 cell)

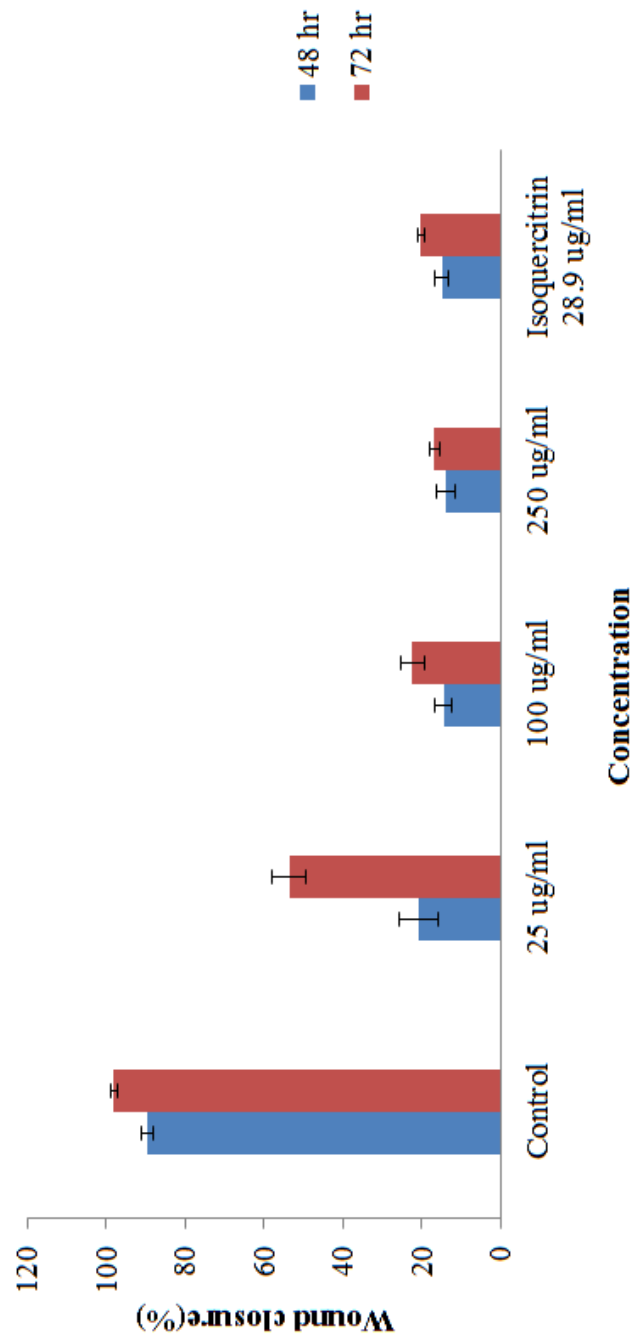


Figure 46. Cell migration (MCF-7 cell)

Cell scratch assay on MCF-7 cell line was observed by inverted microscope and analyzed with Image J program.

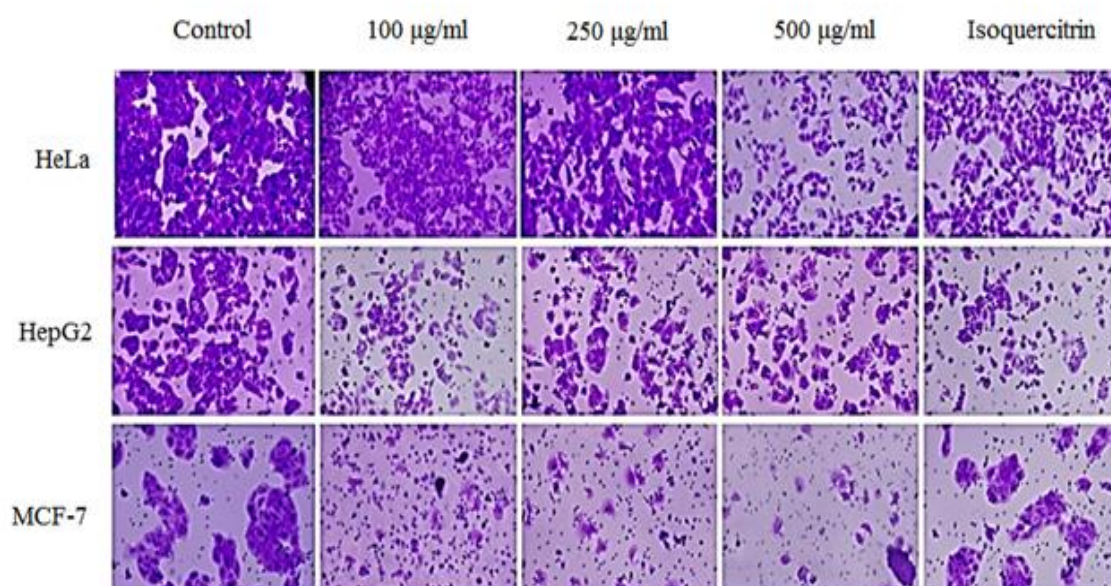
Values represent gap distance compared to control cells and plots are mean  $\pm$  SD (n=3). \*p < 0.05 versus non treated controls.

The Okra seed extract displayed inhibition of migration in two of the three cancer cell lines (MCF-7 and HepG2) in the cell scratch assay that were statistically significant. The effect of the OSE on the HeLa cell line was negligible but even at low doses of 25 ug/ml, this effect was most pronounced with the MCF-7 cell line exhibiting the highest level of migration inhibition. The effect on the HepG2 cells was different. The HepG2 cells grow and divide in groups in overlapping layers; hence, the split and side of the heel appears less noticeable when the HepG2 cells were scratched while the MCF-7 prefer to divide horizontally into a monolayer rather than overlapping.

## 7. Cells invasion inhibition assay

The cells invasion inhibition assay studies the vertical movement by culturing the cells on the transwell plate to simulate metastasis. The Boyden chamber migration test revealed statistically significant dose dependent effects on all 3 cell lines and all 3 doses of the Okra seed extract, already appearing at the lowest dose tested. At all doses, the MCF-7 cell line exhibited the highest level of invasion inhibition followed by the HepG2 cells and HeLa cells respectively. Our results are in agreement with the findings of Dai et al where apigenin could resist the migration and invasion of colorectal cancer (Dai et al., 2016) and hesperidin and nobiletin in *Citrus reticulata* cv. *Suavissima* that could resist the migration of several cancer cells, e.g. human liver cancer HepG2, promyelocytic leukemia HL-60, and breast cancer MDA-MB-231 as seen by Zhang et al (Zhang et al., 2014). Isoquercitrin alone used as control resulted in similar effects, in the inverse order of effect on the three cell lines. This might be because isoquercitrin alone is not sufficiently effective in inhibiting migration and invasion but may require more components to enhance its effect or activity. Several mechanisms may be involved in migration and invasion as for example, the proteolytic of conversion pro-uPA to be uPA (urokinase) to stimulate uPA receptor resulting in differentiation and invasion, PI3K/AKT pathway related to proliferation of cancer cells inducing metastasis and invasion faster or the TK2 protein tyrosine kinase 2 (PTK2), also known as focal adhesion kinase (FAK) that

is related to the attachment and spreading of cancer cells (Jiang et al., 2015, Krakhmal et al., 2015). Flavonoids impact differently on different pathways associated with invasion and migration e.g., quercitrin inhibiting the miR-16/HOXA10 process in oral cancer (Zhao et al., 2019), apigenin inhibiting the NEDD9 process of colorectal cancer (Dai et al., 2016), or delphinidin inhibiting Brain-derived neurotrophic factor (BDNF) in ovarian cancer (Lim et al., 2017). It is therefore hypothesized that the crude extract may present a better and more efficient approach than the use of isoquercitrin alone.



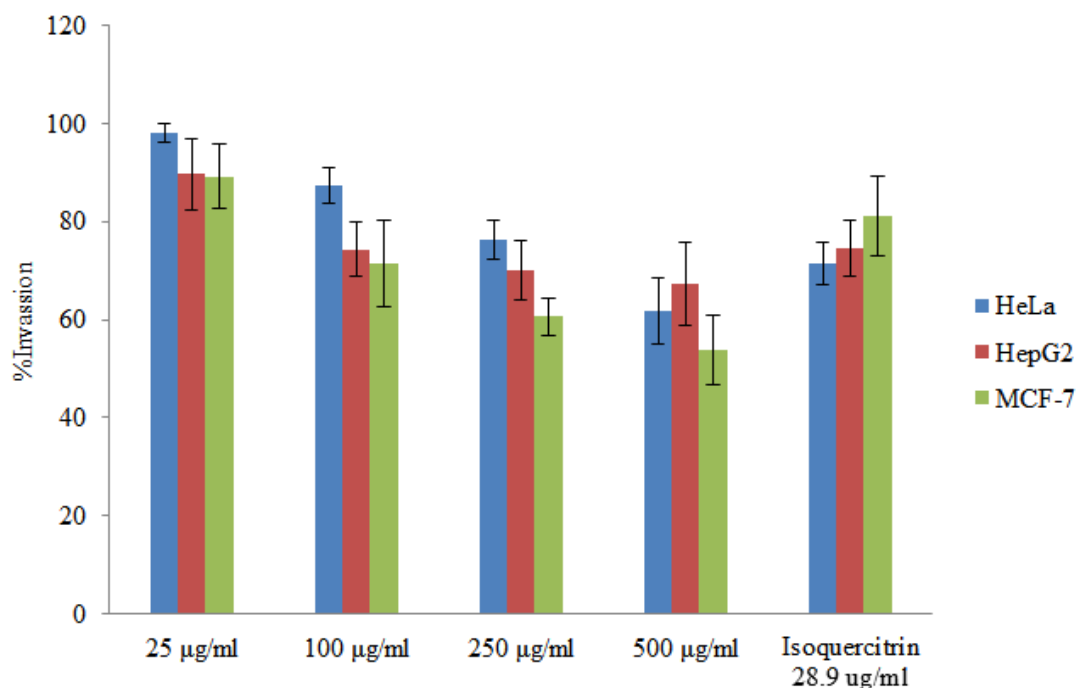


Figure 47. Cell invasion inhibition.

Cells were left untreated or treated with various concentrations of the Okra seed extract for 48 hrs. Cell invasion was determined by crystal violet staining and cell lysate before being evaluated on a microplate reader at a wavelength of 590 nm. Values represented are relative cell invasion compared to control cells. Plots are mean  $\pm$  SD (n=3). \*P < 0.05 versus non treated controls.

จุฬาลงกรณ์มหาวิทยาลัย  
CHULALONGKORN UNIVERSITY

## 8. Apoptosis induction test

Cell death, particularly apoptosis, is widely-studied. Understanding apoptosis in disease conditions is very important as it not only gives insights into the pathogenesis of a disease but may also leave clues on how the disease can be treated. The mechanism of apoptosis is complex involving many pathways. Defects can occur at any point along these pathways, leading to malignant transformation of the affected cells, tumour metastasis and resistance to anticancer drugs (Wong, 2011). Disrupted balance of pro-apoptotic and anti-apoptotic proteins such as p53 protein or Bcl-2 protein, a decrease of caspase, or Impaired receptor signaling pathway all can result in reduced apoptosis and enhanced tumor growth and development. As a consequence, cancer treatment by stimulating its apoptosis is

very interesting. Substances in the flavonoid group are being intensely researched (Abotaleb et al., 2018), such as the stimulation of protein Bcl-2 of morin flavonoid of Moraceae plant (Nguyen et al., 2017) or quercetin disturbing Foxo3a in breast cancer, resulting in apoptosis (Hyun et al., 2015). The analyses of apoptosis in cells is as follows: measuring the increase of caspase enzyme, measuring the destroyed DNA or the change of the cell membrane. Cells during early apoptosis will express phosphatidylserine at the outer membrane. In this study we selected to label phosphatidylserine by annexin V and 7AAD and measured with flow cytometry thus allowing for the monitoring of the apoptosis state.

Earlier in the results section of current study we evaluated the Okra seed extract's cytotoxic effect and reported that such effects were dose and time dependent and highest for the breast cancer MCF-7 cell lines, followed by the liver cancer HepG2 while the effect was minimal for the cervical cancer HeLa cell line indicating resistance to the extract. The incubation with the extract showed a significant effect on the apoptosis assay. Table 15 shows that cells treated with 25, 50, 100, 250, 500, 750 and 1,000  $\mu\text{g/mL}$  Okra seed extract for 48 h resulted in a significant increase in the percentage of apoptotic cells (early and late apoptosis) in a manner consistent with its cytotoxic effects. Thus, the breast cancer MCF-7 cell line was the most responsive to induction of early and late apoptosis in a dose dependent manner already at low doses, but slightly declined at the highest dose. Similar albeit weaker effects were noted for the cervical HeLa and liver HepG2 cancer cell lines. The apoptosis stimulation increases due to the concentration of the extract. However, the death of cells begins to change from early apoptosis to late apoptosis, called necrosis, if the extract is very intense (table 15). The results are consistent with numerous studies that found that substances in the flavonoid group may induce apoptosis of cancer cells. In addition, different types of flavonoid may exhibit differential effects in a multitude of cancer cells, such as flavonoids extracted from propolis may induce more apoptosis in breast cancer than in colon cancer. The chemical structure of different flavonoids may affect their antiradical activity and thus induce differential effects on cancer cell inhibition.

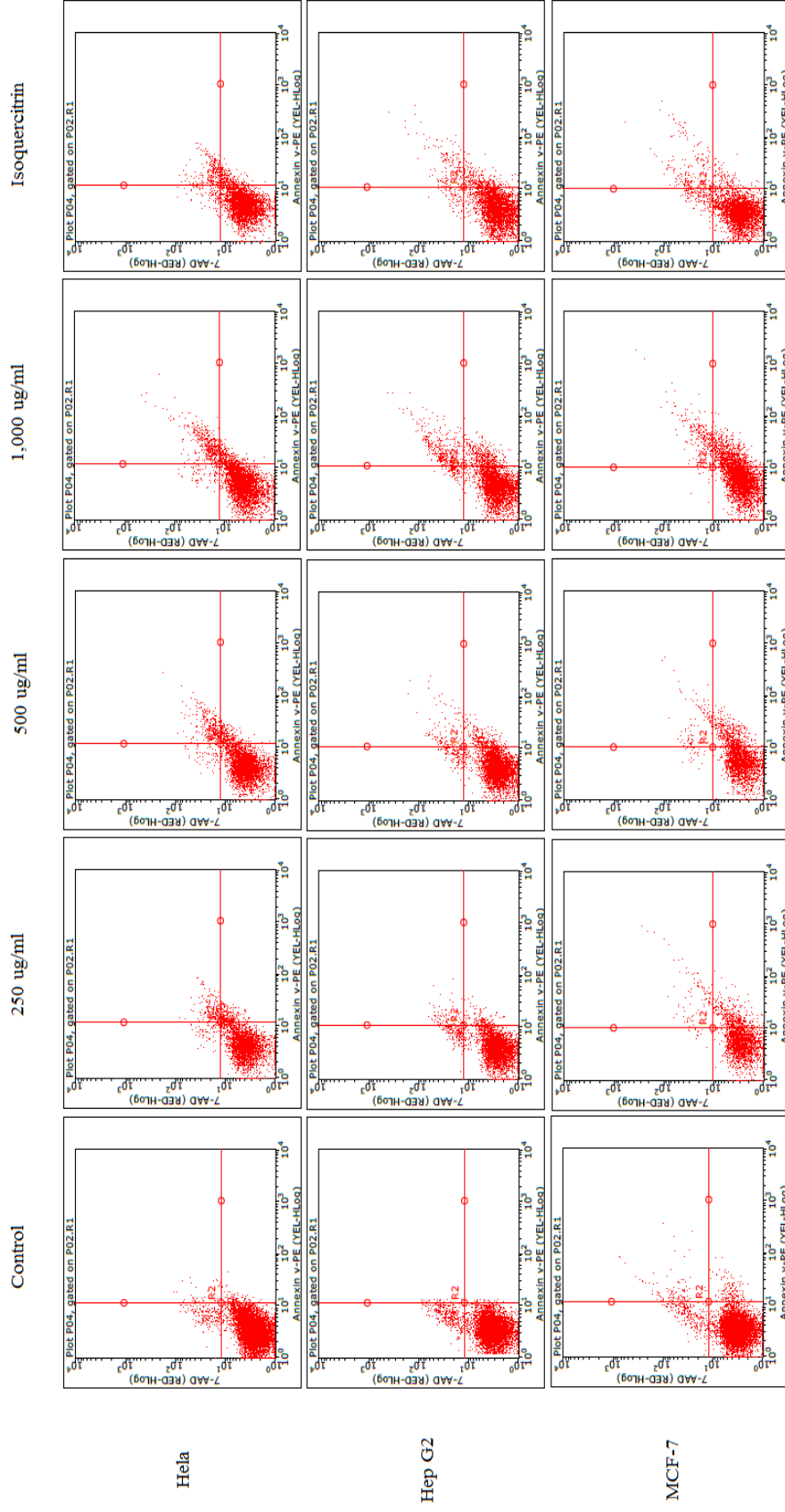


Figure 48. Cell apoptosis.

Table 15 Cell apoptosis.

	Control	25	50	100	250	500	750	1,000	Iso quercitrin
HeLa	Early apoptotic	4.13±0.13*	3.92±0.72*	4.20±0.18*	6.18±0.38*	6.41±0.23*	6.69±0.63*	6.55±0.13*	5.51±0.22*
	Necrosis	3.57±0.43*	5.23±1.03*	4.26±0.23*	5.18±0.91*	5.89±0.17*	7.85±0.62*	8.38±0.06*	3.87±0.08*
HepG2	Early apoptotic	3.21±0.09*	3.97±0.81*	5.19±0.21*	5.23±0.45*	5.36±0.24*	12.59±1.12*	10.59±0.21*	5.83±0.50*
	Necrosis	1.73±0.11*	1.67±0.19*	1.72±0.08*	2.00±0.12*	2.19±0.20*	3.47±0.38*	8.66±0.58*	3.22±0.32*
MCF-7	Early apoptotic	5.37±0.83*	5.60±2.46*	12.63±0.12*	15.21±1.14*	15.62±2.47*	21.78±6.08*	19.34±2.33*	3.11±0.73*
	Necrosis	3.34±0.58	3.29±0.61	4.60±0.73*	3.87±1.72*	5.52±0.47*	7.84±1.77*	8.05±2.16*	3.94±0.40

Cells were left untreated or treated with various concentrations of the Okra seed extract for 48 hrs. Cell apoptosis was determined by Annexin V and 7-AAD staining and cell lysate before being evaluated with flow cytometry. Values represented are relative apoptotic cells compared to control cells. Plots are mean  $\pm$  SD (n=3). \*P < 0.05 versus non treated controls.

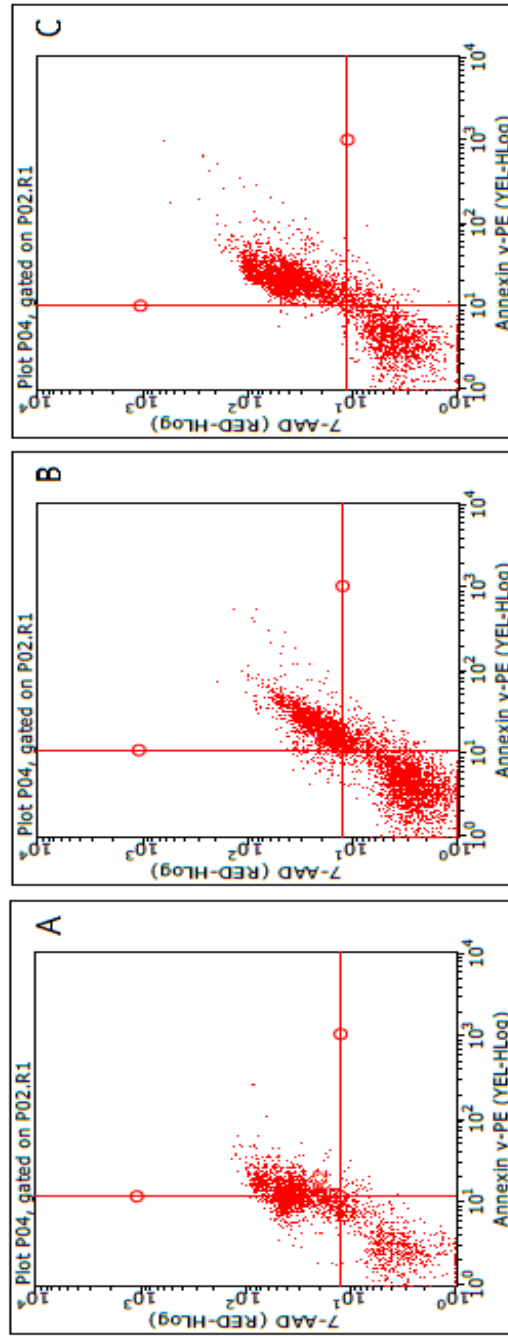


Figure 49. Cisplatin induce cell death (A: HeLa, B: HepG2 and C: MCF-7).

Compared to chemotherapy presently used, such as cisplatin and the Okra seed extract, it was found that cisplatin has higher necrosis death induction of cancer cells than apoptosis death. The disadvantage of this type of dead cells is that necrosis death often means the explosion of cells or leakage of cytoplasm. This will release cytokines to cause inflammation or fever after the death of cells. The Okra seed extract contains the induction effect to the apoptosis death, this is the good point for further development.

### 9. Anti- vascular endothelial growth factor test

Cancer cells use angiogenesis factor to promote their spread by creating new blood vessels. Factors involved are among others the Vascular Endothelial Growth Factor (VEGF). Many reports have established a relationship between VEGF and the progress of cancer (Hegde, Wallin and Mancao, 2018, Apte, Chen and Ferrara, 2019). The cancer will promote release VEGF to stimulate new blood vessel creation around it.. Therefore, the use of drugs or substances that can resist angiogenesis is another way to fight cancer.

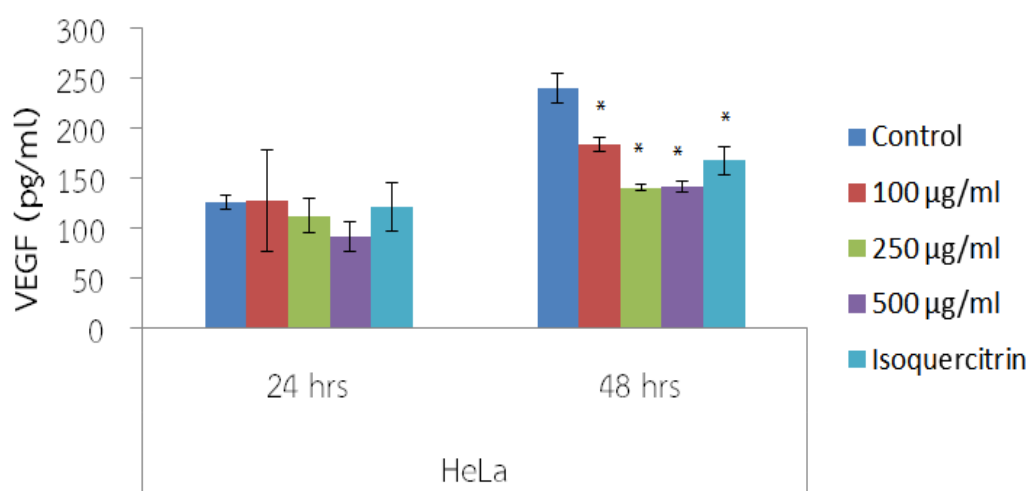


Figure 50. Anti-vascular endothelial growth factor (HeLa cell).

HeLa cells were left untreated or treated with various concentrations of the Okra seed extract for 48 hrs. VEGF was determined by sandwich Elisa assay. Values represented are relative VEGF concentrations compared to control cells.

Plots are mean  $\pm$  SD (n=3). \*P < 0.05 versus non treated controls.

In the present study, we observed that the OSE exerted its VEGF inhibition in a dose depended manner on all 3 cell lines both at 24 and 48 hours but this effect was only significant at 48 hours in accordance with previous reports on flavonoids and isoquercitrin. In the cervical Hela cancer cell line, VEGF inhibition is evident at 48 hours (figure48) at 250 ug/ml and 500 ug/ml, and significantly more efficient than isoquercitrin.

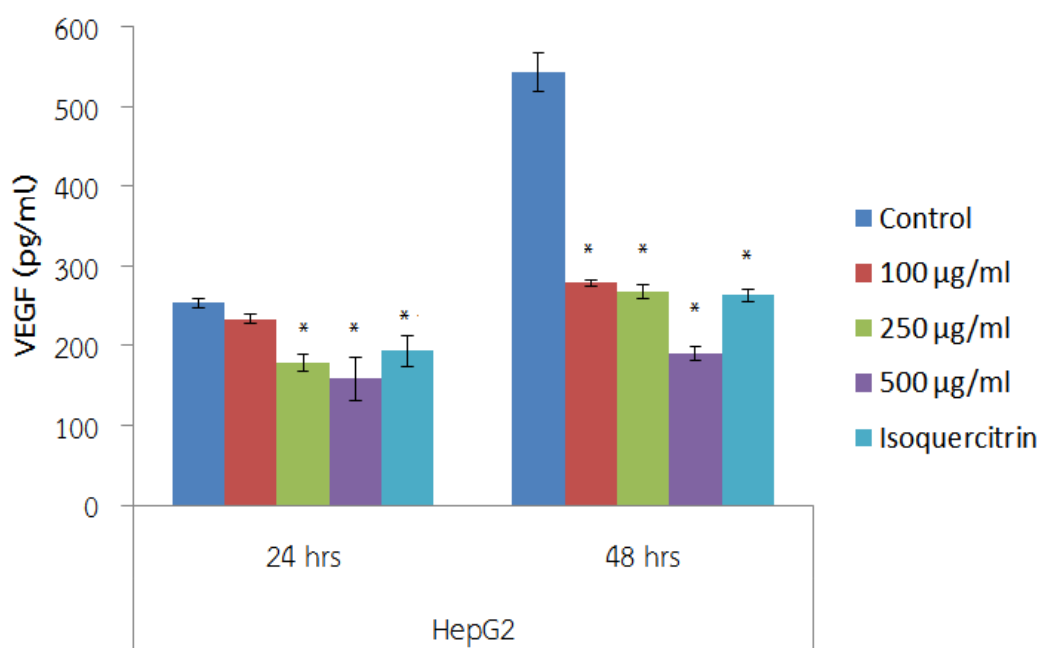


Figure 51. Anti-vascular endothelial growth factor (HepG2 cell).

HepG2 cells were left untreated or treated with various concentrations of the Okra seed extract for 48 hrs. VEGF was determined by sandwich Elisa assay. Values represented are relative VEGF concentrations compared to control cells.

Plots are mean  $\pm$  SD (n=3). \*P < 0.05 versus non treated controls

In the liver cancer cell line, OSE exerted its VEGF inhibition at 24 hours (figure49) with statistical significance. The effect is dose dependent, meaning the higher the concentration, the higher the VEGF inhibition. At 48 hours, the best effect was noted for the 500 ug/ml concentration. Isoquercitrin still displayed the same results as in other experiments, meaning the efficiency is not as good as when using the extract.

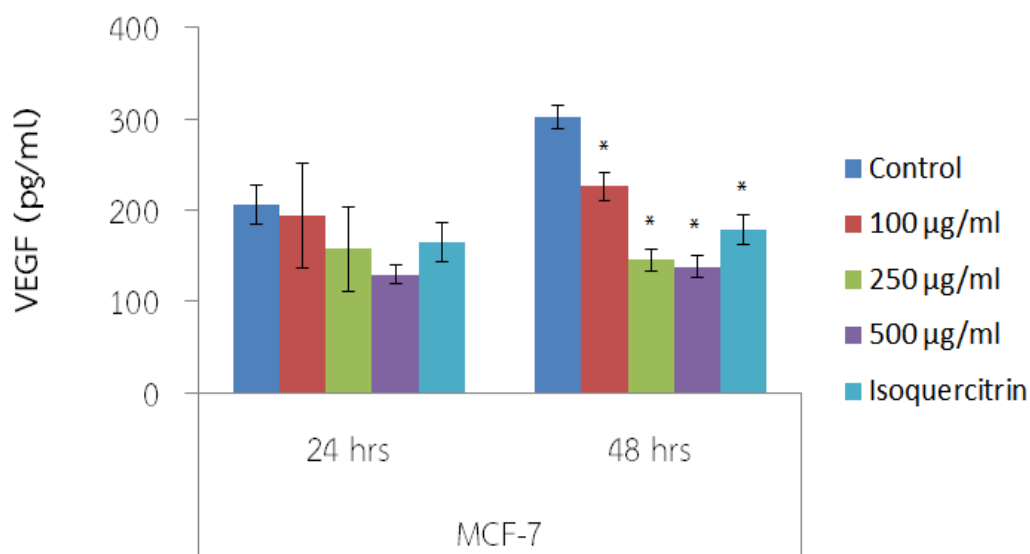


Figure 52. Anti-vascular endothelial growth factor (MCF-7 cell).

MCF-7 cells were left untreated or treated with various concentrations of the Okra seed extract for 48 hrs. VEGF was determined by sandwich Elisa assay. Values represented are relative VEGF concentrations compared to control cells.

Plots are mean  $\pm$  SD (n=3). \*P < 0.05 versus non treated controls.

In the breast cancer cell line (MCF-7) results were similar as for cervical cancer. Already at 24 hours there was a non-significant tendency to VEGF inhibition. After 48 hours of incubation, results became significant with dose dependent increase of inhibition effect. In the control group VEGF measured  $302.26 \pm 12.64$  pg/ml, while the groups of 100 µg/ml, 250 µg/ml, and 500 µg/ml concentrated OSE extract, the VEGF measured  $225.89 \pm 15.75$  pg/ml,  $145.22 \pm 11.76$  pg/ml, and  $137.81 \pm 11.56$  pg/ml, respectively. It was obvious that the release of VEGF was almost completely resisted since using the concentration at 250 µg/ml. Furthermore, VEGF release observed in liver cancer cell was the highest due to the fact that liver cells normally make new vessels. In other cancer cell types, VEGF values reported were 363 pg/ml for colorectal cancer and 399 pg/ml for other cancers (Kut,Mac Gabhann and Popel, 2007).

## 10. Formulation of Okra seed extract loaded polymeric micelles

After realizing the properties of the Okra seed extract and the pharmaceutical activity relating to cancer cells, the Okra seed extract could be developed into a drug delivery system. We selected the polymeric micelles carrier system to increase the solubility to the extract and test its efficiency on whether or not our delivery system could enhance the efficiency in resisting cancer cells. In the preparation, the thin film hydration method was used to compare the chemical and physical properties such as the size of the particle, zeta value, and entrapment efficiency.

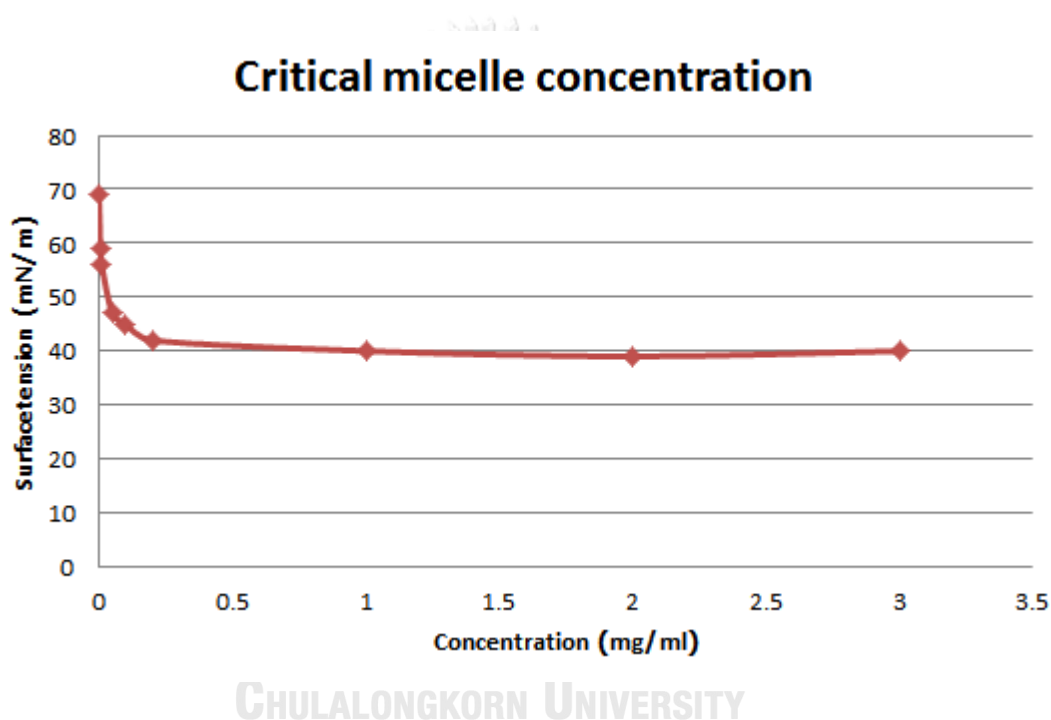


Figure 53. Critical micelle concentration of poloxamer 407.

Before starting the preparation of the particles for the polymeric micelle, the critical micelle concentration (CMC) was tested by Dunouy ring tensiometer for analysis of the surface tension of the poloxamer 407 to evaluate its concentration. The graph between the surface tension and the concentration at the lowest level before stabilizing the surface tension was plotted, which is called critical micelle concentration. The poloxamer 407 is a surfactant substance; therefore, the interfacial phenomena appeared in the form of positive absorption, which means the molecule of the poloxamer 407 will replace the molecule of water on the edge between

water and air. As a consequence, the surface tension reduced when the poloxamer 407's molecule was multiplied, until the molecule of poloxamer 407 would position in order to stabilize the surface tension and started to produce micelle (figure52). According to the experiment, it was found that poloxamer 407 had a CMC value = 0.04 mg/ml (figure51), which is similar to previous research (Ćirin, Krstonošić and Poša, 2017). The formula prepared and applied in this work used 50 mg of poloxamer 407 with the CMC approximately 1,250 fold. It was demonstrated that it could produce micelles at the lowest concentration to prepare particles.

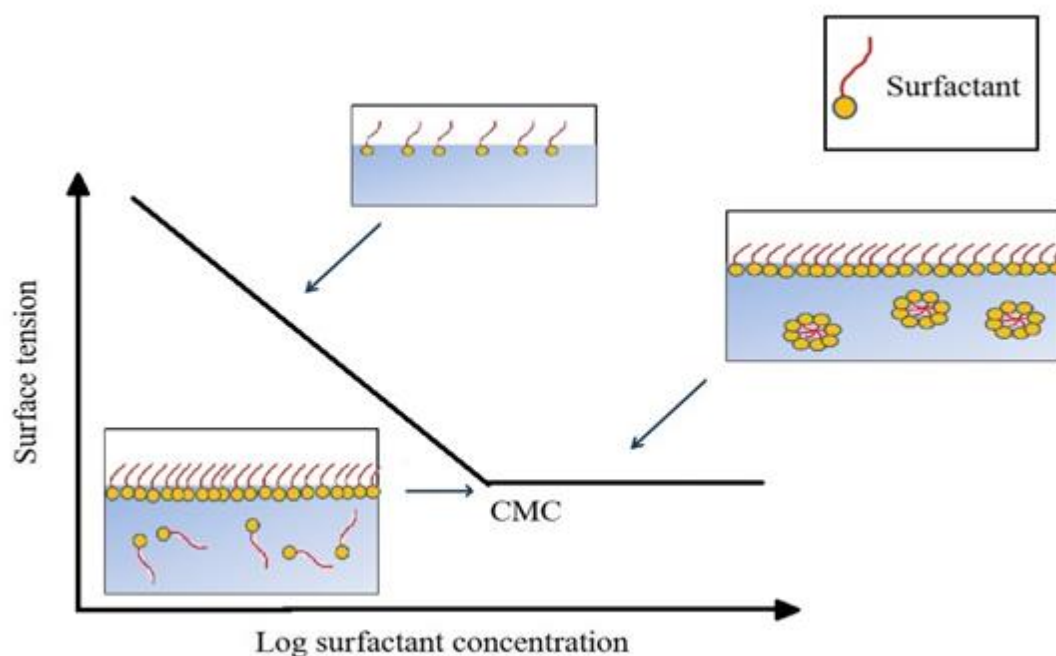


Figure 54. Surface tension and critical micelle concentration.

Table 16 Characterization of Okra seed extract loaded polymeric micelles.(n=3)

	Ratio (mg: mg) (extract: poloxamer)	Size (nm)	PDI	Zeta-potential	% EE
F1	50:50	391.63±43.52	0.36±0.04	-9.54±3.42	79.82±0.29
F2	50:100	404.03±36.46	0.42±0.08	-15.00±5.10	83.57±0.75
F3	50: 200	442.72±72.43	0.44±0.05	-15.27±3.88	86.56±0.54
F4	50: 500	190.23±46.96	0.34±0.05	-14.70±4.88	93.43±2.45
F5	50:1,000	167.57±110.58	0.99±0.01	-16.02±6.72	86.88±1.93
B1	0:200	381.57±49.17	0.26±0.16	-9.72±4.46	
B2	0:500	164.92±63.16	0.56±0.52	-11.48±5.19	
B3	0:1,000	174.91±93.03	0.97±0.12	-10.61±7.58	

In the process of micelle preparation, we observed that when the concentration of poloxamer 407 increases more than the CMC, the poloxamer molecules will move down from the water surface to form micelles, the size of which will increase continuously until an optimum level is reached. Particle size will then start decreasing due to the thermodynamic effect of micelle surface tension decreasing below the surface free energy level. Therefore, in order to maintain thermodynamic stability, micelle size decreased as to increase surface area (Yotsumoto et al., 2018, Janćzuk and Zdziennicka, 2019). In any case, according to the equation F5, we observed that when the concentration of Poloxamer407 increases the value of polydisperse index (PDI) also increases. Due to the high number of micelles, aggregation occurs which results in the formation of a new molecular size, from spherical to the rod shaped or bilayer sheet (Kamranfar and Jamialahmadi, 2014).

When considering the result of poloxamer 407 towards zeta-potential, it was found that the poloxamer 407 does not affect the change of polarity due to it being a nonionic surfactant although increasing its concentration, the zeta-potential still remains indifferent or near 0. It represented a small number of anions because the substance of flavonoid entrapped inside contains anions from the hydroxyl group in the structure of the phenol area. The final stage is to consider the concentration of the poloxamer 407 towards the entrapment of the extract. The proportion of 50:500 entrapped the drug at the highest level, or  $93.43 \pm 2.45\%$ . Regarding the factors resulting in the difference of drug entrapment, it could be explained through the result of micelles production towards the concentration of poloxamer 407. At the early stage, F1-F3 with the low concentration of poloxamer 407 produced incomplete micelles and the particles are large. However, PDI is low, which demonstrated the loose order arrangement of poloxamer 407's molecules. This resulted in micelle's instability and small entrapment capacity. When the concentration of poloxamer 407 increased to 500 mg, the quantity of surfactant was expected to be sufficient for the complete production of micelles. The particles were apparently small, resulting in better drug entrapment. As seen in figures 59-63, the difference in physical properties is visible. As in figure 62, the concentration is 50:500, so the solvent turned yellow the most. This conformed to the analytical result of entrapment efficiency that found the drug was entrapped in micelles the most. Meanwhile, at a proportion of 50:1,000 (F5), it was found that the entrapment efficiency reduced. In compliance with the result of particles, when the concentration of poloxamer 407 was multiplied until reaching 1,000 mg, though the particles were smaller the dispersion of particle size was high. Micelles positioned in order and size was larger to pass the membrane filter before analysis with UV-visible. The result, therefore, showed lower entrapment.



Figure 55 Okra seed extract loaded polymeric micelles (50:50)



Figure 56. Okra seed extract loaded polymeric micelles (50:100)



Figure 57. Okra seed extract loaded polymeric micelles (50:200)



Figure 58. Okra seed extract loaded polymeric micelles (50:500)



Figure 59. Okra seed extract loaded polymeric micelles (50:1,000)

The possibility of flavonoid substance entrapment in micelles from poloxamer 407 was expected when the poloxamer 407 formed micelles and they arranged in U-shape molecules by turning its polyoxyethylene, which is a hydrophilic chain to the outside, and turned the middle hydrophobic chain, which has the structure of polypropylene to the inside. The substance of flavonoid would cause charge interaction between flavonoid molecule and poloxamer 407 molecule with hydrogen bond (figure 58). This affected the polymeric micelles system that is able to carry the substance of flavonoid (Chat et al., 2011). With respect to the characterization data of the prepared delivery system, we could select the formula 50:500(F4) to apply in further study due to the size of particles being small and the entrapment efficiency being high.

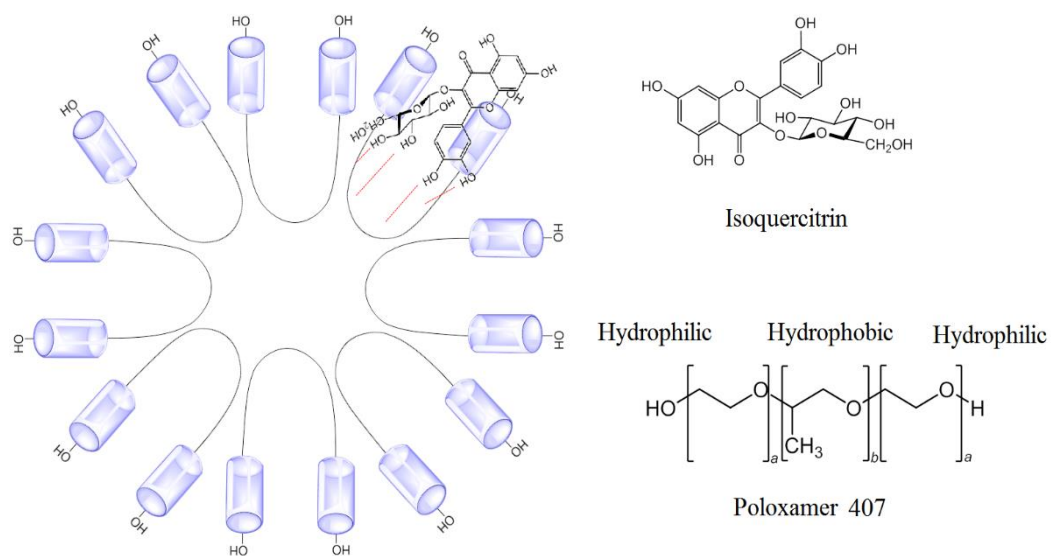


Figure 60. Possible location of isoquercitrin in micelles.

Based on the principle of colloids, OSE-loaded in polymeric micelles (F4) were tested with the chromatography method (Pozzi et al., 2013). Due to the negative charge of the cellulose made filter paper, OSE can be partitioned in the mobile phase (distilled water) when put as a spot on filter paper as flavonoids is OSE are negatively charged. Therefore, there is a repulsion force between flavonoid and filter paper. But if the particle is positively charged or neutral then the filter paper will attract it. In the present study, all of the micelles are expected to be able to load the flavonoid in the OSE, rendering the movement of the OSE in the micelles invisible and since poloxamer407 is a nonionic surfactant no negative charge is seen to repel from the hydroxyl group on filter paper.

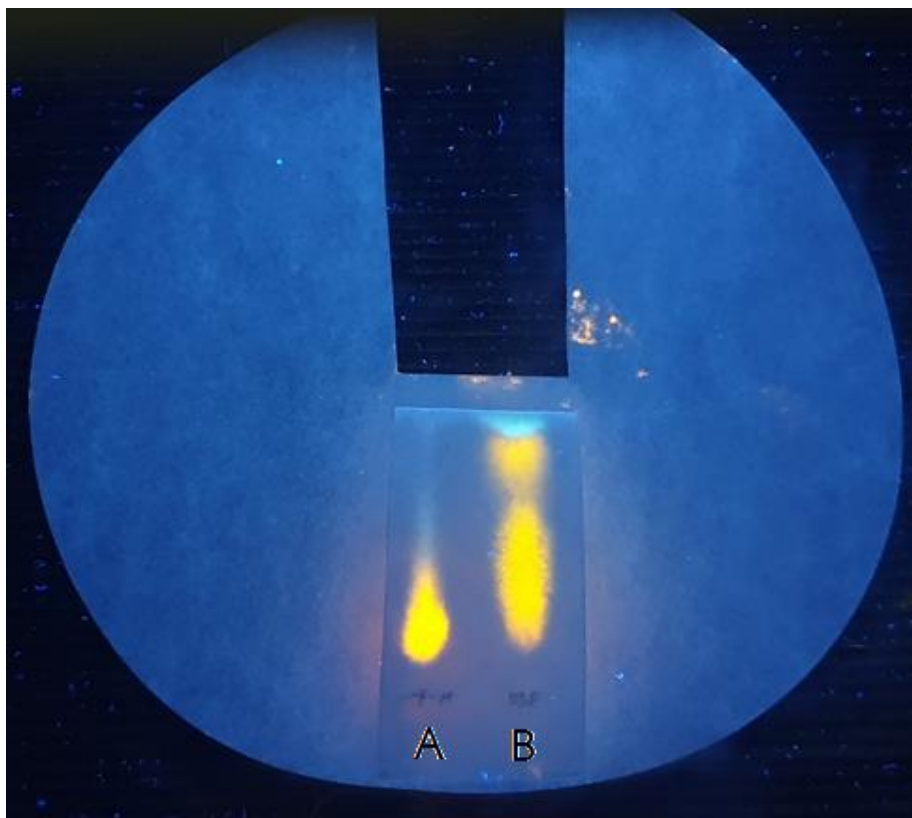


Figure 61. Chromatographic elution of Okra seed extract (A: OSE-micelles, B: OSE).

According to the test (figure59), after running TLC, the paper that was sprayed by NP-PEG reagent was used to check the difference. It was apparent that spot A, which was the Okra seed extract entrapped in the polymeric micelles delivery, moved through the mobile phase less than the crude. As a consequence, it was discovered by testing that the delivery system could entrap the extract.

### 11. Anticancer activity of Okra seed extract loaded polymeric micelles

In the experiment of anticancer activity efficiency of the polymeric micelles delivery system we compared the crude 500 ug/ml Okra seed extract, the Okra seed extract loaded polymeric micelles, in which the concentration was equivalent to the 500 ug/ml Okra seed extract and the blank polymeric micelle (figure60).

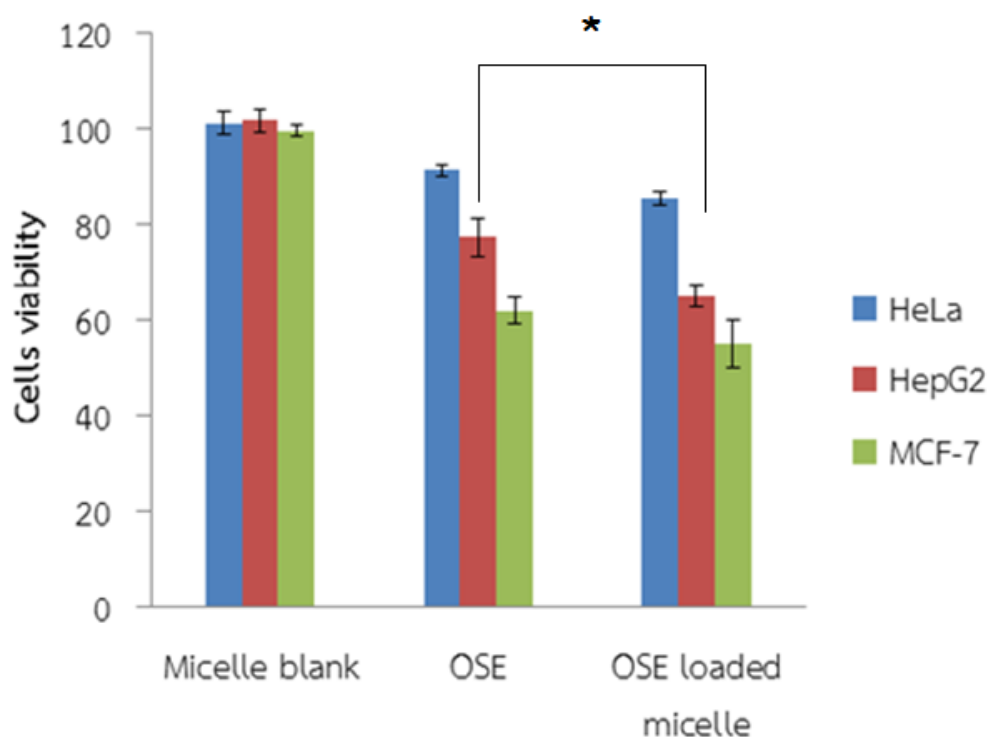


Figure 62. Cytotoxic activity of Okra seed extract loaded polymeric micelles. Cells were left treated for 48 hrs. with Okra seed extract loaded in polymeric micelles and were compared with unloaded Okra seed extract treatment. Cell viability was determined by presto blue assay. Values shown are relative cell viability compared to control cells. Plots are mean  $\pm$  SD (n=3).

\*P < 0.05 versus OSE-unloaded in polymeric micelles.

The blank polymeric micelles did not exert any cytotoxic effect to any of the cancer cell lines. When Okra seed extract was added to the polymeric micelles water solubility increased and cytotoxicity was enhanced (figure 60). The increased water solubility might increase the extract's penetration rate into the cells, thereby inhibiting their growth. However, the polymeric micelles delivery system's cytotoxicity increase was only significant in the HepG2 cell line with little change in the MCF-7 and HeLa lines. Previous studies reported that efflux pumps and p-glycoproteins are localized on the cell membrane of breast cancer cells and help transport substances in and out of the cells, potentially rendering them resistant to chemotherapy. Similar reports have been published on cervical cancer. In a recent

report, Hela cells appear to favor protein or peptide uptake more than positive charged nanoparticles (Mohebbi et al., 2019). The polymeric micelles delivery system used in the present study was an initial prototype aimed to increase the solubility of the Okra seed extract. Future studies are in order to devise more specific drug targeting system to cancer cells, such as conjugation to folic acid (Sharma and Agnihotri, 2019) or polymeric mixed micelle preparation to change surface charge of micelles in order to increase cellular uptake in some cancer cells (Yang et al., 2019a, Yang et al., 2019b).

## 12. Stability test

In the stability test of OSE-polymeric micelle after lyophilization, the products appeared as a white cake without adding the bulking agent in the original formula. After the stability test for 2 states, at 40°C and 4°C, the physical characteristics after 3 months did not change for either state. They still remained as white cakes in vials. After re-dispersal by water, particle size analysis, and zeta potential (table 17), the size of particles was not different in each month. The micelles after lyophilization became larger than when prepared before being lyophilized. The particle size became larger in the range 500-600 nm. The reason for the enlargement was due to re-dispersal without reducing particles with sonication as in the preparation process, thus simulating real world/hospital use where the use of a sonication is not available. So, when the micelles are produced in the early stage, their particles are large because of thermodynamic stability. If needed to reduce size, mechanical force is required to induce the system vibration, causing the size to decrease to preserve the thermodynamic stability. However, zeta potential was not different and remained in -10 mV range.

Table 17 Physical stability of the Okra seed extract loaded polymeric micelle after lyophilization. (n=3)

Condition/Time	0 month	1 month	2 month	3 month
Particle size				
4 Celsius degree	578.32±59.03	612.43±63.02	589.03±53.96	582.81±58.74
40 Celsius degree		593.24±48.61	605.72±68.23	584.28±53.16
Zata-potential				
4 Celsius degree	-12.56±2.18	-15.03±3.82	-9.64±5.73	-13.54±5.04
40 Celsius degree		-10.94±2.61	-12.38±2.41	-14.49±3.97

The analysis of flavonoid quantity after 3-month collection using UV-visible spectrophotometry at the 353 nm of wavelength reported that the quantity of flavonoid significantly decreased compared to day 0 after when stored at 40°C. In month 3, the quantity of flavonoid was 71.85%, compared to 92.17% on day 0 at 4°C (figure61). This was in agreement with the report that flavonoid substances may degrade easily due to catalysis from heat, humidity, or light. Standard isoquercitrin (Sigma Aldrich Company) should be handled at -20°C as slow degradation was reported in 4°C. This data may aid future product maintenance.

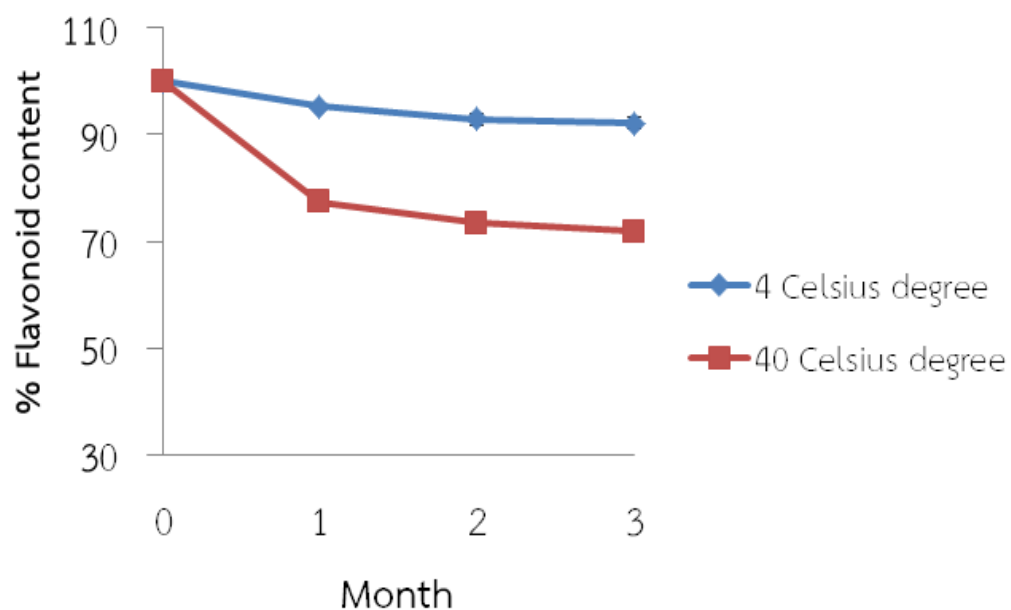


Figure 63. Stability of Okra seed extract loaded in polymeric micelle.

The flavonoid content of Okra seed extract loaded in polymeric micelle was determined by UV-visible spectrophotometry lamda 353 nm. Values represent flavonoid content at 4°C and 40°C. Plots are mean  $\pm$  SD (n=3).

## CHAPTER V

### CONCLUSION

The aim of the present study was to elucidate the phytochemical composition of the Okra seed extract and study the anticancer activity of its flavonoid-rich fraction, delivered in its native form as well as in the form of a polymeric micelle with enhanced solubility, in three carcinoma cell lines.

The physical characteristics of the extract included a yellow-brown powder without fragrance, though it could be liquid at room temperature. The extraction %yield was  $4.27 \pm 0.45\%$  and the DSC thermogram observed degradation starting at  $100^{\circ}\text{C}$ .

The phytochemical screening of the Okra seed extract reported reactions to the ferric chloride test, Shinoda test, sodium hydroxide test, and Molisch's test. These results demonstrate the presence of phenolic, flavonoid, and glycoside compounds, respectively.

Spectrophotometry analysis using FTIR, the major spectra are found as follows: OH stretching of OH group in the structures of flavonoid and glycoside, CH stretching of the alkyl group, the glycoside structure, and C=O ketone in flavonoid. After processing, it was expected that the extract would display flavonoid glycoside compounds. Considering the analytical results of HPLC chromatogram, it was found that the Okra seed extract contained 4 major components. The retention time is as follows: 16.948, 17.916, 20.065, and 21.187 minutes. One of the major components was isoquercitrin.

Antioxidant testing of the Okra seed extract by DPPH and ABTS employing free radical scavenging, the crude Okra seed extract, provided the highest antioxidant

readings at  $IC_{50} = 48.59 \pm 5.57$   $\mu\text{g/ml}$  and  $43.76 \pm 0.12$   $\mu\text{g/ml}$ , respectively. In the ethanol fraction, the Okra seed provided inferior antioxidant efficacy at  $IC_{50} = 56.65 \pm 8.80$   $\mu\text{g/ml}$  and  $49.04 \pm 0.43$   $\mu\text{g/ml}$ , respectively. The ethanol fraction displayed lower readings probably due to the degradation of the extract during partition and evaporation. Furthermore, the dichloromethane fraction and hexane fraction, could not be analyzed due to the fact that none of the components were found in these 2 layers because most of the contents have poles.

Regarding the extract's cytotoxic activity at studies in the cervical HeLa, liver HepG2, and breast MCF-7 cancer cell lines, the direct delivery of the crude Okra seed extract had the highest cytotoxic effect on the breast cancer cell line (MCF-7), followed by the hepatocellular carcinoma (HepG2) and cervical carcinoma (HeLa) cell lines in that order without any observed cytotoxicity on normal keratinocyte cells (HaCat).

The Okra seed extract's effect demonstrated a dose and time dependent cell proliferation and migration inhibition with differential effects in the 3 cancer cell lines. In the HeLa cell line, the Okra seed extract could significantly resist the migration of HeLa cells differently as compared to the control group, although the division resistance was not sufficiently effective. The effect on the HepG2 cells was different. The HepG2 cells grow and divide in groups in overlapping layers; hence, the split and side of the heel appears less noticeable when the HepG2 cells were scratched while the MCF-7 prefer to divide horizontally into a monolayer rather than overlapping. Monitoring apoptosis by labelling the cell membrane with annexin V and 7-AAD, we observed that the Okra seed extract could stimulate apoptosis and provide better efficiency than using isoquercitrin alone. The above described effects

are plausibly due to VEGF production inhibition, leading to apoptosis and cell death. The observed OSE effects on cancer cell lines may stem from the four flavonoid compounds observed in the current study, one of which was isoquercitrin. However, in view of the latter compound's isolated effects being inferior to those observed by the OSE, we hypothesize that either isoquercitrin requires the biological synergy of any one or all of the observed flavonoids, or any of the three in isolation or all in concert are responsible. Further studies are required to elucidate the nature of the three unknown compounds.

Finally, this study extracted Okra seed and prepared it in the form of polymeric micelles to apply in further industrial development. The study compared the proportion of poloxamer 407, which is a non-ionic surfactant, for preparing polymeric micelles at several proportions. It was discovered that the increase of poloxamer 407 resulted in smaller size micelles and increased efficiency in drug entrapment. The optimal proportions to use is 500 mg of poloxamer 407 and 50 mg of Okra seed extract; the particle size was  $190.23 \pm 46.96$  nm and the entrapment efficiency was  $93.43 \pm 2.45\%$ . The polymeric micelles delivery system's cytotoxicity increase was only significant in the HepG2 cell line with little change in the MCF-7 and HeLa lines. After the stability test, the delivery system was developed into dry powder for lyophilization with the intention of keeping the product longer and for easier delivery, including pharmaceutical applications using either oral route or injection. The prepared polymeric micelles were dried up and the final product looked as a white cake that could dissolve in water. However, we encountered some issue upon dissolving it in water resulting in bigger particle size than expected.

Furthermore, the amount of flavonoids was significantly reduced at 40°C. This information needs to be taken into account in future pharmaceutical applications.

Further studies are required to elucidate the nature of the three unknown compounds. Furthermore, as we encountered significant problems in dissolving the Okra seed extract and creating the polymeric micelles, further studies are needed to devise a clinically beneficial delivery and targeting system. Further studies are required to evaluate future pharmaceutical development in the form of products or combination with chemotherapy in order to increase efficiency of therapeutics effects and will expanded as well as research about concerning long-term safety and stability of a potential product.



## REFERENCES

- Abotaleb, M., Samuel, S. M., Varghese, E., Varghese, S., Kubatka, P., Liskova, A. and Büsselberg, D. (2018). Flavonoids in Cancer and Apoptosis. *Cancers*, 11, 28.
- Ahmed, N., Konduru, N. K., Ahmad, S. and Owais, M. (2014). Synthesis of flavonoids based novel tetrahydropyran conjugates (Prins products) and their antiproliferative activity against human cancer cell lines. *European Journal of Medicinal Chemistry*, 75, 233-246.
- Ahmed, S., Khan, H., Fratantonio, D., Hasan, M. M., Sharifi, S., Fathi, N., Ullah, H. and Rastrelli, L. (2019). Apoptosis induced by luteolin in breast cancer: Mechanistic and therapeutic perspectives. *Phytomedicine*, 152883.
- Alba, K., Laws, A. P. and Kontogiorgos, V. (2015). Isolation and characterization of acetylated LM-pectins extracted from okra pods. *Food Hydrocolloids*, 43, 726-735.
- Amado, N. G., Predes, D., Fonseca, B. F., Cerqueira, D. M., Reis, A. H., Dudenhoeffer, A. C., Borges, H. L., Mendes, F. A. and Abreu, J. G. (2014). Isoquercitrin suppresses colon cancer cell growth in vitro by targeting the Wnt/beta-catenin signaling pathway. *J Biol Chem*, 289, 35456-67.
- Amiji, M. M., Lai, P.-K., Shenoy, D. B. and Rao, M. (2002). Intratumoral Administration of Paclitaxel in an In Situ Gelling Poloxamer 407 Formulation. *Pharmaceutical Development and Technology*, 7, 195-202.
- Apte, R. S., Chen, D. S. and Ferrara, N. (2019). VEGF in Signaling and Disease: Beyond Discovery and Development. *Cell*, 176, 1248-1264.
- Batra, P. and Sharma, A. K. (2013). Anti-cancer potential of flavonoids: recent trends and future perspectives. *3 Biotech*, 3, 439-459.
- Belkhir, M., Rebai, O., Dhaouadi, K., Congiu, F., Tuberoso, C. I. G., Amri, M. and Fattouch, S. (2013). Comparative Analysis of Tunisian Wild *Crataegus azarolus* (Yellow Azarole) and *Crataegus monogyna* (Red Azarole) Leaf, Fruit, and Traditionally Derived Syrup: Phenolic Profiles and Antioxidant and Antimicrobial Activities of the Aqueous-Acetone Extracts. *Journal of Agricultural and Food Chemistry*, 61, 9594-9601.
- ben Sghaier, M., Pagano, A., Mousslim, M., Ammari, Y., Kovacic, H. and Luis, J. (2016). Rutin inhibits proliferation, attenuates superoxide production and decreases adhesion and migration of human cancerous cells. *Biomedicine & Pharmacotherapy*, 84, 1972-1978.

- Bhatia, N., Kaur, G., Soni, V., Kataria, J. and Dhawan, R. K. (2016). Evaluation of the wound healing potential of isoquercetin-based cream on scald burn injury in rats. *Burns & Trauma*, 4, 7-7.
- Biesaga, M. (2011). Influence of extraction methods on stability of flavonoids. *Journal of Chromatography A*, 1218, 2505-2512.
- Chanh, P. H., Ifansyah, N., Chahine, R., Mounayar-Chalfoun, A., Gleye, J. and Moulis, C. (1986). Comparative effects of total flavonoids extracted from *Ribes nigrum* leaves, rutin and isoquercitrin on biosynthesis and release of prostaglandins in the ex vivo rabbit heart. *Prostaglandins Leukot Med*, 22, 295-300.
- Chat, O. A., Najar, M. H., Mir, M. A., Rather, G. M. and Dar, A. A. (2011). Effects of surfactant micelles on solubilization and DPPH radical scavenging activity of Rutin. *Journal of Colloid and Interface Science*, 355, 140-149.
- Chen, C.-H., Huang, T.-S., Wong, C.-H., Hong, C.-L., Tsai, Y.-H., Liang, C.-C., Lu, F.-J. and Chang, W.-H. (2009). Synergistic anti-cancer effect of baicalein and silymarin on human hepatoma HepG2 Cells. *Food and Chemical Toxicology*, 47, 638-644.
- Chen, F., Chen, X., Yang, D., Che, X., Wang, J., Li, X., Zhang, Z., Wang, Q., Zheng, W., Wang, L., Wang, X. and Song, X. (2016). Isoquercitrin inhibits bladder cancer progression in vivo and in vitro by regulating the PI3K/Akt and PKC signaling pathways. *Oncol Rep*, 36, 165-72.
- Chen, H., Khemtong, C., Yang, X., Chang, X. and Gao, J. (2011). Nanonization strategies for poorly water-soluble drugs. *Drug discovery today*, 16, 354-360.
- Chen, Q., Li, P., Xu, Y., Li, Y. and Tang, B. (2015). Isoquercitrin inhibits the progression of pancreatic cancer in vivo and in vitro by regulating opioid receptors and the mitogen-activated protein kinase signalling pathway. *Oncol Rep*, 33, 840-8.
- Chen, Y.-J., Cheng, Y.-J., Hung, A. C., Wu, Y.-C., Hou, M.-F., Tyan, Y.-C. and Yuan, S.-S. F. (2013). The synthetic flavonoid WYC02-9 inhibits cervical cancer cell migration/invasion and angiogenesis via MAPK14 signaling. *Gynecologic Oncology*, 131, 734-743.
- Cimmino, L., Neel, B. G. and Aifantis, I. (2018). Vitamin C in Stem Cell Reprogramming and Cancer. *Trends in Cell Biology*, 28, 698-708.
- Ćirin, D., Krstonošić, V. and Poša, M. (2017). Properties of poloxamer 407 and polysorbate mixed micelles: Influence of polysorbate hydrophobic chain. *Journal of Industrial and Engineering Chemistry*, 47, 194-201.
- Dai, J., Van Wie, P. G., Fai, L. Y., Kim, D., Wang, L., Poyil, P., Luo, J. and Zhang, Z. (2016). Downregulation of NEDD9 by apigenin suppresses migration, invasion, and metastasis of colorectal cancer cells. *Toxicology and Applied Pharmacology*,

311, 106-112.

- Dai, X., Huang, Q., Zhou, B., Gong, Z., Liu, Z. and Shi, S. (2013). Preparative isolation and purification of seven main antioxidants from *Eucommia ulmoides* Oliv. (Du-zhong) leaves using HSCCC guided by DPPH-HPLC experiment. *Food Chemistry*, 139, 563-570.
- de Sousa Ferreira Soares, G., Assreuy, A. M. S., de Almeida Gadelha, C. A., de Moraes Gomes, V., Delatorre, P., da Conceição Simões, R., Cavada, B. S., Leite, J. F., Nagano, C. S., Pinto, N. V., de Luna Freire Pessoa, H. and Santi-Gadelha, T. (2012). Purification and Biological Activities of *Abelmoschus esculentus* Seed Lectin. *The Protein Journal*, 31, 674-680.
- Dela Cruz, C. S., Tanoue, L. T. and Matthay, R. A. (2011). Lung Cancer: Epidemiology, Etiology, and Prevention. *Clinics in chest medicine*, 32, 10.1016/j.ccm.2011.09.001.
- Esan, A. M., Masisi, K., Dada, F. A. and Olaiya, C. O. (2017). Comparative effects of indole acetic acid and salicylic acid on oxidative stress marker and antioxidant potential of okra (*Abelmoschus esculentus*) fruit under salinity stress. *Scientia Horticulturae*, 216, 278-283.
- Fan, S., Zhang, Y., Sun, Q., Yu, L., Li, M., Zheng, B., Wu, X., Yang, B., Li, Y. and Huang, C. (2014). Extract of okra lowers blood glucose and serum lipids in high-fat diet-induced obese C57BL/6 mice. *The Journal of Nutritional Biochemistry*, 25, 702-709.
- Farombi, E. O., Akinmoladun, A. C. and Owumi, S. E. (2019). Anti-cancer Foods: Flavonoids. In: Melton, L., Shahidi, F. and Varelis, P. (eds.) *Encyclopedia of Food Chemistry*. Oxford: Academic Press.
- Fernandes, M. D., Lima, F. S., Rodrigues, D., Handa, C., Guelfi, M., Garcia, S. and Ida, E. I. (2017). Evaluation of the isoflavone and total phenolic contents of kefir-fermented soymilk storage and after the in vitro digestive system simulation. *Food Chemistry*, 229, 373-380.
- Gates, J. (2013). Ethnomedicinal, phytochemical and pharmacological profile of genus *Abelmoschus*. *Phytopharmacology*, 4, 648-663.
- Ghori, M. U., Mohammad, M. A., Rudrangi, S. R. S., Fleming, L. T., Merchant, H. A., Smith, A. M. and Conway, B. R. (2017). Impact of purification on physicochemical, surface and functional properties of okra biopolymer. *Food Hydrocolloids*, 71, 311-320.
- Hegde, P. S., Wallin, J. J. and Mancao, C. (2018). Predictive markers of anti-VEGF and emerging role of angiogenesis inhibitors as immunotherapeutics. *Seminars in*

*Cancer Biology*, 52, 117-124.

- Hernández-Corroto, E., Marina, M. L. and García, M. C. (2018). Multiple protective effect of peptides released from *Olea europaea* and *Prunus persica* seeds against oxidative damage and cancer cell proliferation. *Food Research International*, 106, 458-467.
- Hu, Y., Li, Y., Zhang, W., Kou, G. and Zhou, Z. (2018). Physical stability and antioxidant activity of citrus flavonoids in arabic gum-stabilized microcapsules: Modulation of whey protein concentrate. *Food Hydrocolloids*, 77, 588-597.
- Hyun, H. B., Lee, W. S., Go, S. I., Nagappan, A., Park, C., Han, M. H., Hong, S. H., Kim, G., Kim, G. Y., Cheong, J., Ryu, C. H., Shin, S. C. and Choi, Y. H. (2015). The flavonoid morin from Moraceae induces apoptosis by modulation of Bcl-2 family members and Fas receptor in HCT 116 cells. *Int J Oncol*, 46, 2670-8.
- Jańczuk, B. and Zdziennicka, A. (2019). Critical micelle concentration, composition and thermodynamic properties of n-octyl- $\beta$ -d-glucopyranoside and sodium dodecylsulfate mixed micelles. *Journal of Molecular Liquids*, 286, 110748.
- Jarial, R., Shard, A., Thakur, S., Sakinah, M., Zularisam, A. W., Rezanian, S., Kanwar, S. S. and Singh, L. (2018). Characterization of flavonoids from fern *Cheilanthes tenuifolia* and evaluation of antioxidant, antimicrobial and anticancer activities. *Journal of King Saud University - Science*, 30, 425-432.
- Jiang, W. G., Sanders, A. J., Kato, M., Ungefroren, H., Gieseler, F., Prince, M., Thompson, S. K., Zollo, M., Spano, D., Dhawan, P., Sliva, D., Subbarayan, P. R., Sarkar, M., Honoki, K., Fujii, H., Georgakilas, A. G., Amedei, A., Niccolai, E., Amin, A., Ashraf, S. S., Ye, L., Helferich, W. G., Yang, X., Boosani, C. S., Guha, G., Ciriolo, M. R., Aquilano, K., Chen, S., Azmi, A. S., Keith, W. N., Bilsland, A., Bhakta, D., Halicka, D., Nowsheen, S., Pantano, F. and Santini, D. (2015). Tissue invasion and metastasis: Molecular, biological and clinical perspectives. *Seminars in Cancer Biology*, 35, S244-S275.
- Jin, X., Zhang, Y., Zhang, Z., Che, D. and Lv, H. (2016). Juglone loaded poloxamer 188/phospholipid mixed micelles evaluated in vitro and in vivo in breast cancer. *International Journal of Pharmaceutics*, 515, 359-366.
- Jindal, N. and Mehta, S. K. (2015). Nevirapine loaded Poloxamer 407/Pluronic P123 mixed micelles: Optimization of formulation and in vitro evaluation. *Colloids and Surfaces B: Biointerfaces*, 129, 100-106.
- Joshi, S., A Kedar, K., V Markana, U., Lodha, S., Shah, P., Vyas, H., B Vyas, R., Vyas, B. and Kalyankar, G. (2011). Alteration of gastric mucus secretion in rats treated with *Abelmoschus esculentus* seed mucilage. *Der Pharmacia Lettre*, 3(5), 183-188.

- Jurikova, T., Sochor, J., Rop, O., Mlcek, J., Balla, S., Szekeres, L., Adam, V. and Kizek, R. (2012). Polyphenolic profile and biological activity of Chinese hawthorn (*Crataegus pinnatifida* BUNGE) fruits. *Molecules (Basel, Switzerland)*, 17, 14490-14509.
- Kabanov, A. V., Batrakova, E. V. and Alakhov, V. Y. (2002). Pluronic® block copolymers for overcoming drug resistance in cancer. *Advanced Drug Delivery Reviews*, 54, 759-779.
- Kamranfar, P. and Jamialahmadi, M. (2014). Effect of surfactant micelle shape transition on the microemulsion viscosity and its application in enhanced oil recovery processes. *Journal of Molecular Liquids*, 198, 286-291.
- Karim, M. R., Islam, M. S., Sarkar, S. M., Murugan, A. C., Makky, E. A., Rashid, S. S. and Yusoff, M. M. (2014). Anti-amylolytic activity of fresh and cooked okra (*Hibiscus esculentus* L.) pod extract. *Biocatalysis and Agricultural Biotechnology*, 3, 373-377.
- Khazaei, S., Salehiniya, H. and Mohammadian-Hafshejani, A. (2015). Some Facts about Cancer in the World using Registered Cancer in 2012. *Iranian Journal of Public Health*, 44, 1559-1560.
- Kibe, S., Ohuchida, K., Ando, Y., Takesue, S., Nakayama, H., Abe, T., Endo, S., Koikawa, K., Okumura, T., Iwamoto, C., Shindo, K., Moriyama, T., Nakata, K., Miyasaka, Y., Shimamoto, M., Ohtsuka, T., Mizumoto, K., Oda, Y. and Nakamura, M. (2019). Cancer-associated acinar-to-ductal metaplasia within the invasive front of pancreatic cancer contributes to local invasion. *Cancer Letters*, 444, 70-81.
- Kim, T.-J., Byun, J.-S., Kwon, H. S. and Kim, D.-Y. (2018). Cellular toxicity driven by high-dose vitamin C on normal and cancer stem cells. *Biochemical and Biophysical Research Communications*, 497, 347-353.
- Kontogiorgos, V., Margelou, I., Georgiadis, N. and Ritzoulis, C. (2012). Rheological characterization of okra pectins. *Food Hydrocolloids*, 29, 356-362.
- Kpodo, F. M., Agbenorhevi, J. K., Alba, K., Bingham, R. J., Oduro, I. N., Morris, G. A. and Kontogiorgos, V. (2017). Pectin isolation and characterization from six okra genotypes. *Food Hydrocolloids*, 72, 323-330.
- Krakhmal, N. V., Zavyalova, M. V., Denisov, E. V., Vtorushin, S. V. and Perelmuter, V. M. (2015). Cancer Invasion: Patterns and Mechanisms. *Acta naturae*, 7, 17-28.
- Kraujalis, P. and Venskutonis, P. R. (2013). Supercritical carbon dioxide extraction of squalene and tocopherols from amaranth and assessment of extracts antioxidant activity. *The Journal of Supercritical Fluids*, 80, 78-85.
- Kut, C., Mac Gabhann, F. and Popel, A. S. (2007). Where is VEGF in the body? A meta-

- analysis of VEGF distribution in cancer. *British journal of cancer*, 97, 978-985.
- Lengsfeld, C., Titgemeyer, F., Faller, G. and Hensel, A. (2004). Glycosylated compounds from okra inhibit adhesion of *Helicobacter pylori* to human gastric mucosa. *J Agric Food Chem*, 52, 1495-503.
- Li, F., Li, C., Zhang, H., Lu, Z., Li, Z., You, Q., Lu, N. and Guo, Q. (2012). VI-14, a novel flavonoid derivative, inhibits migration and invasion of human breast cancer cells. *Toxicology and Applied Pharmacology*, 261, 217-226.
- Lim, W.-C., Kim, H., Kim, Y.-J., Park, S.-H., Song, J.-H., Lee, K. H., Lee, I. H., Lee, Y.-K., So, K. A., Choi, K.-C. and Ko, H. (2017). Delphinidin inhibits BDNF-induced migration and invasion in SKOV3 ovarian cancer cells. *Bioorganic & Medicinal Chemistry Letters*, 27, 5337-5343.
- Lima, A. I. G., Mota, J., Monteiro, S. A. V. S. and Ferreira, R. M. S. B. (2016). Legume seeds and colorectal cancer revisited: Protease inhibitors reduce MMP-9 activity and colon cancer cell migration. *Food Chemistry*, 197, 30-38.
- Lin, C., Wu, M. and Dong, J. (2012). Quercetin-4'-O- $\beta$ -D-glucopyranoside (QODG) Inhibits Angiogenesis by Suppressing VEGFR2-Mediated Signaling in Zebrafish and Endothelial Cells. *PLoS One*, 7, e31708.
- Liu, J., Zhao, Y., Wu, Q., John, A., Jiang, Y., Yang, J., Liu, H. and Yang, B. (2017). Structure characterisation of polysaccharides in vegetable "okra" and evaluation of hypoglycemic activity. *Food Chemistry*.
- Lu, Y. and Park, K. (2013). Polymeric micelles and alternative nanonized delivery vehicles for poorly soluble drugs. *International journal of pharmaceutics*, 453, 198-214.
- Mairuae, N., Connor, J. R., Lee, S. Y., Cheepsunthorn, P. and Tongjaroenbuangam, W. (2015). The effects of okra (*Abelmoschus esculentus* Linn.) on the cellular events associated with Alzheimer's disease in a stably expressed HFE neuroblastoma SH-SY5Y cell line. *Neuroscience Letters*, 603, 6-11.
- Males, Z., Plazibat, M., Vundac, V. B. and Zuntar, I. (2006). Qualitative and quantitative analysis of flavonoids of the strawberry tree - *Arbutus unedo* L. (Ericaceae). *Acta Pharm*, 56, 245-50.
- Maqsood, M., Qureshi, R., Ikram, M., Ahmad, M. S., Jabeen, B., Asi, M. R., Khan, J. A., Ali, S. and Lilge, L. (2018). In vitro anticancer activities of *Withania coagulans* against HeLa, MCF-7, RD, RG2, and INS-1 cancer cells and phytochemical analysis. *Integrative Medicine Research*, 7, 184-191.
- Masuko, T., Minami, A., Iwasaki, N., Majima, T., Nishimura, S.-I. and Lee, Y. C. (2005). Carbohydrate analysis by a phenol-sulfuric acid method in microplate format.

*Analytical Biochemistry*, 339, 69-72.

- Mendez-Lagunas, L., Rodríguez-Ramírez, J., Cruz-Gracida, M., Sandoval-Torres, S. and Barriada-Bernal, G. (2017). Convective drying kinetics of strawberry (*Fragaria ananassa*): Effects on antioxidant activity, anthocyanins and total phenolic content. *Food Chemistry*, 230, 174-181.
- Mérida-Ortega, Á., Hernández-Alcaraz, C., Hernández-Ramírez, R. U., García-Martínez, A., Trejo-Valdivia, B., Salinas-Rodríguez, A., Svensson, K., Cebrián, M. E., Franco-Marina, F. and López-Carrillo, L. (2016). Phthalate exposure, flavonoid consumption and breast cancer risk among Mexican women. *Environment International*, 96, 167-172.
- Messing, J., Thole, C., Niehues, M., Shevtsova, A., Glocker, E., Boren, T. and Hensel, A. (2014). Antiadhesive properties of *Abelmoschus esculentus* (Okra) immature fruit extract against *Helicobacter pylori* adhesion. *PLoS One*, 9, 1-10.
- Mohamed, E. A., Abu Hashim, I. I., Yusif, R. M., Suddek, G. M., Shaaban, A. A. A. and Badria, F. A. E. (2017). Enhanced in vitro cytotoxicity and anti-tumor activity of vorinostat-loaded pluronic micelles with prolonged release and reduced hepatic and renal toxicities. *European Journal of Pharmaceutical Sciences*, 96, 232-242.
- Mohebbi, S., Tohidi Moghadam, T., Nikkhah, M. and Behmanesh, M. (2019). RGD-HK Peptide-Functionalized Gold Nanorods Emerge as Targeted Biocompatible Nanocarriers for Biomedical Applications. *Nanoscale Research Letters*, 14, 13.
- Monte, L. G., Santi-Gadelha, T., Reis, L. B., Braganhol, E., Prietsch, R. F., Dellagostin, O. A., e Lacerda, R. R., Gadelha, C. A. A., Conceição, F. R. and Pinto, L. S. (2014). Lectin of *Abelmoschus esculentus* (okra) promotes selective antitumor effects in human breast cancer cells. *Biotechnology Letters*, 36, 461-469.
- Nafees, S., Mehdi, S. H., Zafaryab, M., Zeya, B., Sarwar, T. and Rizvi, M. A. (2018). Synergistic Interaction of Rutin and Silibinin on Human Colon Cancer Cell Line. *Archives of Medical Research*, 49, 226-234.
- Newton, A. M. J., Indana, V. L. and Kumar, J. (2015). Chronotherapeutic drug delivery of Tamarind gum, Chitosan and Okra gum controlled release colon targeted directly compressed Propranolol HCl matrix tablets and in-vitro evaluation. *International Journal of Biological Macromolecules*, 79, 290-299.
- Nguyen, L. T., Lee, Y.-H., Sharma, A. R., Park, J.-B., Jagga, S., Sharma, G., Lee, S.-S. and Nam, J.-S. (2017). Quercetin induces apoptosis and cell cycle arrest in triple-negative breast cancer cells through modulation of Foxo3a activity. *The Korean journal of physiology & pharmacology : official journal of the Korean*

- Physiological Society and the Korean Society of Pharmacology*, 21, 205-213.
- Olennikov, D. N., Tankhaeva, L. M., Partilkhayev, V. V. and Rokhin, A. V. (2012). Chemical constituents of *Caragana bungei* shoots. *Revista Brasileira de Farmacognosia*, 22, 490-496.
- Pellosi, D. S., Tessaro, A. L., Moret, F., Gaio, E., Reddi, E., Caetano, W., Quaglia, F. and Hioka, N. (2016). Pluronic® mixed micelles as efficient nanocarriers for benzoporphyrin derivatives applied to photodynamic therapy in cancer cells. *Journal of Photochemistry and Photobiology A: Chemistry*, 314, 143-154.
- Pozzi, F., Shibayama, N., Leona, M. and Lombardi, J. R. (2013). TLC-SERS study of Syrian rue (*Peganum harmala*) and its main alkaloid constituents. *Journal of Raman Spectroscopy*, 44, 102-107.
- Roswall, N. and Weiderpass, E. (2015). Alcohol as a Risk Factor for Cancer: Existing Evidence in a Global Perspective. *Journal of Preventive Medicine and Public Health*, 48, 1-9.
- Russo, A., Pellosi, D. S., Pagliara, V., Milone, M. R., Pucci, B., Caetano, W., Hioka, N., Budillon, A., Ungaro, F., Russo, G. and Quaglia, F. (2016). Biotin-targeted Pluronic® P123/F127 mixed micelles delivering niclosamide: A repositioning strategy to treat drug-resistant lung cancer cells. *International Journal of Pharmaceutics*, 511, 127-139.
- Seal, T. (2016). Quantitative HPLC analysis of phenolic acids, flavonoids and ascorbic acid in four different solvent extracts of two wild edible leaves, *Sonchus arvensis* and *Oenanthe linearis* of North-Eastern region in India. *Journal of Applied Pharmaceutical Science*, 6, 157-166.
- Sengkhamparn, N., Sagis, L. M. C., de Vries, R., Schols, H. A., Sajjaanantakul, T. and Voragen, A. G. J. (2010). Physicochemical properties of pectins from okra (*Abelmoschus esculentus* (L.) Moench). *Food Hydrocolloids*, 24, 35-41.
- Sengkhamparn, N., Verhoef, R., Schols, H. A., Sajjaanantakul, T. and Voragen, A. G. (2009). Characterisation of cell wall polysaccharides from okra (*Abelmoschus esculentus* (L.) Moench). *Carbohydr Res*, 344, 1824-32.
- Shanmugapriya, K., Kim, H. and Kang, H. W. (2019). In vitro antitumor potential of astaxanthin nanoemulsion against cancer cells via mitochondrial mediated apoptosis. *International Journal of Pharmaceutics*, 560, 334-346.
- Sharma, B. and Agnihotri, N. (2019). Role of cholesterol homeostasis and its efflux pathways in cancer progression. *The Journal of Steroid Biochemistry and Molecular Biology*, 191, 105377.
- Sharma, K., Ko, E. Y., Assefa, A. D., Ha, S., Nile, S. H., Lee, E. T. and Park, S. W. (2015).

- Temperature-dependent studies on the total phenolics, flavonoids, antioxidant activities, and sugar content in six onion varieties. *Journal of Food and Drug Analysis*, 23, 243-252.
- Singla, P., Singh, O., Chabba, S., Aswal, V. K. and Mahajan, R. K. (2018). Sodium deoxycholate mediated enhanced solubilization and stability of hydrophobic drug Clozapine in pluronic micelles. *Spectrochimica Acta Part A: Molecular and Biomolecular Spectroscopy*, 191, 143-154.
- Stankovic, M. (2011). Total phenolic content, flavonoid concentration and antioxidant activity of Marrubium peregrinum L. Extracts. *Kragujevac J. Sci.* 33, 33, 63-72.
- Stankovic, M. S., Niciforovic, N., Topuzovic, M. and Solujic, S. (2011). Total Phenolic Content, Flavonoid Concentrations and Antioxidant Activity, of the Whole Plant and Plant Parts Extracts from Teucrium Montanum L. Var. Montanum, F. Supinum (L.) Reichenb. *Biotechnology & Biotechnological Equipment*, 25, 2222-2227.
- Tian, Z. H., Miao, F. T., Zhang, X., Wang, Q. H., Lei, N. and Guo, L. C. (2015). Therapeutic effect of okra extract on gestational diabetes mellitus rats induced by streptozotocin. *Asian Pac J Trop Med*, 8, 1038-1042.
- Tima, S., Anuchapreeda, S., Ampasavate, C., Berkland, C. and Okonogi, S. (2017). Stable curcumin-loaded polymeric micellar formulation for enhancing cellular uptake and cytotoxicity to FLT3 overexpressing EoL-1 leukemic cells. *European Journal of Pharmaceutics and Biopharmaceutics*, 114, 57-68.
- Valentová, K., Vrba, J., Banciřová, M., Ulrichová, J. and Křen, V. (2014). Isoquercitrin: Pharmacology, toxicology, and metabolism. *Food and Chemical Toxicology*, 68, 267-282.
- Vayssade, M., Sengkhampan, N., Verhoef, R., Delaigue, C., Goundiam, O., Vigneron, P., Voragen, A. G., Schols, H. A. and Nagel, M. D. (2010). Antiproliferative and proapoptotic actions of okra pectin on B16F10 melanoma cells. *Phytother Res*, 24, 982-9.
- Vemuri, S. K., Banala, R. R., Subbaiah, G. P. V., Srivastava, S. K., Reddy, A. V. G. and Malarvili, T. (2017). Anti-cancer potential of a mix of natural extracts of turmeric, ginger and garlic: A cell-based study. *Egyptian Journal of Basic and Applied Sciences*, 4, 332-344.
- Venturelli, S., Burkard, M., Biendl, M., Lauer, U. M., Frank, J. and Busch, C. (2016). Prenylated chalcones and flavonoids for the prevention and treatment of cancer. *Nutrition*, 32, 1171-1178.
- Vlase, L., Parvu, M., Parvu, E. A. and Toiu, A. (2012). Chemical constituents of three

- Allium species from Romania. *Molecules*, 18, 114-27.
- Wang, H., Lai, Y.-J., Chan, Y.-L., Li, T.-L. and Wu, C.-J. (2011). Epigallocatechin-3-gallate effectively attenuates skeletal muscle atrophy caused by cancer cachexia. *Cancer Letters*, 305, 40-49.
- Wang, J., Gong, A., Gu, S., Cui, H. and Wu, X. (2015a). Ultrafast synthesis of isoquercitrin by enzymatic hydrolysis of rutin in a continuous-flow microreactor. *J. Serb. Chem. Soc.*, 80, 853-866.
- Wang, J., Gong, A., Yang, C. F., Bao, Q., Shi, X. Y., Han, B. B., Wu, X. Y. and Wu, F. A. (2015b). An effective biphasic system accelerates hesperidinase-catalyzed conversion of rutin to isoquercitrin. *Sci Rep*, 5, 8682.
- Wang, J., Man, G. C. W., Chan, T. H., Kwong, J. and Wang, C. C. (2017). A prodrug of green tea polyphenol (–)-epigallocatechin-3-gallate (Pro-EGCG) serves as a novel angiogenesis inhibitor in endometrial cancer. *Cancer Letters*.
- Wang, Z.-H. and Zhan-Sheng, H. (2018). Catalpol inhibits migration and induces apoptosis in gastric cancer cells and in athymic nude mice. *Biomedicine & Pharmacotherapy*, 103, 1708-1719.
- Wen, L., Wu, D., Jiang, Y., Prasad, K. N., Lin, S., Jiang, G., He, J., Zhao, M., Luo, W. and Yang, B. (2014). Identification of flavonoids in litchi (*Litchi chinensis* Sonn.) leaf and evaluation of anticancer activities. *Journal of Functional Foods*, 6, 555-563.
- Wong, R. S. Y. (2011). Apoptosis in cancer: from pathogenesis to treatment. *Journal of experimental & clinical cancer research : CR*, 30, 87-87.
- Xia, F., Zhong, Y., Li, M., Chang, Q., Liao, Y., Liu, X. and Pan, R. (2015). Antioxidant and Anti-Fatigue Constituents of Okra. *Nutrients*, 7, 8846-58.
- Xia, R., Xu, G., Huang, Y., Sheng, X., Xu, X. and Lu, H. (2018). Hesperidin suppresses the migration and invasion of non-small cell lung cancer cells by inhibiting the SDF-1/CXCR-4 pathway. *Life Sciences*, 201, 111-120.
- Xu, W., Ling, P. and Zhang, T. (2013). Polymeric micelles, a promising drug delivery system to enhance bioavailability of poorly water-soluble drugs. *Journal of drug delivery*, 2013.
- Yang, C., Li, F., Zhang, X., Wang, L., Zhou, Z. and Wang, M. (2013). Phenolic antioxidants from *Rosa soulieana* flowers. *Natural Product Research*, 27, 2055-2058.
- Yang, C., Yuan, C., Liu, W., Guo, J., Feng, D., Yin, X., Lin, W., Shuttleworth, P. S. and Yue, H. (2019a). DPD studies on mixed micelles self-assembled from MPEG-PDEAEMA and MPEG-PCL for controlled doxorubicin release. *Colloids and Surfaces B: Biointerfaces*, 178, 56-65.
- Yang, M., Ding, H., Zhu, Y., Ge, Y. and Li, L. (2019b). Co-delivery of paclitaxel and

- doxorubicin using mixed micelles based on the redox sensitive prodrugs. *Colloids and Surfaces B: Biointerfaces*, 175, 126-135.
- Yotsumoto, K., Ishii, K., Kokubo, M. and Yasuoka, S. (2018). Improvement of the skin penetration of hydrophobic drugs by polymeric micelles. *International Journal of Pharmaceutics*, 553, 132-140.
- Yun, J., Lee, H., Ko, H. J., Woo, E.-R. and Lee, D. G. (2015). Fungicidal effect of isoquercitrin via inducing membrane disturbance. *Biochimica et Biophysica Acta (BBA) - Biomembranes*, 1848, 695-701.
- Zang, M., Hu, L., Zhang, B., Zhu, Z., Li, J., Zhu, Z., Yan, M. and Liu, B. (2017). Luteolin suppresses angiogenesis and vasculogenic mimicry formation through inhibiting Notch1-VEGF signaling in gastric cancer. *Biochemical and Biophysical Research Communications*, 490, 913-919.
- Zhang, H. X., Du, G. H. and Zhang, J. T. (2004). Assay of mitochondrial functions by resazurin in vitro. *Acta Pharmacol Sin*, 25, 385-9.
- Zhang, J., Wu, Y., Zhao, X., Luo, F., Li, X., Zhu, H., Sun, C. and Chen, K. (2014). Chemopreventive effect of flavonoids from Ougan (*Citrus reticulata* cv. Suavissima) fruit against cancer cell proliferation and migration. *Journal of Functional Foods*, 10, 511-519.
- Zhang, Y., Chen, S., Wei, C., Rankin, G. O., Ye, X. and Chen, Y. C. (2018). Flavonoids from Chinese bayberry leaves induced apoptosis and G1 cell cycle arrest via Erk pathway in ovarian cancer cells. *European Journal of Medicinal Chemistry*, 147, 218-226.
- Zhao, J., Fang, Z., Zha, Z., Sun, Q., Wang, H., Sun, M. and Qiao, B. (2019). Quercetin inhibits cell viability, migration and invasion by regulating miR-16/HOXA10 axis in oral cancer. *European Journal of Pharmacology*, 847, 11-18.
- Zheng, A.-W., Chen, Y.-Q., Fang, J., Zhang, Y.-L. and Jia, D.-D. (2017a). Xiaoaiping combined with cisplatin can inhibit proliferation and invasion and induce cell cycle arrest and apoptosis in human ovarian cancer cell lines. *Biomedicine & Pharmacotherapy*, 89, 1172-1177.
- Zheng, A.-W., Chen, Y.-Q., Fang, J., Zhang, Y.-L. and Jia, D.-D. (2017b). Xiaoaiping combined with cisplatin can inhibit proliferation and invasion and induce cell cycle arrest and apoptosis in human ovarian cancer cell lines. *Biomedicine & Pharmacotherapy*, 89, 1172-1177.

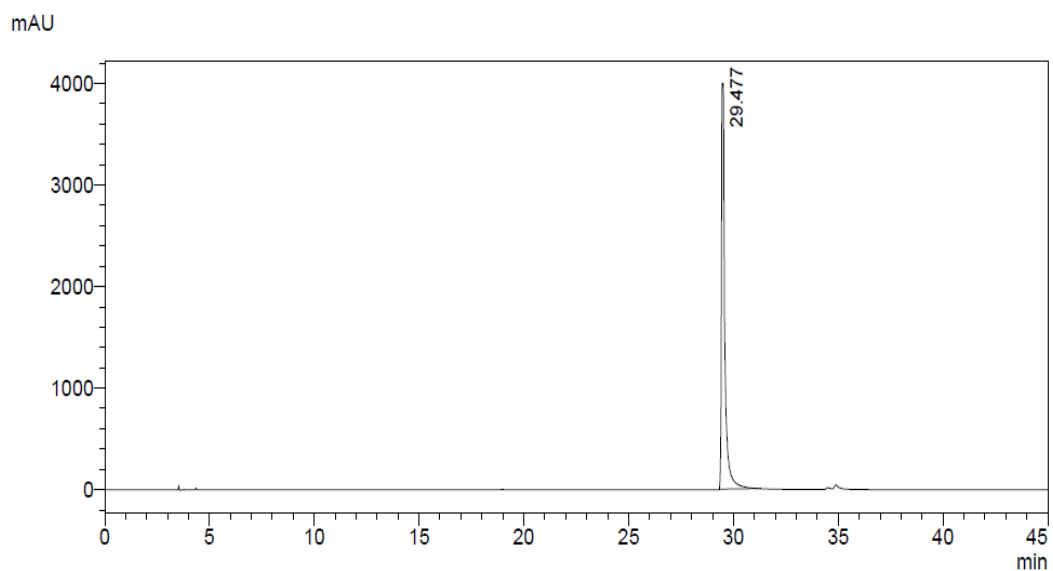


## Appendices

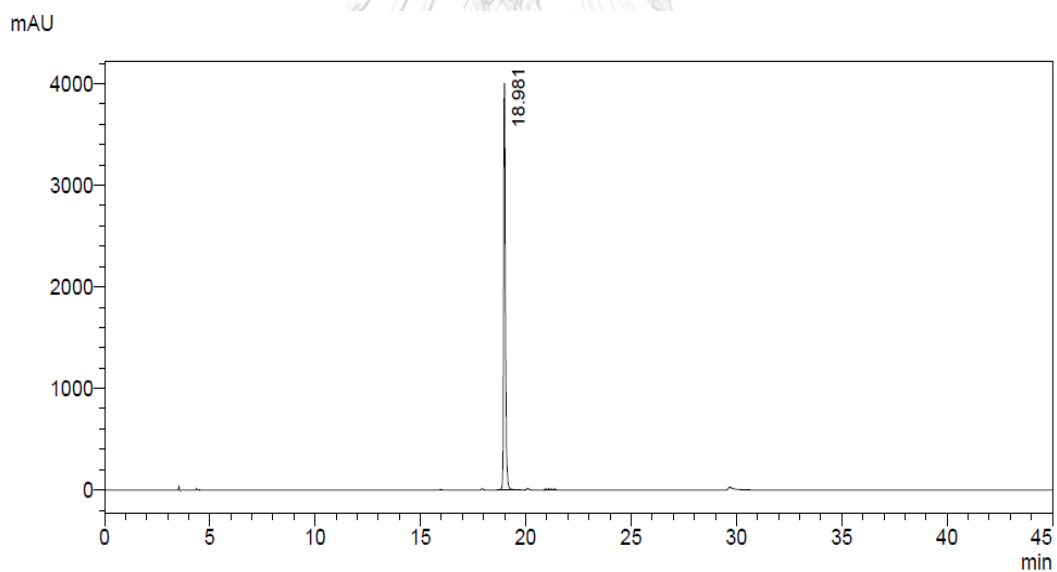
จุฬาลงกรณ์มหาวิทยาลัย  
**CHULALONGKORN UNIVERSITY**

## Appendix A

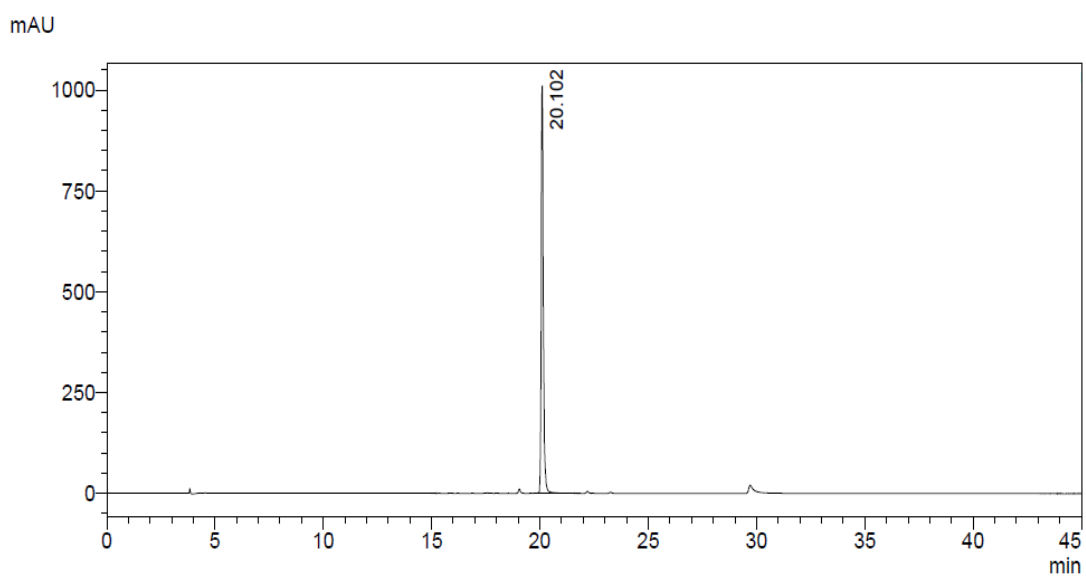
HPLC chromatogram



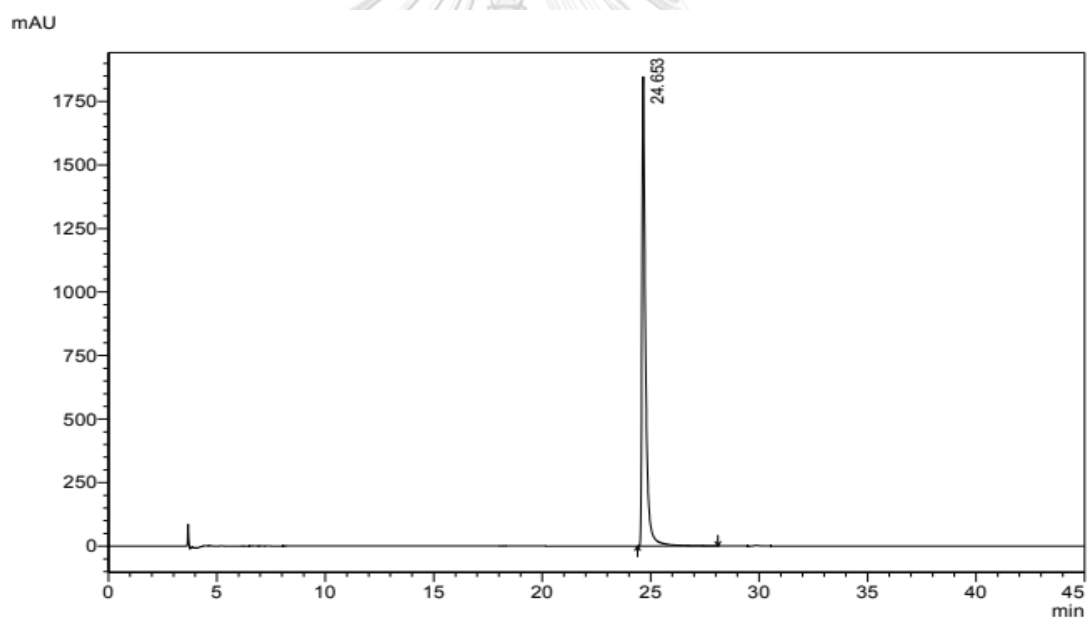
HPLC chromatogram of the standard quercetin



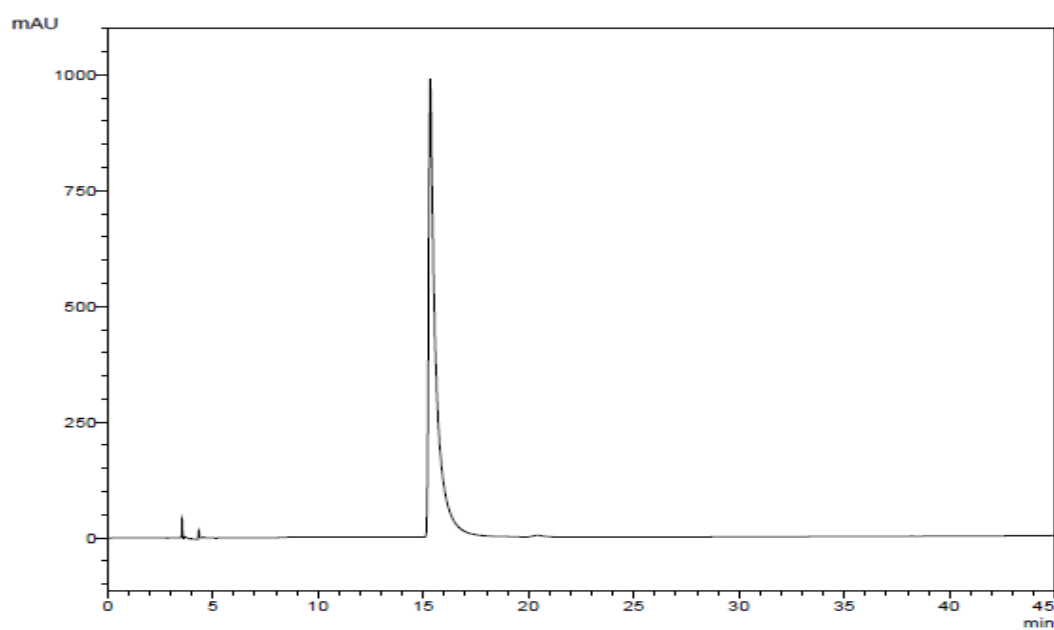
HPLC chromatogram of the standard rutin



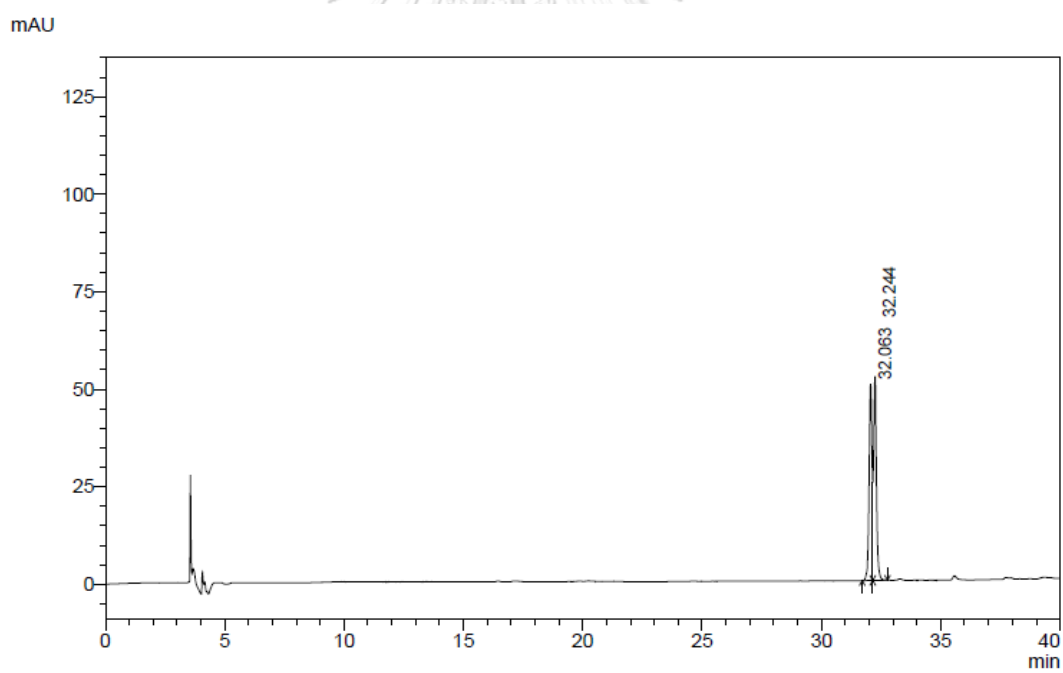
HPLC chromatogram of the standard isoquercitrin



HPLC chromatogram of the standard myricetin

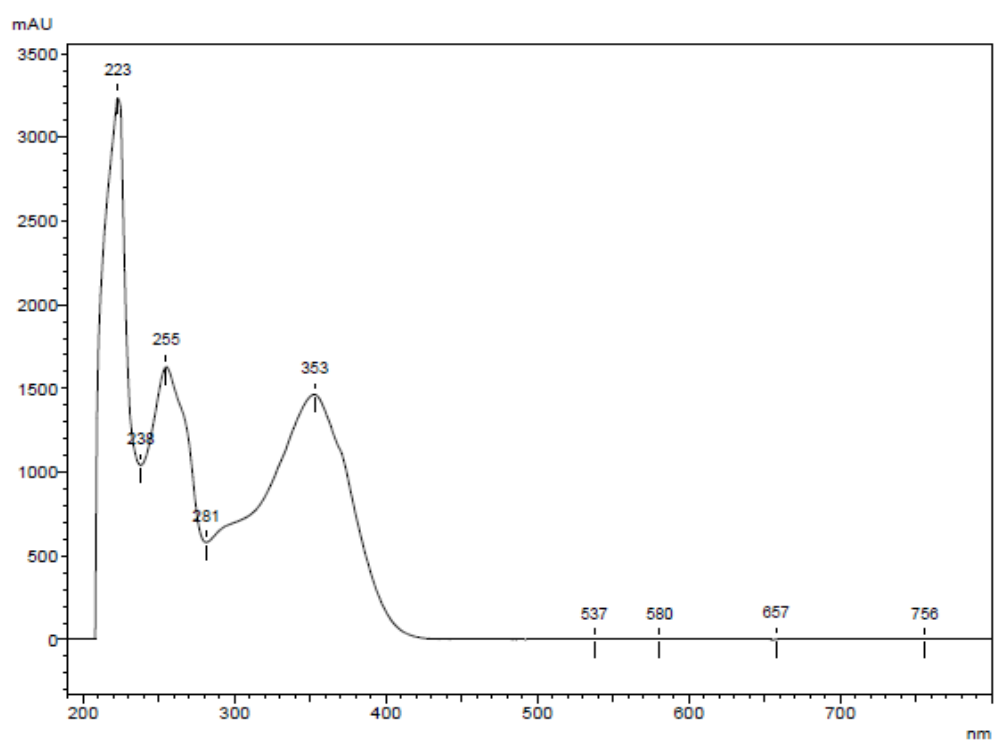


HPLC chromatogram of the standard epigallocatechin-3-gallate (EGCG)



HPLC chromatogram of the standard siribinin

==== Shimadzu LabSolutions UV Spectrum ====

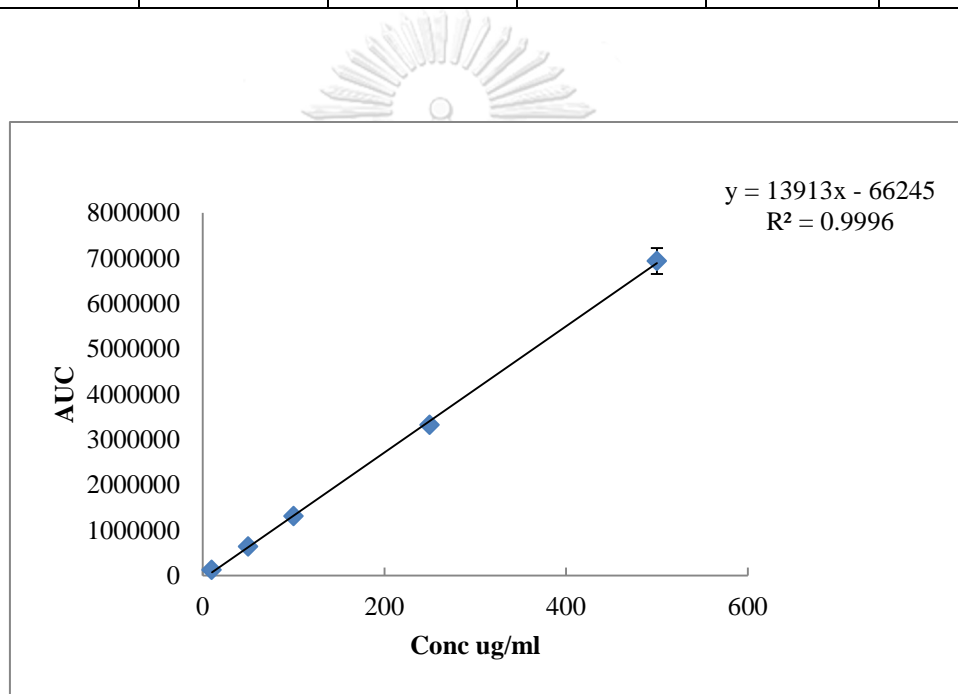


UV spectrum of Okra seed extract

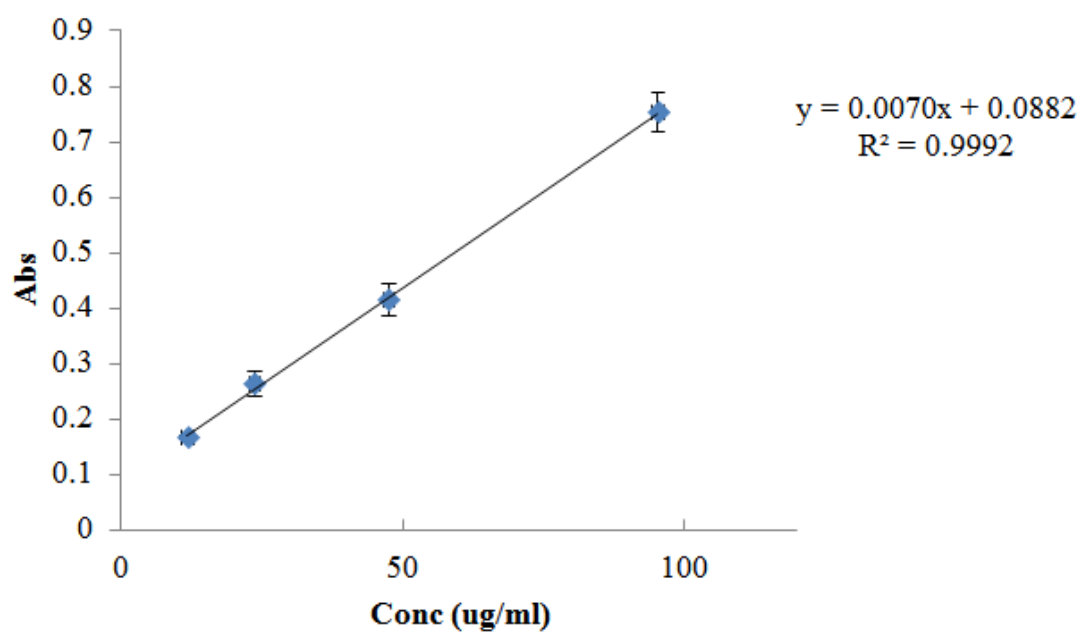
## Appendix B

Data for calibration curve of isoquercitrin

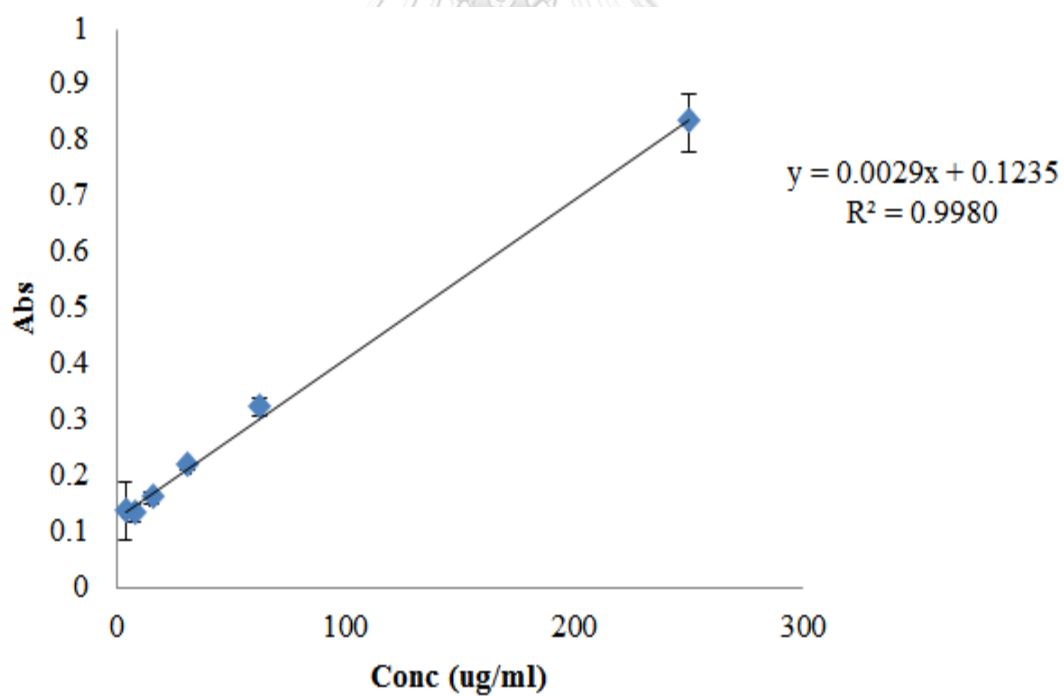
Concentration	AUC	AUC	AUC	mean	SD
1,000 ug/ml	18,302,780	18,176,805	18,717,160	18,398,915	± 282,714.2
500 ug/ml	6,896,720	6,948,796	6,962,690	6,936,069	± 34,777.85
250 ug/ml	3,308,832	3,326,747	3,336,907	3,324,162	± 14,214.89
100 ug/ml	1,303,316	1,305,960	1,312,149	1,307,142	± 4,533.511
50 ug/ml	635,349	636,469	640,843	637,554	± 2,903.168
10 ug/ml	124,715	124,416	125,596	124,909	± 613.455



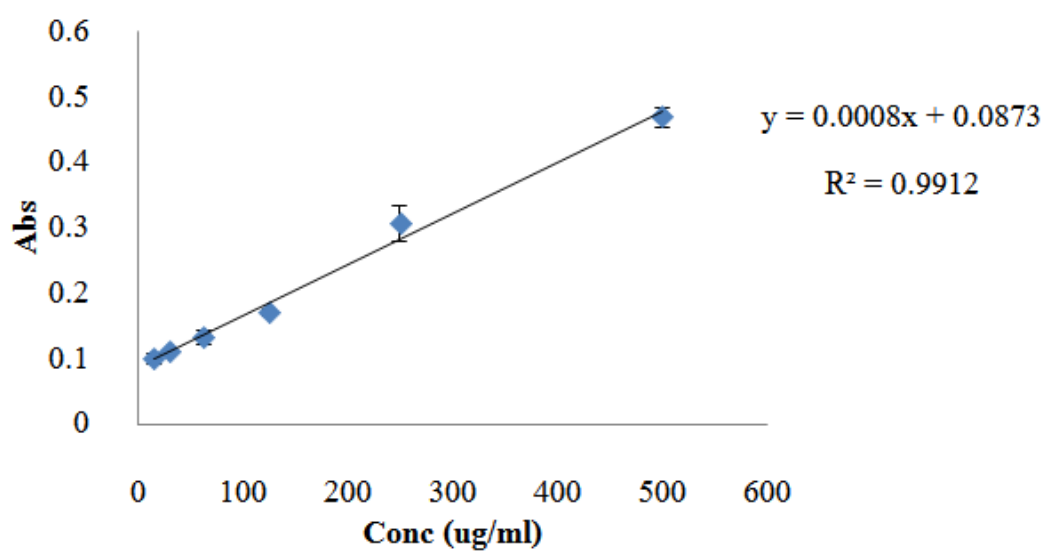
Standard curve of isoquercitrin



Total phenolic content of standard Gallic acid



Total phenolic content of standard Quercetin



Total phenolic content of standard Glucose



Data in DPPH assay of OSE-EtOH

MeOH+DPPH			Average
0.412	0.376	0.405	0.398

blank MeOH			Average
0.036	0.037	0.036	0.036

OSE+MeOH	Absorbance			Average
	1	2	3	
1000	0.048	0.044	0.045	0.046
500	0.038	0.038	0.040	0.039
250	0.039	0.036	0.039	0.038
125	0.038	0.038	0.045	0.040
62.5	0.037	0.039	0.037	0.038
31.25	0.039	0.038	0.037	0.038
15.63	0.037	0.038	0.038	0.038
7.81	0.036	0.036	0.037	0.036
3.91	0.038	0.036	0.041	0.038
1.95	0.038	0.037	0.036	0.037

Conc.OSE(ug/ml)	Absorbance		
	1	2	3
1000	0.073	0.069	0.072
500	0.064	0.066	0.066
250	0.067	0.067	0.065
125	0.077	0.073	0.073
62.5	0.217	0.165	0.167
31.25	0.303	0.261	0.258
15.63	0.354	0.356	0.343
7.81	0.382	0.370	0.380

3.91	0.396	0.400	0.391
1.95	0.412	0.413	0.404

Conc.OSE (ug/ml)	(OSE+MeOH)-(blank MeOH)	Abs. sample			%Inhibition		
		1	2	3	1	2	3
1000	0.010	0.063	0.059	0.06	84.07	85.08	84.33
500	0.003	0.061	0.063	0.063	84.58	84.07	84.07
250	0.002	0.065	0.065	0.063	83.65	83.65	84.16
125	0.004	0.073	0.069	0.069	81.73	82.73	82.73
62.5	0.002	0.215	0.163	0.165	45.85	58.93	58.42
31.25	0.002	0.301	0.259	0.256	24.31	34.87	35.62
15.63	0.002	0.352	0.354	0.341	11.40	10.90	14.17
7.81	0.000	0.382	0.37	0.38	4.02	7.04	4.53
3.91	0.002	0.394	0.398	0.389	1.01	0.00	2.26
1.95	0.001	0.411	0.412	0.403	-3.35	-3.60	-1.34

Data in DPPH assay of OSE-crude

MeOH+DPPH			Average
0.356	0.361	0.357	0.358

blank MeOH			
0.036	0.035	0.036	0.036

OSE+MeOH	Absorbance			Average
	1	2	3	
1000	0.042	0.047	0.046	0.045
500	0.041	0.042	0.042	0.042
250	0.050	0.040	0.039	0.043
125	0.038	0.039	0.039	0.039
62.5	0.053	0.046	0.037	0.045
31.25	0.037	0.036	0.037	0.037
15.63	0.039	0.038	0.037	0.038
7.81	0.039	0.038	0.039	0.039
3.91	0.040	0.037	0.037	0.038
1.95	0.037	0.039	0.039	0.038

Conc.EtOH(ug/ml)	Absorbance		
	1	2	3
1000	0.068	0.069	0.073
500	0.065	0.062	0.065
250	0.062	0.065	0.064
125	0.076	0.101	0.102
62.5	0.129	0.170	0.166
31.25	0.203	0.230	0.230
15.63	0.264	0.284	0.237
7.81	0.288	0.317	0.318

3.91	0.323	0.335	0.340
1.95	0.338	0.354	0.356

Conc.OSE (ug/ml)	(OSE+MeOH)- (blank MeOH)	Abs. sample			%Inhibition		
		1	2	3	1	2	3
1000	0.010	0.063	0.059	0.06	84.07	85.08	84.33
500	0.003	0.061	0.063	0.063	84.58	84.07	84.07
250	0.002	0.065	0.065	0.063	83.65	83.65	84.16
125	0.004	0.073	0.069	0.069	81.73	82.73	82.73
62.5	0.002	0.215	0.163	0.165	45.85	58.93	58.42
31.25	0.002	0.301	0.259	0.256	24.31	34.87	35.62
15.63	0.002	0.352	0.354	0.341	11.40	10.90	14.17
7.81	0.000	0.382	0.37	0.38	4.02	7.04	4.53
3.91	0.002	0.394	0.398	0.389	1.01	0.00	2.26
1.95	0.001	0.411	0.412	0.403	-3.35	-3.60	-1.34

Data in ABTS assay of OSE-EtOH

MeOH+ABTS			Average
0.418	0.416	0.424	0.419

blank MeoH			Average
0.037	0.039	0.039	0.038

ABTS			Average
0.829	0.844	0.848	0.840

OSE+MeOH	Absorbance			Average
(ug/ml)	1	2	3	
1000	0.050	0.049	0.048	0.049
500	0.041	0.040	0.040	0.040
250	0.039	0.041	0.040	0.040
125	0.045	0.043	0.040	0.043
62.5	0.038	0.038	0.040	0.039
31.25	0.038	0.038	0.041	0.039
15.63	0.040	0.040	0.039	0.040
7.81	0.039	0.040	0.039	0.039
3.91	0.040	0.039	0.038	0.039
1.95	0.040	0.041	0.039	0.040

Conc.OSE(ug/ml)	Absorbance		
	1	2	3
1000	0.045	0.046	0.049
500	0.040	0.041	0.044
250	0.040	0.038	0.037
125	0.084	0.081	0.085
62.5	0.164	0.166	0.166

31.25	0.271	0.270	0.276
15.63	0.334	0.340	0.340
7.81	0.374	0.375	0.378
3.91	0.396	0.392	0.395
1.95	0.424	0.422	0.426

Conc.OSE (ug/ml)	(OSE+MeOH)- (blank MeOH)	Abs. sample			%Inhibition		
		1	2	3	1	2	3
1000	0.012	0.0328	0.0338	0.04	92.18	91.94	91.22
500	0.004	0.0365	0.0375	0.04	91.30	91.07	90.35
250	0.003	0.0368	0.0348	0.03	91.22	91.70	91.94
125	0.006	0.0781	0.0751	0.08	81.37	82.08	81.13
62.5	0.002	0.1621	0.1641	0.16	61.34	60.86	60.81
31.25	0.002	0.2688	0.2678	0.27	35.90	36.14	34.71
15.63	0.003	0.3311	0.3371	0.34	21.03	19.60	19.60
7.81	0.003	0.3715	0.3725	0.38	11.41	11.18	10.46
3.91	0.002	0.3938	0.3898	0.39	6.09	7.04	6.33
1.95	0.003	0.4208	0.4188	0.42	-0.35	0.13	-0.83

Data in ABTS assay of OSE-Crude

MeOH+ABTS			Average
0.418	0.416	0.424	0.419

blank MeoH			Average
0.037	0.039	0.039	0.038

ABTS			Average
0.829	0.844	0.848	0.840

OSE+MeOH (ug/ml)	Absorbance			Average
	1	2	3	
1000	0.050	0.049	0.048	0.049
500	0.041	0.040	0.040	0.040
250	0.039	0.041	0.040	0.040
125	0.045	0.043	0.040	0.043
62.5	0.038	0.038	0.040	0.039
31.25	0.038	0.038	0.041	0.039
15.63	0.040	0.040	0.039	0.040
7.81	0.039	0.040	0.039	0.039
3.91	0.040	0.039	0.038	0.039
1.95	0.040	0.041	0.039	0.040

Conc.OSE(ug/ml)	Absorbance			Average
	1	2	3	
1000	0.042	0.043	0.044	0.043
500	0.038	0.041	0.042	0.040
250	0.038	0.038	0.037	0.038
125	0.044	0.044	0.043	0.044
62.5	0.144	0.141	0.142	0.142

31.25	0.245	0.254	0.250	0.250
15.63	0.320	0.320	0.320	0.320
7.81	0.361	0.367	0.360	0.363
3.91	0.386	0.382	0.389	0.386
1.95	0.404	0.402	0.412	0.406

Conc.OSE (ug/ml)	(OSE+MeOH)-(blank MeOH)	Abs. sample			%Inhibition		
		1	2	3	1	2	3
1000	0.012	0.0298	0.0308	0.03	92.89	92.66	92.42
500	0.004	0.0345	0.0375	0.04	91.78	91.07	90.83
250	0.003	0.0348	0.0348	0.03	91.70	91.70	91.94
125	0.006	0.0381	0.0381	0.04	90.91	90.91	91.14
62.5	0.002	0.1421	0.1391	0.14	66.10	66.82	66.58
31.25	0.002	0.2428	0.2518	0.25	42.10	39.95	40.91
15.63	0.003	0.3171	0.3171	0.32	24.37	24.37	24.37
7.81	0.003	0.3585	0.3645	0.36	14.52	13.08	14.75
3.91	0.002	0.3838	0.3798	0.39	8.47	9.43	7.76
1.95	0.003	0.4008	0.3988	0.41	4.42	4.90	2.51

## Appendix C

### *In vitro* cells base assay

#### Cytotoxicity test

Percent cells viability in each fraction

	OSE-Hex	OSE-DCM	OSE-EtOH	OSE	Mixed fraction
HeLa	98.24±0.94	99.02±2.97	95.12±2.00	91.40±1.29	95.06±1.66
HepG2	99.04±0.85	98.63±0.56	83.08±6.96	77.41±4.11	90.51±2.38
MCF-7	99.59±1.71	97.75±1.72	77.89±4.65	62.11±2.81	84.49±3.00

#### ANOVA

	Sum of Squares	df	Mean Square	F	Sig.
Between Groups	5018.363	14	358.455	39.919	.000
Within Groups	269.383	30	8.979		
Total	5287.747	44			

#### Multiple Comparisons

##### Tukey HSD

(I) Conc	(J) Conc	Mean Difference (I-J)	Std. Error	Sig.	95% Confidence Interval	
					Lower Bound	Upper Bound
HeLa-Hex	HeLa-DCM	-.77333	2.44669	1.000	-9.7894	8.2427
	HeLa-EtOH	3.12667	2.44669	.991	-5.8894	12.1427
	HeLa-crude	6.84667	2.44669	.300	-2.1694	15.8627
	HeLa-mix	3.19000	2.44669	.990	-5.8261	12.2061
HeLa-DCM	HeLa-Hex	.77333	2.44669	1.000	-8.2427	9.7894
	HeLa-EtOH	3.90000	2.44669	.947	-5.1161	12.9161

	HeLa-crude	7.62000	2.44669	.169	-1.3961	16.6361
	HeLa-mix	3.96333	2.44669	.941	-5.0527	12.9794
HeLa-EtOH	HeLa-Hex	-3.12667	2.44669	.991	-12.1427	5.8894
	HeLa-DCM	-3.90000	2.44669	.947	-12.9161	5.1161
	HeLa-crude	3.72000	2.44669	.963	-5.2961	12.7361
	HeLa-mix	.06333	2.44669	1.000	-8.9527	9.0794
HeLa-crude	HeLa-Hex	-6.84667	2.44669	.300	-15.8627	2.1694
	HeLa-DCM	-7.62000	2.44669	.169	-16.6361	1.3961
	HeLa-EtOH	-3.72000	2.44669	.963	-12.7361	5.2961
	HeLa-mix	-3.65667	2.44669	.968	-12.6727	5.3594
HeLa-mix	HeLa-Hex	-3.19000	2.44669	.990	-12.2061	5.8261
	HeLa-DCM	-3.96333	2.44669	.941	-12.9794	5.0527
	HeLa-EtOH	-.06333	2.44669	1.000	-9.0794	8.9527
	HeLa-crude	3.65667	2.44669	.968	-5.3594	12.6727
HepG2-Hex	HepG2-DCM	.40667	2.44669	1.000	-8.6094	9.4227
	HepG2-EtOH	15.95667 <sup>*</sup>	2.44669	.000	6.9406	24.9727
	HepG2-crude	21.63000 <sup>*</sup>	2.44669	.000	12.6139	30.6461
	HepG2-Mix	8.53333	2.44669	.078	-.4827	17.5494
HepG2-DCM	HepG2-Hex	-.40667	2.44669	1.000	-9.4227	8.6094
	HepG2-EtOH	15.55000 <sup>*</sup>	2.44669	.000	6.5339	24.5661
	HepG2-crude	21.22333 <sup>*</sup>	2.44669	.000	12.2073	30.2394
	HepG2-Mix	8.12667	2.44669	.112	-.8894	17.1427
HepG2-EtOH	HepG2-Hex	-15.95667 <sup>*</sup>	2.44669	.000	-24.9727	-6.9406
	HepG2-DCM	-15.55000 <sup>*</sup>	2.44669	.000	-24.5661	-6.5339
	HepG2-crude	5.67333	2.44669	.586	-3.3427	14.6894
	HepG2-Mix	-7.42333	2.44669	.197	-16.4394	1.5927
HepG2-crude	HepG2-Hex	-21.63000 <sup>*</sup>	2.44669	.000	-30.6461	-12.6139

	HepG2-DCM	-21.22333 <sup>*</sup>	2.44669	.000	-30.2394	-12.2073
	HepG2-EtOH	-5.67333	2.44669	.586	-14.6894	3.3427
	HepG2-Mix	-13.09667 <sup>*</sup>	2.44669	.001	-22.1127	-4.0806
HepG2-Mix	HepG2-Hex	-8.53333	2.44669	.078	-17.5494	.4827
	HepG2-DCM	-8.12667	2.44669	.112	-17.1427	.8894
	HepG2-EtOH	7.42333	2.44669	.197	-1.5927	16.4394
	HepG2-crude	13.09667 <sup>*</sup>	2.44669	.001	4.0806	22.1127
MCF-Hex	MCF-DCM	1.84333	2.44669	1.000	-7.1727	10.8594
	MCF-EtOH	21.70000 <sup>*</sup>	2.44669	.000	12.6839	30.7161
	MCF-crude	37.48000 <sup>*</sup>	2.44669	.000	28.4639	46.4961
	MCF-Mix	15.10000 <sup>*</sup>	2.44669	.000	6.0839	24.1161
MCF-DCM	MCF-Hex	-1.84333	2.44669	1.000	-10.8594	7.1727
	MCF-EtOH	19.85667 <sup>*</sup>	2.44669	.000	10.8406	28.8727
	MCF-crude	35.63667 <sup>*</sup>	2.44669	.000	26.6206	44.6527
	MCF-Mix	13.25667 <sup>*</sup>	2.44669	.001	4.2406	22.2727
MCF-EtOH	MCF-Hex	-21.70000 <sup>*</sup>	2.44669	.000	-30.7161	-12.6839
	MCF-DCM	-19.85667 <sup>*</sup>	2.44669	.000	-28.8727	-10.8406
	MCF-crude	15.78000 <sup>*</sup>	2.44669	.000	6.7639	24.7961
	MCF-Mix	-6.60000	2.44669	.352	-15.6161	2.4161
MCF-crude	MCF-Hex	-37.48000 <sup>*</sup>	2.44669	.000	-46.4961	-28.4639
	MCF-DCM	-35.63667 <sup>*</sup>	2.44669	.000	-44.6527	-26.6206
	MCF-EtOH	-15.78000 <sup>*</sup>	2.44669	.000	-24.7961	-6.7639
	MCF-Mix	-22.38000 <sup>*</sup>	2.44669	.000	-31.3961	-13.3639
MCF-Mix	MCF-Hex	-15.10000 <sup>*</sup>	2.44669	.000	-24.1161	-6.0839
	MCF-DCM	-13.25667 <sup>*</sup>	2.44669	.001	-22.2727	-4.2406
	MCF-EtOH	6.60000	2.44669	.352	-2.4161	15.6161
	MCF-crude	22.38000 <sup>*</sup>	2.44669	.000	13.3639	31.3961

## Percent cells viability in Okra seed extract

HeLa

Concentration	%Inhibit	SD
25ug/ml	100.04	±1.23
50ug/ml	99.38	±0.29
100ug/ml	98.64	±0.63
250ug/ml	95.75	±1.97
500ug/ml	91.40	±1.29
750ug/ml	88.56	±4.44
1,000ug/ml	83.38	±1.81
Isoquercetin	97.09	±1.70

## ANOVA

	Sum of Squares	df	Mean Square	F	Sig.
Between Groups	749.233	7	107.033	26.202	.000
Within Groups	61.274	15	4.085		
Total	810.507	22			

## Multiple Comparisons

Tukey HSD

(I) Conc	(J) Conc	Mean Difference (I-J)	Std. Error	Sig.	95% Confidence Interval	
					Lower Bound	Upper Bound
25 ug/ml	50 ug/ml	.66000	1.65024	1.000	-5.1044	6.4244
	100 ug/ml	1.40000	1.65024	.987	-4.3644	7.1644

	250 ug/ml	4.28667	1.65024	.230	-1.4777	10.0510
	500 ug/ml	8.64000 <sup>*</sup>	1.65024	.002	2.8756	14.4044
	750 ug/ml	11.47667 <sup>*</sup>	1.65024	.000	5.7123	17.2410
	1,000 ug/ml	16.66000 <sup>*</sup>	1.65024	.000	10.8956	22.4244
	Isoquercitrin	1.96500	1.84503	.955	-4.4797	8.4097
50 ug/ml	25 ug/ml	-.66000	1.65024	1.000	-6.4244	5.1044
	100 ug/ml	.74000	1.65024	1.000	-5.0244	6.5044
	250 ug/ml	3.62667	1.65024	.404	-2.1377	9.3910
	500 ug/ml	7.98000 <sup>*</sup>	1.65024	.004	2.2156	13.7444
	750 ug/ml	10.81667 <sup>*</sup>	1.65024	.000	5.0523	16.5810
	1,000 ug/ml	16.00000 <sup>*</sup>	1.65024	.000	10.2356	21.7644
	Isoquercitrin	1.30500	1.84503	.995	-5.1397	7.7497
100 ug/ml	25 ug/ml	-1.40000	1.65024	.987	-7.1644	4.3644
	50 ug/ml	-.74000	1.65024	1.000	-6.5044	5.0244
	250 ug/ml	2.88667	1.65024	.659	-2.8777	8.6510
	500 ug/ml	7.24000 <sup>*</sup>	1.65024	.009	1.4756	13.0044
	750 ug/ml	10.07667 <sup>*</sup>	1.65024	.000	4.3123	15.8410
	1,000 ug/ml	15.26000 <sup>*</sup>	1.65024	.000	9.4956	21.0244
	Isoquercitrin	.56500	1.84503	1.000	-5.8797	7.0097
250 ug/ml	25 ug/ml	-4.28667	1.65024	.230	-10.0510	1.4777
	50 ug/ml	-3.62667	1.65024	.404	-9.3910	2.1377
	100 ug/ml	-2.88667	1.65024	.659	-8.6510	2.8777
	500 ug/ml	4.35333	1.65024	.216	-1.4110	10.1177
	750 ug/ml	7.19000 <sup>*</sup>	1.65024	.010	1.4256	12.9544
	1,000 ug/ml	12.37333 <sup>*</sup>	1.65024	.000	6.6090	18.1377
	Isoquercitrin	-2.32167	1.84503	.901	-8.7664	4.1231
500 ug/ml	25 ug/ml	-8.64000 <sup>*</sup>	1.65024	.002	-14.4044	-2.8756

	50 ug/ml	-7.98000 <sup>*</sup>	1.65024	.004	-13.7444	-2.2156
	100 ug/ml	-7.24000 <sup>*</sup>	1.65024	.009	-13.0044	-1.4756
	250 ug/ml	-4.35333	1.65024	.216	-10.1177	1.4110
	750 ug/ml	2.83667	1.65024	.677	-2.9277	8.6010
	1,000 ug/ml	8.02000 <sup>*</sup>	1.65024	.004	2.2556	13.7844
	Isoquercitrin	-6.67500 <sup>*</sup>	1.84503	.040	-13.1197	-.2303
750 ug/ml	25 ug/ml	-11.47667 <sup>*</sup>	1.65024	.000	-17.2410	-5.7123
	50 ug/ml	-10.81667 <sup>*</sup>	1.65024	.000	-16.5810	-5.0523
	100 ug/ml	-10.07667 <sup>*</sup>	1.65024	.000	-15.8410	-4.3123
	250 ug/ml	-7.19000 <sup>*</sup>	1.65024	.010	-12.9544	-1.4256
	500 ug/ml	-2.83667	1.65024	.677	-8.6010	2.9277
	1,000 ug/ml	5.18333	1.65024	.094	-.5810	10.9477
	Isoquercitrin	-9.51167 <sup>*</sup>	1.84503	.002	-15.9564	-3.0669
1,000 ug/ml	25 ug/ml	-16.66000 <sup>*</sup>	1.65024	.000	-22.4244	-10.8956
	50 ug/ml	-16.00000 <sup>*</sup>	1.65024	.000	-21.7644	-10.2356
	100 ug/ml	-15.26000 <sup>*</sup>	1.65024	.000	-21.0244	-9.4956
	250 ug/ml	-12.37333 <sup>*</sup>	1.65024	.000	-18.1377	-6.6090
	500 ug/ml	-8.02000 <sup>*</sup>	1.65024	.004	-13.7844	-2.2556
	750 ug/ml	-5.18333	1.65024	.094	-10.9477	.5810
	Isoquercitrin	-14.69500 <sup>*</sup>	1.84503	.000	-21.1397	-8.2503
Isoquercitrin	25 ug/ml	-1.96500	1.84503	.955	-8.4097	4.4797
	50 ug/ml	-1.30500	1.84503	.995	-7.7497	5.1397
	100 ug/ml	-.56500	1.84503	1.000	-7.0097	5.8797
	250 ug/ml	2.32167	1.84503	.901	-4.1231	8.7664
	500 ug/ml	6.67500 <sup>*</sup>	1.84503	.040	.2303	13.1197
	750 ug/ml	9.51167 <sup>*</sup>	1.84503	.002	3.0669	15.9564
	1,000 ug/ml	14.69500 <sup>*</sup>	1.84503	.000	8.2503	21.1397

HepG2

Concentration	%Inhibit	SD
25ug/ml	101.40	±2.27
50ug/ml	99.19	±0.38
100ug/ml	94.85	±3.29
250ug/ml	84.78	±2.24
500ug/ml	77.41	±4.11
750ug/ml	68.72	±3.21
1,000ug/ml	60.97	±2.26
Isoquercetin	89.38	±1.84

ANOVA

	Sum of Squares	df	Mean Square	F	Sig.
Between Groups	4456.032	7	636.576	89.571	.000
Within Groups	113.712	16	7.107		
Total	4569.744	23			

## Multiple Comparisons

Tukey HSD

(I) Conc	(J) Conc	Mean Difference (I-J)	Std. Error	Sig.	95% Confidence Interval	
					Lower Bound	Upper Bound
25 ug/ml	50 ug/ml	2.21000	2.17669	.965	-5.3260	9.7460
	100 ug/ml	6.55000	2.17669	.114	-.9860	14.0860
	250 ug/ml	16.62333*	2.17669	.000	9.0873	24.1594

	500 ug/ml	23.99333 <sup>*</sup>	2.17669	.000	16.4573	31.5294
	750 ug/ml	32.68000 <sup>*</sup>	2.17669	.000	25.1440	40.2160
	1,000 ug/ml	40.43000 <sup>*</sup>	2.17669	.000	32.8940	47.9660
	Isoquercitrin	12.02000 <sup>*</sup>	2.17669	.001	4.4840	19.5560
50 ug/ml	25 ug/ml	-2.21000	2.17669	.965	-9.7460	5.3260
	100 ug/ml	4.34000	2.17669	.514	-3.1960	11.8760
	250 ug/ml	14.41333 <sup>*</sup>	2.17669	.000	6.8773	21.9494
	500 ug/ml	21.78333 <sup>*</sup>	2.17669	.000	14.2473	29.3194
	750 ug/ml	30.47000 <sup>*</sup>	2.17669	.000	22.9340	38.0060
	1,000 ug/ml	38.22000 <sup>*</sup>	2.17669	.000	30.6840	45.7560
	Isoquercitrin	9.81000 <sup>*</sup>	2.17669	.007	2.2740	17.3460
100 ug/ml	25 ug/ml	-6.55000	2.17669	.114	-14.0860	.9860
	50 ug/ml	-4.34000	2.17669	.514	-11.8760	3.1960
	250 ug/ml	10.07333 <sup>*</sup>	2.17669	.005	2.5373	17.6094
	500 ug/ml	17.44333 <sup>*</sup>	2.17669	.000	9.9073	24.9794
	750 ug/ml	26.13000 <sup>*</sup>	2.17669	.000	18.5940	33.6660
	1,000 ug/ml	33.88000 <sup>*</sup>	2.17669	.000	26.3440	41.4160
	Isoquercitrin	5.47000	2.17669	.257	-2.0660	13.0060
250 ug/ml	25 ug/ml	-16.62333 <sup>*</sup>	2.17669	.000	-24.1594	-9.0873
	50 ug/ml	-14.41333 <sup>*</sup>	2.17669	.000	-21.9494	-6.8773
	100 ug/ml	-10.07333 <sup>*</sup>	2.17669	.005	-17.6094	-2.5373
	500 ug/ml	7.37000	2.17669	.058	-.1660	14.9060
	750 ug/ml	16.05667 <sup>*</sup>	2.17669	.000	8.5206	23.5927
	1,000 ug/ml	23.80667 <sup>*</sup>	2.17669	.000	16.2706	31.3427
	Isoquercitrin	-4.60333	2.17669	.446	-12.1394	2.9327
500 ug/ml	25 ug/ml	-23.99333 <sup>*</sup>	2.17669	.000	-31.5294	-16.4573
	50 ug/ml	-21.78333 <sup>*</sup>	2.17669	.000	-29.3194	-14.2473

	100 ug/ml	-17.44333 <sup>*</sup>	2.17669	.000	-24.9794	-9.9073
	250 ug/ml	-7.37000	2.17669	.058	-14.9060	.1660
	750 ug/ml	8.68667 <sup>*</sup>	2.17669	.018	1.1506	16.2227
	1,000 ug/ml	16.43667 <sup>*</sup>	2.17669	.000	8.9006	23.9727
	Isoquercitrin	-11.97333 <sup>*</sup>	2.17669	.001	-19.5094	-4.4373
750 ug/ml	25 ug/ml	-32.68000 <sup>*</sup>	2.17669	.000	-40.2160	-25.1440
	50 ug/ml	-30.47000 <sup>*</sup>	2.17669	.000	-38.0060	-22.9340
	100 ug/ml	-26.13000 <sup>*</sup>	2.17669	.000	-33.6660	-18.5940
	250 ug/ml	-16.05667 <sup>*</sup>	2.17669	.000	-23.5927	-8.5206
	500 ug/ml	-8.68667 <sup>*</sup>	2.17669	.018	-16.2227	-1.1506
	1,000 ug/ml	7.75000 <sup>*</sup>	2.17669	.042	.2140	15.2860
	Isoquercitrin	-20.66000 <sup>*</sup>	2.17669	.000	-28.1960	-13.1240
1,000 ug/ml	25 ug/ml	-40.43000 <sup>*</sup>	2.17669	.000	-47.9660	-32.8940
	50 ug/ml	-38.22000 <sup>*</sup>	2.17669	.000	-45.7560	-30.6840
	100 ug/ml	-33.88000 <sup>*</sup>	2.17669	.000	-41.4160	-26.3440
	250 ug/ml	-23.80667 <sup>*</sup>	2.17669	.000	-31.3427	-16.2706
	500 ug/ml	-16.43667 <sup>*</sup>	2.17669	.000	-23.9727	-8.9006
	750 ug/ml	-7.75000 <sup>*</sup>	2.17669	.042	-15.2860	-.2140
	Isoquercitrin	-28.41000 <sup>*</sup>	2.17669	.000	-35.9460	-20.8740
Isoquercitrin	25 ug/ml	-12.02000 <sup>*</sup>	2.17669	.001	-19.5560	-4.4840
	50 ug/ml	-9.81000 <sup>*</sup>	2.17669	.007	-17.3460	-2.2740
	100 ug/ml	-5.47000	2.17669	.257	-13.0060	2.0660
	250 ug/ml	4.60333	2.17669	.446	-2.9327	12.1394
	500 ug/ml	11.97333 <sup>*</sup>	2.17669	.001	4.4373	19.5094
	750 ug/ml	20.66000 <sup>*</sup>	2.17669	.000	13.1240	28.1960
	1,000 ug/ml	28.41000 <sup>*</sup>	2.17669	.000	20.8740	35.9460

MCF-7

Concentration	%Inhibit	SD
25ug/ml	98.60	±0.84
50ug/ml	99.9	±2.47
100ug/ml	89.07	±2.09
250ug/ml	78.35	±3.09
500ug/ml	62.11	±2.82
750ug/ml	51.39	±3.78
1,000ug/ml	43.60	±4.13
Isoquercetin	79.99	±3.43

ANOVA

	Sum of Squares	df	Mean Square	F	Sig.
Between Groups	9357.811	7	1336.830	149.187	.000
Within Groups	143.372	16	8.961		
Total	9501.183	23			

Multiple Comparisons

Tukey HSD

(I) Conc	(J) Conc	Mean Difference (I-J)	Std. Error	Sig.	95% Confidence Interval	
					Lower Bound	Upper Bound
25 ug/ml	50 ug/ml	-1.29667	2.44415	.999	-9.7587	7.1653
	100 ug/ml	9.53667 <sup>*</sup>	2.44415	.022	1.0747	17.9987

	250 ug/ml	20.25667 <sup>*</sup>	2.44415	.000	11.7947	28.7187
	500 ug/ml	36.49333 <sup>*</sup>	2.44415	.000	28.0313	44.9553
	750 ug/ml	47.21333 <sup>*</sup>	2.44415	.000	38.7513	55.6753
	1,000 ug/ml	55.00000 <sup>*</sup>	2.44415	.000	46.5380	63.4620
	Isoquercitrin	18.61667 <sup>*</sup>	2.44415	.000	10.1547	27.0787
50 ug/ml	25 ug/ml	1.29667	2.44415	.999	-7.1653	9.7587
	100 ug/ml	10.83333 <sup>*</sup>	2.44415	.008	2.3713	19.2953
	250 ug/ml	21.55333 <sup>*</sup>	2.44415	.000	13.0913	30.0153
	500 ug/ml	37.79000 <sup>*</sup>	2.44415	.000	29.3280	46.2520
	750 ug/ml	48.51000 <sup>*</sup>	2.44415	.000	40.0480	56.9720
	1,000 ug/ml	56.29667 <sup>*</sup>	2.44415	.000	47.8347	64.7587
	Isoquercitrin	19.91333 <sup>*</sup>	2.44415	.000	11.4513	28.3753
100 ug/ml	25 ug/ml	-9.53667 <sup>*</sup>	2.44415	.022	-17.9987	-1.0747
	50 ug/ml	-10.83333 <sup>*</sup>	2.44415	.008	-19.2953	-2.3713
	250 ug/ml	10.72000 <sup>*</sup>	2.44415	.008	2.2580	19.1820
	500 ug/ml	26.95667 <sup>*</sup>	2.44415	.000	18.4947	35.4187
	750 ug/ml	37.67667 <sup>*</sup>	2.44415	.000	29.2147	46.1387
	1,000 ug/ml	45.46333 <sup>*</sup>	2.44415	.000	37.0013	53.9253
	Isoquercitrin	9.08000 <sup>*</sup>	2.44415	.031	.6180	17.5420
250 ug/ml	25 ug/ml	-20.25667 <sup>*</sup>	2.44415	.000	-28.7187	-11.7947
	50 ug/ml	-21.55333 <sup>*</sup>	2.44415	.000	-30.0153	-13.0913
	100 ug/ml	-10.72000 <sup>*</sup>	2.44415	.008	-19.1820	-2.2580
	500 ug/ml	16.23667 <sup>*</sup>	2.44415	.000	7.7747	24.6987
	750 ug/ml	26.95667 <sup>*</sup>	2.44415	.000	18.4947	35.4187
	1,000 ug/ml	34.74333 <sup>*</sup>	2.44415	.000	26.2813	43.2053
	Isoquercitrin	-1.64000	2.44415	.997	-10.1020	6.8220
500 ug/ml	25 ug/ml	-36.49333 <sup>*</sup>	2.44415	.000	-44.9553	-28.0313

	50 ug/ml	-37.79000 <sup>*</sup>	2.44415	.000	-46.2520	-29.3280
	100 ug/ml	-26.95667 <sup>*</sup>	2.44415	.000	-35.4187	-18.4947
	250 ug/ml	-16.23667 <sup>*</sup>	2.44415	.000	-24.6987	-7.7747
	750 ug/ml	10.72000 <sup>*</sup>	2.44415	.008	2.2580	19.1820
	1,000 ug/ml	18.50667 <sup>*</sup>	2.44415	.000	10.0447	26.9687
	Isoquercitrin	-17.87667 <sup>*</sup>	2.44415	.000	-26.3387	-9.4147
750 ug/ml	25 ug/ml	-47.21333 <sup>*</sup>	2.44415	.000	-55.6753	-38.7513
	50 ug/ml	-48.51000 <sup>*</sup>	2.44415	.000	-56.9720	-40.0480
	100 ug/ml	-37.67667 <sup>*</sup>	2.44415	.000	-46.1387	-29.2147
	250 ug/ml	-26.95667 <sup>*</sup>	2.44415	.000	-35.4187	-18.4947
	500 ug/ml	-10.72000 <sup>*</sup>	2.44415	.008	-19.1820	-2.2580
	1,000 ug/ml	7.78667	2.44415	.083	-.6753	16.2487
	Isoquercitrin	-28.59667 <sup>*</sup>	2.44415	.000	-37.0587	-20.1347
1,000 ug/ml	25 ug/ml	-55.00000 <sup>*</sup>	2.44415	.000	-63.4620	-46.5380
	50 ug/ml	-56.29667 <sup>*</sup>	2.44415	.000	-64.7587	-47.8347
	100 ug/ml	-45.46333 <sup>*</sup>	2.44415	.000	-53.9253	-37.0013
	250 ug/ml	-34.74333 <sup>*</sup>	2.44415	.000	-43.2053	-26.2813
	500 ug/ml	-18.50667 <sup>*</sup>	2.44415	.000	-26.9687	-10.0447
	750 ug/ml	-7.78667	2.44415	.083	-16.2487	.6753
	Isoquercitrin	-36.38333 <sup>*</sup>	2.44415	.000	-44.8453	-27.9213
Isoquercitrin	25 ug/ml	-18.61667 <sup>*</sup>	2.44415	.000	-27.0787	-10.1547
	50 ug/ml	-19.91333 <sup>*</sup>	2.44415	.000	-28.3753	-11.4513
	100 ug/ml	-9.08000 <sup>*</sup>	2.44415	.031	-17.5420	-.6180
	250 ug/ml	1.64000	2.44415	.997	-6.8220	10.1020
	500 ug/ml	17.87667 <sup>*</sup>	2.44415	.000	9.4147	26.3387
	750 ug/ml	28.59667 <sup>*</sup>	2.44415	.000	20.1347	37.0587
	1,000 ug/ml	36.38333 <sup>*</sup>	2.44415	.000	27.9213	44.8453

HaCat

Concentration	%Inhibit	SD
25ug/ml	98.94	±2.24
100ug/ml	99.60	±2.49
250ug/ml	103.34	±4.72
500ug/ml	99.35	±4.79
750ug/ml	106.12	±6.24
1,000ug/ml	93.20	±4.53



## Cell scratch assay

## Hela

	24 hr.		72 hr	
	%wound closing	SD	%wound closing	SD
Control	81.50	±7.87	93.73	±2.97
25 ug/ml	28.67	±4.25	46.92	±4.60
100 ug/ml	18.44	±6.14	27.73	±5.25
250 ug/ml	15.77	±5.98	19.48	±4.69
Isoquercitrin	24.64	±3.97	42.95	±3.36

## HepG2

	24 hr.		72 hr	
	%wound closing	SD	%wound closing	SD
Control	9.77	±1.83	30.44	±5.59
25 ug/ml	9.71	±4.33	16.97	±1.14
100 ug/ml	8.35	±1.33	15.05	±1.67
250 ug/ml	8.77	±1.56	15.41	±2.18
Isoquercitrin	7.75	±0.38	16.29	±1.74

## MCF-7

	24 hr.		72 hr	
	%wound closing	SD	%wound closing	SD
Control	89.70	1.43	98.14	0.94
25 ug/ml	20.80	4.86	53.69	4.25
100 ug/ml	14.51	2.11	22.38	2.91
250 ug/ml	13.98	2.48	16.80	1.17
Isoquercitrin	14.98	1.69	20.35	0.92

## Cell invasion assay

Concentration	HeLa	HepG2	MCF-7
25 ug/ml	98.01±1.82	89.67±7.31	89.25±6.78
100 ug/ml	87.34±3.54	74.32±5.67	71.46±8.72
250 ug/ml	76.25±4.17	70.12±6.18	60.63±3.80
500 ug/ml	61.73±6.80	67.35±8.42	53.71±7.14
Isoquercitrin	71.43±4.23	74.41±5.79	81.06±8.26

HeLa

## ANOVA

	Sum of Squares	df	Mean Square	F	Sig.
Between Groups	3473.047	5	694.609	42.872	.000
Within Groups	194.422	12	16.202		
Total	3667.468	17			

## Multiple Comparisons

Tukey HSD

(I) Conc	(J) Conc	Mean Difference (I-J)	Std. Error	Sig.	95% Confidence Interval	
					Lower Bound	Upper Bound
control	25 ug/ml	1.23000	3.28652	.999	-9.8092	12.2692
	100 ug/ml	13.20000*	3.28652	.016	2.1608	24.2392
	250 ug/ml	22.38667*	3.28652	.000	11.3475	33.4258
	1000 ug/ml	38.34000*	3.28652	.000	27.3008	49.3792
	Isoquercitrin	28.01667*	3.28652	.000	16.9775	39.0558

25 ug/ml	control	-1.23000	3.28652	.999	-12.2692	9.8092
	100 ug/ml	11.97000 <sup>*</sup>	3.28652	.031	.9308	23.0092
	250 ug/ml	21.15667 <sup>*</sup>	3.28652	.000	10.1175	32.1958
	1000 ug/ml	37.11000 <sup>*</sup>	3.28652	.000	26.0708	48.1492
	Isoquercitrin	26.78667 <sup>*</sup>	3.28652	.000	15.7475	37.8258
100 ug/ml	control	-13.20000 <sup>*</sup>	3.28652	.016	-24.2392	-2.1608
	25 ug/ml	-11.97000 <sup>*</sup>	3.28652	.031	-23.0092	-.9308
	250 ug/ml	9.18667	3.28652	.126	-1.8525	20.2258
	1000 ug/ml	25.14000 <sup>*</sup>	3.28652	.000	14.1008	36.1792
	Isoquercitrin	14.81667 <sup>*</sup>	3.28652	.007	3.7775	25.8558
250 ug/ml	control	-22.38667 <sup>*</sup>	3.28652	.000	-33.4258	-11.3475
	25 ug/ml	-21.15667 <sup>*</sup>	3.28652	.000	-32.1958	-10.1175
	100 ug/ml	-9.18667	3.28652	.126	-20.2258	1.8525
	1000 ug/ml	15.95333 <sup>*</sup>	3.28652	.004	4.9142	26.9925
	Isoquercitrin	5.63000	3.28652	.549	-5.4092	16.6692
1000 ug/ml	control	-38.34000 <sup>*</sup>	3.28652	.000	-49.3792	-27.3008
	25 ug/ml	-37.11000 <sup>*</sup>	3.28652	.000	-48.1492	-26.0708
	100 ug/ml	-25.14000 <sup>*</sup>	3.28652	.000	-36.1792	-14.1008
	250 ug/ml	-15.95333 <sup>*</sup>	3.28652	.004	-26.9925	-4.9142
	Isoquercitrin	-10.32333	3.28652	.072	-21.3625	.7158
Isoquercitrin	control	-28.01667 <sup>*</sup>	3.28652	.000	-39.0558	-16.9775
	25 ug/ml	-26.78667 <sup>*</sup>	3.28652	.000	-37.8258	-15.7475
	100 ug/ml	-14.81667 <sup>*</sup>	3.28652	.007	-25.8558	-3.7775
	250 ug/ml	-5.63000	3.28652	.549	-16.6692	5.4092
	1000 ug/ml	10.32333	3.28652	.072	-.7158	21.3625

\*. The mean difference is significant at the 0.05 level.

HepG2

## ANOVA

	Sum of Squares	df	Mean Square	F	Sig.
Between Groups	2211.633	5	442.327	11.503	.000
Within Groups	461.450	12	38.454		
Total	2673.084	17			



## Multiple Comparisons

Tukey HSD

(I) Conc	(J) Conc	Mean Difference (I-J)	Std. Error	Sig.	95% Confidence Interval	
					Lower Bound	Upper Bound
control	25 ug/ml	10.67333	5.06321	.345	-6.3336	27.6803
	100 ug/ml	25.81000*	5.06321	.003	8.8031	42.8169
	250 ug/ml	27.78333*	5.06321	.001	10.7764	44.7903
	1000 ug/ml	31.67667*	5.06321	.000	14.6697	48.6836
	Isoquercitrin	24.42333*	5.06321	.004	7.4164	41.4303
25 ug/ml	control	-10.67333	5.06321	.345	-27.6803	6.3336
	100 ug/ml	15.13667	5.06321	.092	-1.8703	32.1436
	250 ug/ml	17.11000*	5.06321	.048	.1031	34.1169
	1000 ug/ml	21.00333*	5.06321	.013	3.9964	38.0103
	Isoquercitrin	13.75000	5.06321	.143	-3.2569	30.7569
100 ug/ml	control	-25.81000*	5.06321	.003	-42.8169	-8.8031
	25 ug/ml	-15.13667	5.06321	.092	-32.1436	1.8703

	250 ug/ml	1.97333	5.06321	.999	-15.0336	18.9803
	1000 ug/ml	5.86667	5.06321	.848	-11.1403	22.8736
	Isoquercitrin	-1.38667	5.06321	1.000	-18.3936	15.6203
250 ug/ml	control	-27.78333 <sup>*</sup>	5.06321	.001	-44.7903	-10.7764
	25 ug/ml	-17.11000 <sup>*</sup>	5.06321	.048	-34.1169	-.1031
	100 ug/ml	-1.97333	5.06321	.999	-18.9803	15.0336
	1000 ug/ml	3.89333	5.06321	.968	-13.1136	20.9003
	Isoquercitrin	-3.36000	5.06321	.983	-20.3669	13.6469
1000 ug/ml	control	-31.67667 <sup>*</sup>	5.06321	.000	-48.6836	-14.6697
	25 ug/ml	-21.00333 <sup>*</sup>	5.06321	.013	-38.0103	-3.9964
	100 ug/ml	-5.86667	5.06321	.848	-22.8736	11.1403
	250 ug/ml	-3.89333	5.06321	.968	-20.9003	13.1136
	Isoquercitrin	-7.25333	5.06321	.709	-24.2603	9.7536
Isoquercitrin	control	-24.42333 <sup>*</sup>	5.06321	.004	-41.4303	-7.4164
	25 ug/ml	-13.75000	5.06321	.143	-30.7569	3.2569
	100 ug/ml	1.38667	5.06321	1.000	-15.6203	18.3936
	250 ug/ml	3.36000	5.06321	.983	-13.6469	20.3669
	1000 ug/ml	7.25333	5.06321	.709	-9.7536	24.2603

\*. The mean difference is significant at the 0.05 level.

## MCF-7

## ANOVA

	Sum of Squares	df	Mean Square	F	Sig.
Between Groups	4566.308	5	913.262	27.074	.000
Within Groups	404.778	12	33.732		
Total	4971.086	17			



## Multiple Comparisons

## Tukey HSD

(I) Conc	(J) Conc	Mean Difference (I-J)	Std. Error	Sig.	95% Confidence Interval	
					Lower Bound	Upper Bound
control	25 ug/ml	10.28000	4.74212	.318	-5.6484	26.2084
	100 ug/ml	27.95333 <sup>*</sup>	4.74212	.001	12.0249	43.8817
	250 ug/ml	39.41667 <sup>*</sup>	4.74212	.000	23.4883	55.3451
	1000 ug/ml	45.72333 <sup>*</sup>	4.74212	.000	29.7949	61.6517
	Isoquercitrin	18.20000 <sup>*</sup>	4.74212	.022	2.2716	34.1284
25 ug/ml	control	-10.28000	4.74212	.318	-26.2084	5.6484
	100 ug/ml	17.67333 <sup>*</sup>	4.74212	.027	1.7449	33.6017
	250 ug/ml	29.13667 <sup>*</sup>	4.74212	.001	13.2083	45.0651
	1000 ug/ml	35.44333 <sup>*</sup>	4.74212	.000	19.5149	51.3717
	Isoquercitrin	7.92000	4.74212	.573	-8.0084	23.8484
100 ug/ml	control	-27.95333 <sup>*</sup>	4.74212	.001	-43.8817	-12.0249
	25 ug/ml	-17.67333 <sup>*</sup>	4.74212	.027	-33.6017	-1.7449

	250 ug/ml	11.46333	4.74212	.224	-4.4651	27.3917
	1000 ug/ml	17.77000 <sup>*</sup>	4.74212	.026	1.8416	33.6984
	Isoquercitrin	-9.75333	4.74212	.368	-25.6817	6.1751
250 ug/ml	control	-39.41667 <sup>*</sup>	4.74212	.000	-55.3451	-23.4883
	25 ug/ml	-29.13667 <sup>*</sup>	4.74212	.001	-45.0651	-13.2083
	100 ug/ml	-11.46333	4.74212	.224	-27.3917	4.4651
	1000 ug/ml	6.30667	4.74212	.764	-9.6217	22.2351
	Isoquercitrin	-21.21667 <sup>*</sup>	4.74212	.008	-37.1451	-5.2883
1000 ug/ml	control	-45.72333 <sup>*</sup>	4.74212	.000	-61.6517	-29.7949
	25 ug/ml	-35.44333 <sup>*</sup>	4.74212	.000	-51.3717	-19.5149
	100 ug/ml	-17.77000 <sup>*</sup>	4.74212	.026	-33.6984	-1.8416
	250 ug/ml	-6.30667	4.74212	.764	-22.2351	9.6217
	Isoquercitrin	-27.52333 <sup>*</sup>	4.74212	.001	-43.4517	-11.5949
Isoquercitrin	control	-18.20000 <sup>*</sup>	4.74212	.022	-34.1284	-2.2716
	25 ug/ml	-7.92000	4.74212	.573	-23.8484	8.0084
	100 ug/ml	9.75333	4.74212	.368	-6.1751	25.6817
	250 ug/ml	21.21667 <sup>*</sup>	4.74212	.008	5.2883	37.1451
	1000 ug/ml	27.52333 <sup>*</sup>	4.74212	.001	11.5949	43.4517

\*. The mean difference is significant at the 0.05 level.

## Antiangiogenesis

VEGF inhibition (pg/ml)

		Control	100 ug/ml	250 ug/ml	500 ug/ml	Isoquercitrin
HeLa	24 hrs	125.96±7.14	128.19±51.24	113.47±17.46	92.26±14.5	121.76±23.91
	48 hrs	240.41±14.67	184.48±7.14	141.15±2.79	141.89±4.84	168.26±14.18

HeLa 24 hrs

**ANOVA**

inhibit

	Sum of Squares	df	Mean Square	F	Sig.
Between Groups	3013.083	4	753.271	1.002	.451
Within Groups	7517.143	10	751.714		
Total	10530.226	14			



## Multiple Comparisons

inhibit  
Tukey HSD

(I) Conc	(J) Conc	Mean Difference (I-J)	Std. Error	Sig.	95% Confidence Interval	
					Lower Bound	Upper Bound
control	100 ug/ml	-2.22222	22.38622	1.000	-75.8971	71.4527
	250 ug/ml	12.96296	22.38622	.975	-60.7119	86.6379
	500 ug/ml	33.70370	22.38622	.581	-39.9712	107.3786
	Isoquercitrin	-4.27037	22.38622	1.000	-77.9453	69.4045
100 ug/ml	control	2.22222	22.38622	1.000	-71.4527	75.8971
	250 ug/ml	15.18519	22.38622	.957	-58.4897	88.8601
	500 ug/ml	35.92593	22.38622	.526	-37.7490	109.6008
	Isoquercitrin	-2.04815	22.38622	1.000	-75.7230	71.6267
250 ug/ml	control	-12.96296	22.38622	.975	-86.6379	60.7119
	100 ug/ml	-15.18519	22.38622	.957	-88.8601	58.4897
	500 ug/ml	20.74074	22.38622	.880	-52.9341	94.4156
	Isoquercitrin	-17.23333	22.38622	.934	-90.9082	56.4416
500 ug/ml	control	-33.70370	22.38622	.581	-107.3786	39.9712
	100 ug/ml	-35.92593	22.38622	.526	-109.6008	37.7490
	250 ug/ml	-20.74074	22.38622	.880	-94.4156	52.9341
	Isoquercitrin	-37.97407	22.38622	.477	-111.6490	35.7008
Isoquercitrin	control	4.27037	22.38622	1.000	-69.4045	77.9453
	100 ug/ml	2.04815	22.38622	1.000	-71.6267	75.7230
	250 ug/ml	17.23333	22.38622	.934	-56.4416	90.9082
	500 ug/ml	37.97407	22.38622	.477	-35.7008	111.6490

HeLa 48 hrs

## ANOVA

	Sum of Squares	df	Mean Square	F	Sig.
Between Groups	20630.433	4	5157.608	51.771	.000
Within Groups	996.242	10	99.624		
Total	21626.675	14			



## Multiple Comparisons

Tukey HSD

(I) Conc	(J) Conc	Mean Difference (I-J)	Std. Error	Sig.	95% Confidence Interval	
					Lower Bound	Upper Bound
control	100 ug/ml	55.92593 <sup>*</sup>	8.14961	.000	29.1049	82.7470
	250 ug/ml	99.25926 <sup>*</sup>	8.14961	.000	72.4382	126.0803
	500 ug/ml	98.51852 <sup>*</sup>	8.14961	.000	71.6975	125.3395
	Isoquercitrin	82.20741 <sup>*</sup>	8.14961	.000	55.3864	109.0284
100 ug/ml	control	-55.92593 <sup>*</sup>	8.14961	.000	-82.7470	-29.1049
	250 ug/ml	43.33333 <sup>*</sup>	8.14961	.002	16.5123	70.1544
	500 ug/ml	42.59259 <sup>*</sup>	8.14961	.003	15.7716	69.4136
	Isoquercitrin	26.28148	8.14961	.055	-.5395	53.1025
250 ug/ml	control	-99.25926 <sup>*</sup>	8.14961	.000	-126.0803	-72.4382
	100 ug/ml	-43.33333 <sup>*</sup>	8.14961	.002	-70.1544	-16.5123
	500 ug/ml	-.74074	8.14961	1.000	-27.5618	26.0803
	Isoquercitrin	-17.05185	8.14961	.294	-43.8729	9.7692
500 ug/ml	control	-98.51852 <sup>*</sup>	8.14961	.000	-125.3395	-71.6975
	100 ug/ml	-42.59259 <sup>*</sup>	8.14961	.003	-69.4136	-15.7716

	250 ug/ml	.74074	8.14961	1.000	-26.0803	27.5618
	Isoquercitrin	-16.31111	8.14961	.331	-43.1321	10.5099
Isoquercitrin	control	-82.20741 <sup>*</sup>	8.14961	.000	-109.0284	-55.3864
	100 ug/ml	-26.28148	8.14961	.055	-53.1025	.5395
	250 ug/ml	17.05185	8.14961	.294	-9.7692	43.8729
	500 ug/ml	16.31111	8.14961	.331	-10.5099	43.1321

\*. The mean difference is significant at the 0.05 level.

		Control	100 ug/ml	250 ug/ml	500 ug/ml	Isoquercitrin
HepG2	24 hrs	253.74±6.12	233.74±5.48	178.56±10.72	158.56±27.31	193.61±19.04
	48 hrs	543.37±23.74	278.93±3.91	267.81±9.45	190.41±8.98	263.24±8.16

HepG2 24 hrs

## ANOVA

	Sum of Squares	df	Mean Square	F	Sig.
Between Groups	18501.056	4	4625.264	18.711	.000
Within Groups	2471.947	10	247.195		
Total	20973.003	14			



## Multiple Comparisons

Tukey HSD

(I) Conc	(J) Conc	Mean Difference (I-J)	Std. Error	Sig.	95% Confidence Interval	
					Lower Bound	Upper Bound
control	100 ug/ml	20.00000	12.83731	.552	-22.2486	62.2486
	250 ug/ml	75.18519 <sup>*</sup>	12.83731	.001	32.9366	117.4338
	500 ug/ml	95.18519 <sup>*</sup>	12.83731	.000	52.9366	137.4338
	Isoquercitrin	59.54074 <sup>*</sup>	12.83731	.006	17.2921	101.7894
100 ug/ml	control	-20.00000	12.83731	.552	-62.2486	22.2486
	250 ug/ml	55.18519 <sup>*</sup>	12.83731	.011	12.9366	97.4338
	500 ug/ml	75.18519 <sup>*</sup>	12.83731	.001	32.9366	117.4338
	Isoquercitrin	39.54074	12.83731	.069	-2.7079	81.7894
250 ug/ml	control	-75.18519 <sup>*</sup>	12.83731	.001	-117.4338	-32.9366
	100 ug/ml	-55.18519 <sup>*</sup>	12.83731	.011	-97.4338	-12.9366
	500 ug/ml	20.00000	12.83731	.552	-22.2486	62.2486
	Isoquercitrin	-15.64444	12.83731	.742	-57.8931	26.6042

500 ug/ml	control	-95.18519 <sup>*</sup>	12.83731	.000	-137.4338	-52.9366
	100 ug/ml	-75.18519 <sup>*</sup>	12.83731	.001	-117.4338	-32.9366
	250 ug/ml	-20.00000	12.83731	.552	-62.2486	22.2486
	Isoquercitrin	-35.64444	12.83731	.110	-77.8931	6.6042
Isoquercitrin	control	-59.54074 <sup>*</sup>	12.83731	.006	-101.7894	-17.2921
	100 ug/ml	-39.54074	12.83731	.069	-81.7894	2.7079
	250 ug/ml	15.64444	12.83731	.742	-26.6042	57.8931
	500 ug/ml	35.64444	12.83731	.110	-6.6042	77.8931

\*. The mean difference is significant at the 0.05 level.



HepG2 48 hrs

#### ANOVA

inhibit					
	Sum of Squares	df	Mean Square	F	Sig.
Between Groups	290116.567	4	72529.142	232.771	.000
Within Groups	3115.906	10	311.591		
Total	293232.473	14			

#### Multiple Comparisons

Tukey HSD

(I) Conc	(J) Conc	Mean	Std. Error	Sig.	95% Confidence Interval	
		Difference (I-J)			Lower Bound	Upper Bound
control	100 ug/ml	309.62963 <sup>*</sup>	14.41274	.000	262.1961	357.0631
	250 ug/ml	364.81481 <sup>*</sup>	14.41274	.000	317.3813	412.2483

	500 ug/ml	384.81481 <sup>*</sup>	14.41274	.000	337.3813	432.2483
	Isoquercitrin	279.40370 <sup>*</sup>	14.41274	.000	231.9702	326.8372
100 ug/ml	control	-309.62963 <sup>*</sup>	14.41274	.000	-357.0631	-262.1961
	250 ug/ml	55.18519 <sup>*</sup>	14.41274	.022	7.7517	102.6187
	500 ug/ml	75.18519 <sup>*</sup>	14.41274	.003	27.7517	122.6187
	Isoquercitrin	-30.22593	14.41274	.292	-77.6594	17.2076
250 ug/ml	control	-364.81481 <sup>*</sup>	14.41274	.000	-412.2483	-317.3813
	100 ug/ml	-55.18519 <sup>*</sup>	14.41274	.022	-102.6187	-7.7517
	500 ug/ml	20.00000	14.41274	.648	-27.4335	67.4335
	Isoquercitrin	-85.41111 <sup>*</sup>	14.41274	.001	-132.8446	-37.9776
500 ug/ml	control	-384.81481 <sup>*</sup>	14.41274	.000	-432.2483	-337.3813
	100 ug/ml	-75.18519 <sup>*</sup>	14.41274	.003	-122.6187	-27.7517
	250 ug/ml	-20.00000	14.41274	.648	-67.4335	27.4335
	Isoquercitrin	-105.41111 <sup>*</sup>	14.41274	.000	-152.8446	-57.9776
Isoquercitrin	control	-279.40370 <sup>*</sup>	14.41274	.000	-326.8372	-231.9702
	100 ug/ml	30.22593	14.41274	.292	-17.2076	77.6594
	250 ug/ml	85.41111 <sup>*</sup>	14.41274	.001	37.9776	132.8446
	500 ug/ml	105.41111 <sup>*</sup>	14.41274	.000	57.9776	152.8446

\*. The mean difference is significant at the 0.05 level.

		Control	100 ug/ml	250 ug/ml	500 ug/ml	Isoquercitrin
MCF-7	24 hrs	205.96±21.92	193.74±57.42	157.44±46.20	129.3±9.86	164.92±21.83
	48 hrs	302.26±12.64	225.89±15.75	145.22±11.76	137.81±11.56	178.48±15.62

MCF-7 24 hrs

## ANOVA

	Sum of Squares	df	Mean Square	F	Sig.
Between Groups	11015.252	4	2753.813	2.143	.150
Within Groups	12850.542	10	1285.054		
Total	23865.795	14			

## Multiple Comparisons

Tukey HSD

(I) Conc	(J) Conc	Mean Difference (I-J)	Std. Error	Sig.	95% Confidence Interval	
					Lower Bound	Upper Bound
control	100 ug/ml	12.22222	29.26949	.993	-84.1061	108.5505
	250 ug/ml	48.51852	29.26949	.498	-47.8098	144.8468
	500 ug/ml	76.66667	29.26949	.140	-19.6616	172.9949
	Isoquercitrin	38.01630	29.26949	.698	-58.3120	134.3446
100 ug/ml	control	-12.22222	29.26949	.993	-108.5505	84.1061
	250 ug/ml	36.29630	29.26949	.730	-60.0320	132.6246
	500 ug/ml	64.44444	29.26949	.254	-31.8838	160.7727
	Isoquercitrin	25.79407	29.26949	.897	-70.5342	122.1224

250 ug/ml	control	-48.51852	29.26949	.498	-144.8468	47.8098
	100 ug/ml	-36.29630	29.26949	.730	-132.6246	60.0320
	500 ug/ml	28.14815	29.26949	.866	-68.1801	124.4764
	Isoquercitrin	-10.50222	29.26949	.996	-106.8305	85.8261
500 ug/ml	control	-76.66667	29.26949	.140	-172.9949	19.6616
	100 ug/ml	-64.44444	29.26949	.254	-160.7727	31.8838
	250 ug/ml	-28.14815	29.26949	.866	-124.4764	68.1801
	Isoquercitrin	-38.65037	29.26949	.686	-134.9787	57.6779
Isoquercitrin	control	-38.01630	29.26949	.698	-134.3446	58.3120
	100 ug/ml	-25.79407	29.26949	.897	-122.1224	70.5342
	250 ug/ml	10.50222	29.26949	.996	-85.8261	106.8305
	500 ug/ml	38.65037	29.26949	.686	-57.6779	134.9787

MCF-7 48 hrs

## ANOVA

inhibit					
	Sum of Squares	df	Mean Square	F	Sig.
Between Groups	61286.732	4	15321.683	103.394	.000
Within Groups	1481.870	10	148.187		
Total	62768.602	14			

### Multiple Comparisons

Tukey HSD

(I) Conc	(J) Conc	Mean Difference (I-J)	Std. Error	Sig.	95% Confidence Interval	
					Lower Bound	Upper Bound
control	100 ug/ml	50.37037 <sup>*</sup>	9.93938	.003	17.6590	83.0817
	250 ug/ml	157.03704 <sup>*</sup>	9.93938	.000	124.3257	189.7484
	500 ug/ml	164.44444 <sup>*</sup>	9.93938	.000	131.7331	197.1558
	Isoquercitrin	123.73593 <sup>*</sup>	9.93938	.000	91.0246	156.4472
100 ug/ml	control	-50.37037 <sup>*</sup>	9.93938	.003	-83.0817	-17.6590
	250 ug/ml	106.66667 <sup>*</sup>	9.93938	.000	73.9553	139.3780
	500 ug/ml	114.07407 <sup>*</sup>	9.93938	.000	81.3628	146.7854
	Isoquercitrin	73.36556 <sup>*</sup>	9.93938	.000	40.6542	106.0769
250 ug/ml	control	-157.03704 <sup>*</sup>	9.93938	.000	-189.7484	-124.3257
	100 ug/ml	-106.66667 <sup>*</sup>	9.93938	.000	-139.3780	-73.9553
	500 ug/ml	7.40741	9.93938	.940	-25.3039	40.1187
	Isoquercitrin	-33.30111 <sup>*</sup>	9.93938	.046	-66.0124	-.5898
500 ug/ml	control	-164.44444 <sup>*</sup>	9.93938	.000	-197.1558	-131.7331
	100 ug/ml	-114.07407 <sup>*</sup>	9.93938	.000	-146.7854	-81.3628
	250 ug/ml	-7.40741	9.93938	.940	-40.1187	25.3039
	Isoquercitrin	-40.70852 <sup>*</sup>	9.93938	.014	-73.4198	-7.9972
Isoquercitrin	control	-123.73593 <sup>*</sup>	9.93938	.000	-156.4472	-91.0246
	100 ug/ml	-73.36556 <sup>*</sup>	9.93938	.000	-106.0769	-40.6542
	250 ug/ml	33.30111 <sup>*</sup>	9.93938	.046	.5898	66.0124
	500 ug/ml	40.70852 <sup>*</sup>	9.93938	.014	7.9972	73.4198

\*. The mean difference is significant at the 0.05 level.

## Okra seed loaded polymeric micelles cytotoxicity

	Micelle blank	Okra seed micelle	Okra seed micelle
HeLa	101.27±2.42	91.40±1.29	85.57±1.54
Hep G2	101.80±2.52	77.41±4.11	65.01±2.17
MCF-7	99.72±1.03	62.11±2.81	55.22±4.87

## ANOVA

	Sum of Squares	df	Mean Square	F	Sig.
Between Groups	7802.722	8	975.340	124.068	.000
Within Groups	141.504	18	7.861		
Total	7944.226	26			

## Multiple Comparisons

## Tukey HSD

(I) Conc	(J) Conc	Mean Difference (I-J)	Std. Error	Sig.	95% Confidence Interval	
					Lower Bound	Upper Bound
HeLa Mi blank	Hela Crude	9.87333 <sup>*</sup>	2.28930	.010	1.8519	17.8947
	HeLa Mi OSE	15.69667 <sup>*</sup>	2.28930	.000	7.6753	23.7181
Hela Crude	HeLa Mi blank	-9.87333 <sup>*</sup>	2.28930	.010	-17.8947	-1.8519
	HeLa Mi OSE	5.82333	2.28930	.275	-2.1981	13.8447
HeLa Mi OSE	HeLa Mi blank	-15.69667 <sup>*</sup>	2.28930	.000	-23.7181	-7.6753
	Hela Crude	-5.82333	2.28930	.275	-13.8447	2.1981
HepG2 Mi blank	HepG2 Crude	24.39333 <sup>*</sup>	2.28930	.000	16.3719	32.4147
	HepG2 Mi OSE	36.79667 <sup>*</sup>	2.28930	.000	28.7753	44.8181

HepG2 Crude	HepG2 Mi blank	-24.39333 <sup>*</sup>	2.28930	.000	-32.4147	-16.3719
	HepG2 Mi OSE	12.40333 <sup>*</sup>	2.28930	.001	4.3819	20.4247
HepG2 Mi OSE	HepG2 Mi blank	-36.79667 <sup>*</sup>	2.28930	.000	-44.8181	-28.7753
	HepG2 Crude	-12.40333 <sup>*</sup>	2.28930	.001	-20.4247	-4.3819
MCF Mi blank	MCF crude	37.61333 <sup>*</sup>	2.28930	.000	29.5919	45.6347
	MCF Mi OSE	44.49667 <sup>*</sup>	2.28930	.000	36.4753	52.5181
MCF crude	MCF Mi blank	-37.61333 <sup>*</sup>	2.28930	.000	-45.6347	-29.5919
	MCF Mi OSE	6.88333	2.28930	.127	-1.1381	14.9047
MCF Mi OSE	MCF Mi blank	-44.49667 <sup>*</sup>	2.28930	.000	-52.5181	-36.4753
	MCF crude	-6.88333	2.28930	.127	-14.9047	1.1381

\*. The mean difference is significant at the 0.05 level.



## VITA

**NAME** Watcharaphong Chaemsawang

**DATE OF BIRTH** 29 May 1986

**PLACE OF BIRTH** Nakhon Sawan, Thailand

**INSTITUTIONS ATTENDED** Bachelor of pharmacy. Faculty of pharmacy. Chiang Mai University

**HOME ADDRESS** 265/1 Village No. 2, Tangew sub-district. Banphotpisai district, Nakhonsawan province

**PUBLICATION**

1. Chaemsawang, W., Prasongchean, W., Papadopoulos, K. I., Sukrong, S., Kao, W. J. and Wattanaarsakit, P. (2018). Emulsion Cross-Linking Technique for Human Fibroblast Encapsulation. International journal of biomaterials, 2018.
2. Chaivichacharn, P., Bunditritidej, P., Phannasorn, P., Chaemsawang, W., Prakongpan, S. and Khongkaew, P. (2016). Stability studies of extemporaneous zinc sulfate injections for hospital use. Bulletin of Health, Science and Technology, 2016, 14(2), 59-63.
3. Charoenphol, T., Pummarin, T., Phensupa, T., Khongkaew, P., Prakongpan, S. and Chaemsawang, W. Development of Stingless bee propolis Solid Lipid Nanoparticle For Delivery of Astaxanthin, The 3rd International Conference on Advanced Pharmaceutical Research (ICAPH 2016), Rangsit University, Thailand.
4. Chaemsawang, W., Prasongchean, W., Papadopoulos, K. I., Kao, W. J. and Wattanaarsakit, P. Alginate encapsulation increases human fibroblast viability in acidic condition. The 2nd International Conference on Advanced Pharmaceutical Research (ICAPH 2015), Rangsit University,

Thailand.

AWARD RECEIVED

-

